MONOTONIC, CREEP-RUPTURE, AND FATIGUE BEHAVIOR OF CARBON FIBER REINFORCED SILICON CARBIDE (C/SIC) AT AN ELEVATED TEMPERATURE

THESIS

John Mark Engesser, Captain, USAF

AFIT/GMS/ENY/04-M01

DEPARTMENT OF THE AIR FORCE
AIR UNIVERSITY

AIR FORCE INSTITUTE OF TECHNOLOGY

Wright-Patterson Air Force Base, Ohio

AFIT/GMS/ENY/04-M01

MONOTONIC, CREEP-RUPTURE, AND FATIGUE BEHAVIOR OF CARBON FIBER REINFORCED SILICON CARBIDE (C/SIC) AT AN ELEVATED TEMPERATURE

THESIS

Presented to the Faculty

Department of Aeronautics and Astronautics

Graduate School of Engineering and Management

Air Force Institute of Technology

Air University

Air Education and Training Command

In Partial Fulfillment of the Requirements for the

Degree of Master of Science (Materials Science)

John Mark Engesser, BS

Captain, USAF

March 2004

AFIT/GMS/ENY/04-M01

MONOTONIC, CREEP-RUPTURE, AND FATIGUE BEHAVIOR OF CARBON FIBER REINFORCED SILICON CARBIDE (C/SIC) AT AN ELEVATED TEMPERATURE

John Mark Engesser, BS
Captain, USAF

Approved:

/signed/	12 Mar 04
Shankar Mall (Chairman)	date
/signed/	12 Mar 04
Theodore Nicholas (Member)	date
/signed/	12 Mar 04
Marina B. Ruggles-Wrenn (Member)	date

Abstract

The main objective of this research effort was to examine the impact that cyclic loading frequency has on the life of a C/SiC composite at an elevated temperature of 550°C. Cyclic loading of C/SiC was investigated at frequencies of 375 Hz, 10 Hz, 1 Hz, and 0.1 Hz. Creep-Rupture tests and tests that were combinations of creep-rupture and fatigue were also accomplished. A monotonic tensile test was performed at 550°C and compared to a room temperature monotonic test.

This study showed that an elevated temperature of 550°C has very little effect on the Ultimate Tensile Strength (UTS) of C/SiC. The UTS of C/SiC at 550°C was 487 MPa, while the room temperature UTS is 493 MPa.

The three creep-rupture tests in this study performed at 350 MPa, 175 MPa and 105 MPa had lives of less than 11 hours despite the fact that the UTS of C/SiC is 487 MPa at 550°C. The short life of the specimens is due to the oxidation of the carbon fibers within the C/SiC composite.

S-N curves developed from the fatigue tests indicate that there is an increase in cycles to failure as the frequency is increased. Another important discovery in this study was the fact that oxidation of the carbon fibers within C/SiC is reduced when frequency of fatigue is increased. At high frequency fatigue (10Hz to 375 Hz), C/SiC composites have longer cycle lives and time lives than at low cycle fatigue. Microscopic and SEM analysis verified that oxidation of carbon within C/SiC is slowed as frequency of fatigue is increased.

To My Wife and Three Kids

Acknowledgments

I would like to thank my family for supporting me during this thesis work. Thank you for understanding all of the late nights. I would also like to thank the AFIT Materials Lab Technician Barry Page for getting the equipment that I needed up and running. Thank you to my readers Dr. Ted Nicholas and Dr. Marina Ruggles-Wrenn. Your insight was very much appreciated. Thank you AFRL/MLL for sponsoring my thesis project.

Lastly, a special thanks goes to my faculty advisor Dr. Shankar Mall. Thanks for all of the guidance and support throughout this thesis effort. I couldn't have done it without you.

John Mark Engesser

Table of Contents

Page

List of Figures

Figure Page

Figure Page

Figure Page

Figure Page

List of Tables

MONOTONIC, CREEP-RUPTURE, AND FATIGUE BEHAVIOR OF CARBON FIBER REINFORCED SILICON CARBIDE (C/SIC) AT AN ELEVATED TEMPERATURE

I. Introduction

A composite material can be defined as a material system consisting of two or more phases on a macroscopic scale, whose performance and properties are designed to be better than the individual materials that make up the composite (1:3). Composite materials have been around since ancient times. Stories in the Bible tell us how the Egyptians made their Hebrew slaves make bricks with mud and straw. Composites have come a long way since the early days of man. The 20th century has seen dramatic increases in composite technology. These new technologies have been responsible for developments such as fiberglass in the 1940's and Metal Matrix Composites (MMCs) in the 1970's. Today, composites are found in many different areas of our lives such as airplanes, cars, sporting equipment, and medical equipment. This explosion in composite use has been fueled largely by the aerospace industry. For instance, the B-2 Stealth Bomber is made almost entirely of composite materials. The never-ending quest to make lighter, faster, and stronger spacecraft and aircraft has seen NASA and the Department of Defense (DoD) increase their composite research efforts. Today, much of their research focuses on high temperature composite materials and their applications. Ceramics are one of the best material classes when it comes to high temperature capabilities. Thus, the

high temperature composites that are garnering much of the attention are Ceramic Matrix Composites (CMCs). Most CMCs are able to withstand extremely high temperatures. However, CMCs do have some limiting factors that affect their performance. One of these limiting factors is the oxidation that occurs within the CMC composite at high temperatures. Carbon Fiber Reinforced Silicon Carbide (C/SiC) is a CMC that succumbs to oxidation at high temperatures. The oxygen in air is able to react with the carbon and oxidize the carbon fibers within the SiC matrix. Despite this oxidation problem, NASA and the U.S. Air Force are considering C/SiC as a composite candidate for many space and aircraft applications such as, heat exchangers, integrally bladed disks, nozzle exit ramps, un-cooled nozzles, combustors, thrust chambers, turbo pump rotors, and re-entry heat shields. These applications will involve cyclic loading with large cycle accumulation at very high temperatures.

Several studies have been conducted that analyze the oxidation that occurs within C/SiC composites. For example, Verilli et al. (2) studied the behavior of C/SiC during creep-rupture and low cycle fatigue loading at temperatures of 550ºC and 650ºC. He concluded that oxidation was the primary damage mechanism during these tests.

One area that has not received much attention is the effect that cyclic loading frequency has on the oxidation of the carbon fibers within C/SiC. This research effort will analyze this effect at an elevated temperature of 550ºC, and also compare it to the creep-rupture data obtained in this study. Cyclic loading of C/SiC will be investigated at very high frequencies as well as low frequencies. This study will also compare monotonic tension tests conducted at room temperature with tests conducted at 550ºC to see if the increased temperature has an adverse effect on the monotonic tensile strength of

C/SiC. Tests will also be performed that combine the characteristics of creep-rupture testing and fatigue testing in order to better understand the oxidation that occurs within C/SiC.

The following chapters will describe this research effort. The background history of C/SiC research will be reviewed. Next, the experimental techniques used in this study will be explained. The results obtained from the tests performed will then be discussed. Lastly, some conclusions and recommendations for this study will be given.

II. Background

This chapter begins with an introduction to Ceramic Matrix Composites (CMCs). A description of the characteristics and applications of carbon fiber reinforced silicon carbide ceramic matrix composites (C/SiCs) are then given. Following that is a discussion of the oxidation that occurs within C/SiC during its exposure to elevated temperature environment. Next, the behavior of C/SiC in creep, tensile, and fatigue tests are explained. Finally, some comments on experiments conducted on C/SiC in various environments are given, and experimental observations from various tests are briefly mentioned.

2.1 Ceramic Matrix Composites

Innovative advancements in technology and research point to a diminished role for the Space Shuttle in the future. Newly developed Reusable Launch Vehicles (RLVs) will soon replace the expensive shuttle. "Within the next 10 years, NASA's goal is to develop a second generation RLV that will increase the safety by two orders of magnitude and reduce the cost of placing payloads in orbit by one order of magnitude, when compared to the performance of the Space Shuttle" (3:435). The materials that will help NASA accomplish this goal are Ceramic Matrix Composites (CMCs). CMCs will increase safety because of their higher strength to density ratio and higher temperature capability, when compared to the current super alloys (4:1). Launch and operational costs would also be decreased due to the lower weights of the RLV components. Another

great advantage of CMCs is that because of their high temperature capability, cooling system requirements could be reduced or even eliminated (5:453). This, in turn, would decrease the weight, cost, and complexity of RLVs. The U.S. Air Force is also interested in CMCs because of their high temperature capability and high strength to density ratio. The Air Force could use these CMC materials to enhance individual Air Force components, thus increasing the performance and capabilities of their future aircraft and spacecraft.

2.2 Carbon Fiber Reinforced Silicon Carbide (C/SiC)

One CMC that has garnered particular attention by NASA and the Air Force is carbon fiber reinforced silicon carbide ceramic matrix composite (C/SiC). This composite consists of continuous carbon fibers in a silicon carbide (SiC) ceramic matrix.

2.2.1 Carbon Fibers.

The carbon fibers that are used quite frequently in C/SiC are T-300 carbon fibers. They have excellent tensile strength at room temperature, 2,760-3,450 MPa, and very high stiffness, 228 GPa (1:28). The density of T-300 carbon fibers is about 1.76 g/cm^3 (1:28). Some of the other advantages of carbon fibers are that they are relatively inexpensive, easily woven into complex architectures, and they possess a high thermal conductivity (6:443). The major disadvantage of T-300 carbon fibers is that they are prone to oxidation at elevated temperatures. The oxidation of the carbon fibers in the SiC matrix will be discussed in section 2.3.

2.2.2 Silicon Carbide (SiC) Ceramic Matrix.

Ceramics are a very attractive material to the aerospace industry because of their ability to maintain strength at high temperatures, their high melting points, and their chemical stability in many hostile environments (7). Ceramics are able to accomplish this because of their very strong chemical bonds, which are both ionic and covalent. However, these strong bonds also cause ceramics to become brittle when a stress is applied. Silicon Carbide (SiC) is a hard covalently bonded ceramic material with a high melting point, low thermal expansion, and excellent thermal conductivity (8). It also has high hardness, good corrosion resistance, and high stiffness. SiC is a material that can be used in applications where high temperature, wear, and corrosion resistant materials are required (8). A disadvantage of SiC is that like all materials, there are flaws and cracks within it. However, when a flaw or crack is present in a ceramic, deformation occurs at these high local stress locations, which then leads to catastrophic failure (7). In a C/SiC composite, the carbon fibers prevent the SiC ceramic matrix from catastrophic failure by stopping the continuation of the matrix cracks through crack bridging (2:257).

2.2.3 C/SiC Characteristics.

The carbon fibers and the SiC ceramic matrix are combined to form C/SiC, which is a very strong high temperature ceramic matrix composite material. C/SiC also has a low density, high stiffness, and high hardness. It can withstand high abrasive action, is chemical resistant, has a low coefficient of thermal expansion, and it has great design flexibility (9:4). There are four techniques that have been developed to manufacture or process C/SiC. These processing techniques include:

slurry infiltration and hot pressing, polymer conversion, silicon melt infiltration, and chemical vapor infiltration (CVI) (10). The technique that was used to manufacture the C/SiC used in this research effort was the CVI process. "The primary advantage of this method is the uniform coating of tailored compositions for multi-layer at relatively low temperatures (900-1100°C)" (11:2). The disadvantages of the CVI process are that it is very expensive, corrosive, toxic, explosive, and it has low deposition rates (11:2). The CVI process is also very time-consuming in that it takes approximately 300-600 hours to complete (12). After C/SiC is manufactured, the SiC matrix regions contain many micro-cracks. These cracks "form upon cooling down from the processing temperature due to stresses that arise from the difference in the coefficients of thermal expansion for the carbon fiber and the SiC matrix" (4:2). During the manufacturing process, a pyrolytic carbon coating can also be applied to the carbon fibers. This coating helps to promote fiber-matrix debonding because pyrolytic carbon is inherently anisotropic and SiC is isotropic (13). The weak bond between the carbon fibers and the SiC matrix is considered beneficial under monotonic tensile loading conditions, but has a negative effect during cyclic loading (14:4-5). The negative effect is due to the internal frictional sliding and heating between the fiber and the matrix.

2.2.4 C/SiC Applications.

C/SiC is being considered as a new material in high temperature and high strength applications by the government as well as many commercial agencies. The different application areas include optics, space technology, automotive, power technology, chemical engineering, nuclear engineering, medical, and defense related

applications. Some of the individual applications include mirrors, telescopes, lifetime brake disks, radiant heater tubes, heat exchangers, wall and blanket components of fusion reactors, integrally bladed disks, large nozzle ramps, nozzle exit ramps, un-cooled nozzles, heat-pipe-cooled leading edges, combustors, thrust chambers, gas generators, vanes, turbo pump rotors, housings, throats, re-entry heat shields, and prosthetic devices (2; 3; 5; 9; 13; 14; 15; 16; 17; 18; 19).

2.3 Oxidation of C/SiC

Oxidation of carbon occurs when it is exposed to oxygen in air at elevated temperatures. If left alone at the elevated temperature, eventually all of the carbon will dissipate in the form of carbon monoxide or carbon dioxide. In a pure oxygen environment, it takes approximately 70 minutes to dissipate an entire 0.4-gram T-300 carbon fiber tow at 600°C (4). The carbon fiber tow will be entirely diffused in 35 minutes at 1200°C (4). Oxidation of the carbon fibers within the SiC matrix is a major concern when considering the high temperature use of carbon fiber reinforced silicon carbide ceramic matrix composites (C/SiCs). The factors that affect the oxidation of the carbon fibers within the SiC matrix include the amount of as-manufactured micro-cracks, crack density, crack closure, temperature, stress, environment, and oxidation inhibitors (20:419). The oxidation of the carbon fibers is able to occur within C/SiC because of the composites porosity and because of the micro-cracks that are formed in the SiC matrix (2). As stated before, these micro-cracks occur in the SiC matrix “upon cooling down from the processing temperature due to stresses that arise from the difference in the

coefficients of thermal expansion for the carbon fiber and the SiC matrix" (4:2). The porosity of C/SiC and the micro-cracks that are present in the SiC matrix allow a path for air to seep into C/SiC. When the composite reaches a high temperature, oxidation between the carbon fibers and the air/oxygen that is in contact with the carbon begins to occur. The carbon fibers that are exposed to the oxygen will eventually be destroyed which will put a greater load on the remaining intact or non-oxidized carbon fibers. If the load is great enough, failure will undoubtedly occur. However, the micro-cracks within the SiC matrix begin to close at C/SiC's processing temperature, approximately 1100°C (4:8). At this processing temperature, the thermal expansion of the carbon fibers and the SiC matrix are matched, which in turn causes the crack edges to come together and stop the seeping of oxygen into the composite. Another positive effect on C/SiC at 1100°C is the growth of silica scale (SiO_2) as the SiC matrix oxidizes. This silica scale helps to fill in matrix cracks, which seal off the fibers from the outside air (4:8). The presence of oxidation within C/SiC is drastically reduced between 1000°C and 1200°C at low stresses (4). At temperatures above 1200°C, both of these anti-oxidizing occurrences begin to diminish. The over expansion of the SiC matrix can cause cracks to widen, and the formation of SiO_2 begins to increase in a parabolic fashion (4:8). Both the over expansion of the matrix and the increase in SiO_2 do much more harm than good to the composite at temperatures greater than 1200°C. Therefore, when designing a system with C/SiC as a main component, oxidation damage of C/SiC must be taken into account at low and at high temperatures, i.e. less than 1000°C or greater than 1200°C.

2.3.1 Oxidation Protection.

"Oxidation protection for C/SiC composites is a key to the true viability of these materials for anything other than limited life applications" (21-3). There has been some research into oxidation protection of C/SiC. It was shown by Halbig et al. (4), that at a low creep stress (69 MPa) and a high temperature (1454°C), the use of boron enhancements in the SiC matrix increased the stress-rupture life of C/SiC by 10 times. In this study, Halbig et al. (4) also demonstrated that at a high creep stress (172 MPa) and a high temperature (1454°C), the use of boron enhancements in the SiC matrix and an external seal coating of carbon, boron, and silicon increased the stress-rupture life of C/SiC by 600-900 times (4:6). However, the research suggested that the enhanced C/SiC would still be susceptible to oxidation at lower temperatures where the protective borosilicate glasses and silica scales do not form (4:9).

2.4 Creep or Stress-Rupture Behavior

A creep or stress-rupture test is a procedure that is quite often used to characterize C/SiC. It is accomplished in order to analyze the stressed oxidation strength of the composite. Therefore, it is usually performed at temperatures greater than 400°C. At temperatures greater than 400°C, oxidation of the carbon fibers is the primary damage mechanism in C/SiC (22). The creep-rupture test, allows oxygen into the composite, which in turn begins to degrade the carbon fibers. As a general rule, when temperature and stress is increased, the life of a sample is decreased (2:246).

2.4.1 Low temperatures (< 750°C).

At low temperatures, oxidation of the carbon fibers within C/SiC occurs uniformly throughout the sample (2:246). However, the oxidation rate increases as the temperature is increased. For example, Verrilli et al. (2) showed that at a stress of 105 MPa the time to failure of C/SiC in air at 650°C was 3.67 hours, whereas, at 550°C the time to failure was 18.28 hours. More carbon fibers were oxidized at 650°C than at 550°C.

2.4.2 Intermediate Temperatures (750-1100°C).

At intermediate temperatures, oxidation of the carbon fibers within C/SiC occurs in a non-uniform manner (2). The oxidation location changes from the areas within the composite that are adjacent to the pre-existing micro-cracks to the surface of the sample. These micro-cracks begin to close as the temperature of the sample approaches the approximate processing temperature of 1100°C (4:8). Therefore, due to the closing of the micro-cracks, and the formation of a silica scale, oxidation of the carbon fibers is inhibited. The creep life at 750°C is less than the creep life at 1000°C. For example, Halbig et al. (4) showed that at a stress of 172 MPa the time to failure of C/SiC in air at 750°C was 91 minutes, whereas, at 1000°C the time to failure was 124 minutes.

2.4.3 High Temperatures (> 1100°C).

The positive effects of micro-crack closure and silica scale formation are diminished at higher temperatures. Oxidation begins to reoccur at a rapid rate within the C/SiC sample at these extreme temperatures. In the Halbig et al. study (4), the

creep-rupture life at 1250°C and 69 MPa was 142 minutes, whereas, at 1500°C the time to failure was 65 minutes (4:5).

2.5 Tensile Behavior

There is considerable variability in the tensile strength of C/SiC. It has a tensile strength between 320 and 610 MPa at room temperature (2; 11; 14; 23; 24). The differences in these values could be attributed to different manufacturing techniques, or to the large plate-to-plate variations of the manufactured C/SiC material (6-447). Weave architecture of the carbon fibers within the matrix can also change the properties of C/SiC (25). C/SiC maintains its tensile strength at elevated temperatures as well. At 1200°C, C/SiC was shown to have a tensile strength of approximately 558 MPa (24). The modulus of C/SiC increases as the sample temperature is increased. The modulus of C/SiC at room temperature is about 47 GPa, however, at 650°C the modulus increases to 100 GPa (14).

2.6 Fatigue Behavior

Cycling frequency plays a role in the fatigue of C/SiC at room temperature (14). This occurs because of the aforementioned weak bond between the carbon fibers and the SiC matrix. When frequency of loading is increased, the fibers and the matrix slide against each other. The internal friction causes an increase in internal heating. If the internal heating gets to a high enough temperature, then oxidation could occur. In a study conducted by Staehler et al. (14), it was shown that at a frequency of 375 Hz at room

temperature, oxidation of the carbon fibers did occur in the internal portions of C/SiC. This caused a reduction in cycles to failure at 375 Hz compared to 4 and 40 Hz (14).

Cycling frequency plays a less significant role in the failure of C/SiC as temperature is increased. This is due to the fact that oxidation becomes the primary damage mechanism to C/SiC at temperatures greater than 400°C (22). Verrilli et al. (2) conducted a test at a temperature of 650°C, a load of 70 MPa, an R ratio of .05, and a frequency of 100 Hz. The number of cycles to failure of this sample was about 3 million, and the time to failure was approximately 9 hours. The same test conducted at a frequency of 0.033 Hz showed 1328 cycles and 11 hours to failure. This data suggests that sample failure at high temperatures is not dependent on the number of cycles but is more reliant on the time that the sample is exposed to the high temperature.

2.7 Tests Conducted in Environments Other Than Air

Many studies have been conducted in environments other than air. For example, tests have been performed in pure oxygen, argon, steam, vacuums, and combinations of these environments (3; 5; 6; 15; 20). The focus of these tests was to try to understand the oxidation of C/SiC. However, these studies will not be addressed because this research effort will focus on tests conducted in an air environment.

2.8 Experimental Observations

There are many disagreements in previous tests conducted by different researchers. For example Verrilli et al. (2) found that the creep-rupture time to failure of C/SiC

manufactured by Allied Signal Composites at 550°C and 175 MPa was 1.53 hours. On the other hand, Halbig et al. (4) found the time to failure of a creep-rupture test of C/SiC manufactured by Honeywell Advanced Composites conducted at 550 °C and 172 MPa to be 25 hours. Both composites were manufactured via CVI and were composed of a SiC matrix reinforced by 2-D plain weave [0/90] preform of T-300 carbon fibers. They were also seal coated with SiC after machining. Verrilli's (2) batch was seal coated via CVI, and Halbig's (4) batch was seal coated via chemical vapor deposition (CVD). The variation in the results could be attributed to the different seal coating methods, slight differences in manufacturing techniques, or the large plate-to-plate variations of the manufactured C/SiC material (6-447). The large error could also occur because of mistakes or differences in experimental techniques. Whatever the case may be, because C/SiC is such a new material, there needs to be more experiments conducted so that results can be compared, and more knowledge can be gained about the behavior of this new material. When numerous experiments have been performed, and the results analyzed, then meaningful conclusions can be drawn regarding the properties of C/SiC at various temperatures and stresses.

III. Material and Experiments

This chapter begins with a description of the C/SiC composite used in this study. The test equipment that was used during the experiments is then mentioned. Next, a discussion of the test procedures that were followed is given. Finally, the post-failure analysis techniques are explained.

3.1 Material Description

The material investigated in this research was a woven carbon fiber-reinforced silicon carbide (C/SiC) ceramic matrix composite manufactured by Honeywell Advanced Composites Inc. (now part of General Electric), Newark, DE. The C/SiC composite was manufactured using the chemical vapor infiltration (CVI) method. Reinforcement of the SiC matrix was accomplished from 26 plies of plain-weave cloth in a [0/90] lay-up. The cloth was woven from 1k tows of T-300 carbon fibers. The fiber pre-form was given a pyrolytic carbon coating in order to promote toughness through fiber-matrix debonding (13). Final fiber volume fraction was approximately 45%. The composite bulk density was reported to be 2.0 g/cm^3. Figure 3-1 gives an enhanced look at the as-manufactured C/SiC composite. The many micro-cracks within the matrix rich regions of the composite can be seen in Figure 3-1. These micro-cracks in the SiC matrix are due to the differences in thermal expansion coefficients between the carbon fibers and the SiC matrix (4:2).

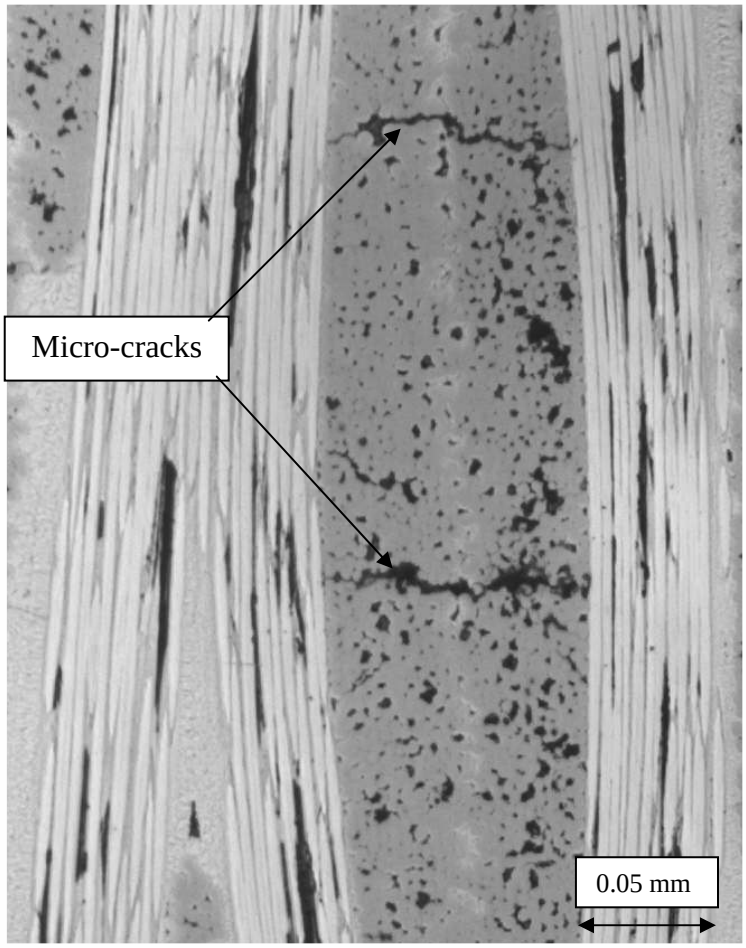

Figure 3-1. Cross-Section Showing Micro-Cracks of C/SiC Composite

Test specimens were cut from the same 216 mm x 216 mm x 3 mm manufactured nominal plate. The specimens were then machined into a dog-bone configuration. The total length of the specimens was 78 mm. Gage section dimensions were 8 mm wide by 12 mm long, while the tab section dimensions were 10 mm wide by 30 mm long. After the machining and cutting of the specimens, they were then seal coated with SiC via chemical vapor deposition (CVD) process. The final thickness of the specimens was approximately 3.4 mm. The as-manufactured test specimen can be seen in Figure 3-2.

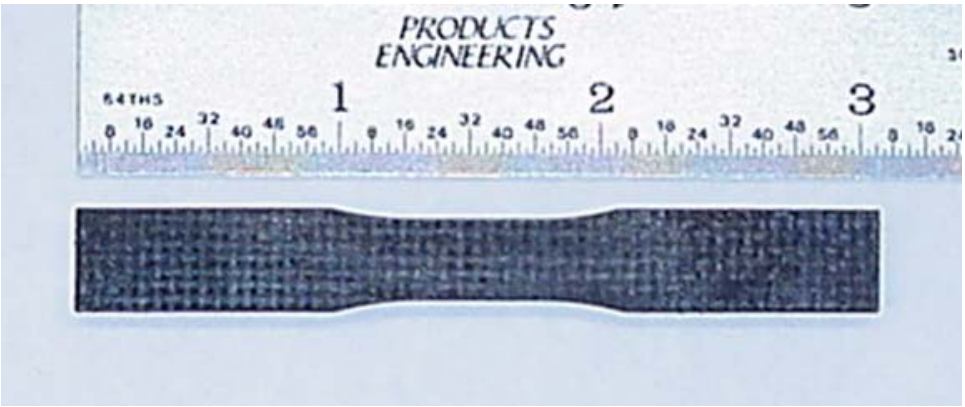

Figure 3-2. Manufactured Test Specimen (scale is in inches)

3.2 Test Equipment

There were five main pieces of equipment used during the testing of the C/SiC composite. They were the servo hydraulic machine, the furnace, the chilled water system, the extensometer, and the computer software.

The servo hydraulic machine used for all of the tests was a Material Test Systems (MTS) Corporation axial test system with a 25 kN (5500 lb) capacity. This horizontally configured machine is shown in Figure 3-3.

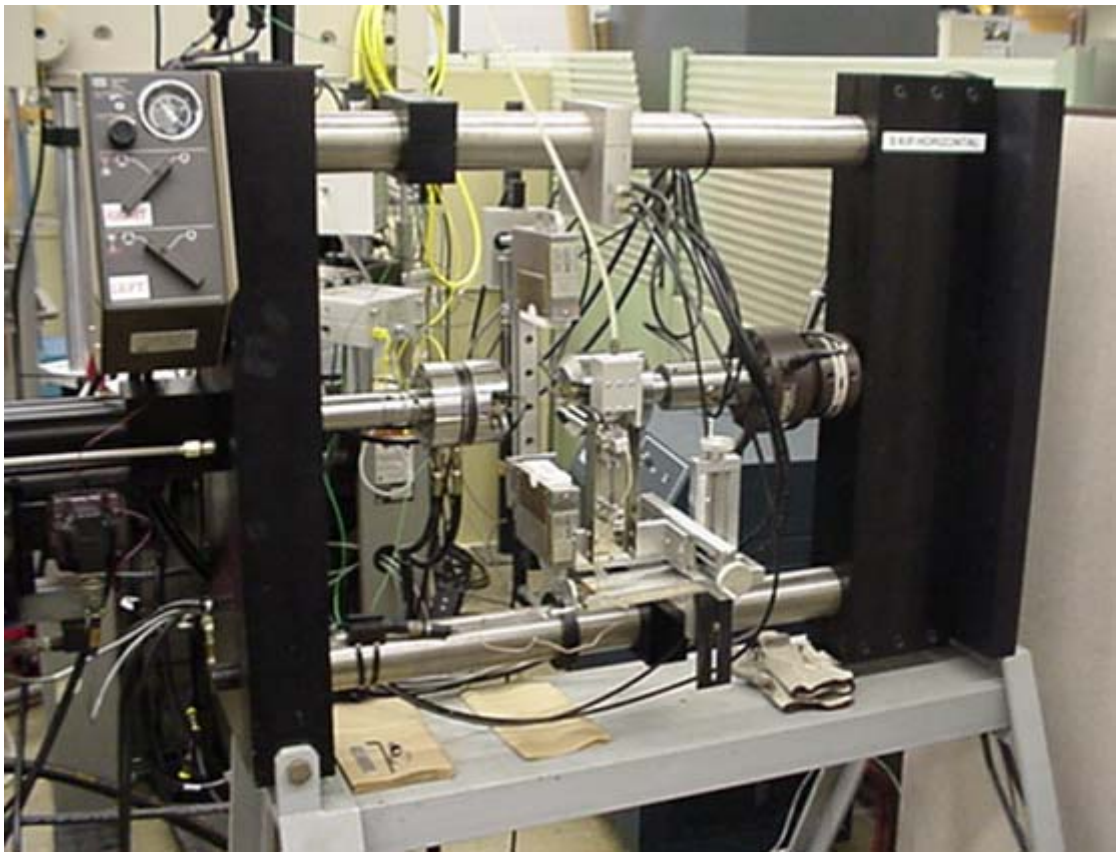

Figure 3-3. Servo Hydraulic Machine Used in Experiments

The grip pressure used on the specimen when placed in this machine was 6.89 MPa (1000 psi). This selected grip pressure was chosen so that it was high enough to prevent the specimen from slipping during loading. The grip pressure was also low enough so that the specimen was not crushed when being gripped. A load cell measured the load

that was placed on the specimen by the servo hydraulic machine. This load cell was an MTS 661.20E-01 load cell with a 25 kN capacity.

The furnace used during the testing of C/SiC was a single zone Amteco Hot-Rail Furnace System with heating elements in the top and bottom portions of the furnace chamber. The C/SiC specimen was held between these two heating elements which heated the specimen on both sides. The furnace chamber was very small and compact with dimensions of 15 mm wide, 50 mm long, and 64 mm deep. A separate MTS 409.83 Temperature Controller unit controlled the temperature inside the furnace chamber. The single zone furnace had a thermocouple placed in the upper portion of the chamber. This thermocouple sent the signal to the Temperature Controller, which then supplied the power to the upper and lower heating elements. Figure 3-4 shows a picture of the bottom portion of the furnace.

The chilled water system was a NESLAB model HX-75. The function of the chiller was to keep the specimen grips and the load cell cool, while the furnace and the surrounding area was very hot. The NESLAB did this by pumping 7°C distilled water through hoses connected to the grips and the load cell isolation block.

Specimen extension was measured with an MTS extensometer model number 632.53E-14. The extensometer consisted of two alumina rods placed 12.7 mm (½ inch) apart. It was held against the specimen with spring pressure. A heat shield was also part of the extensometer setup. Cooling was accomplished by room temperature air being forced through the diffuser on an air-cooling attachment. An MTS calibrator model 650.03 was used to periodically calibrate the extensometer.

The computer software used to control the servo hydraulic machine and the furnace was MTS TestStar IV software. The Multi Purpose Testware (MPT) feature of the software was used to program the various tests and to acquire data throughout the duration of the test. Data acquisition was accomplished in logarithmic intervals (cycles 1,2,3,4,5,6,7,8,9,10,20,30, etc.) and in various timed intervals. Figure 3-5 shows an example of the MTS software program used in the specimen tests.

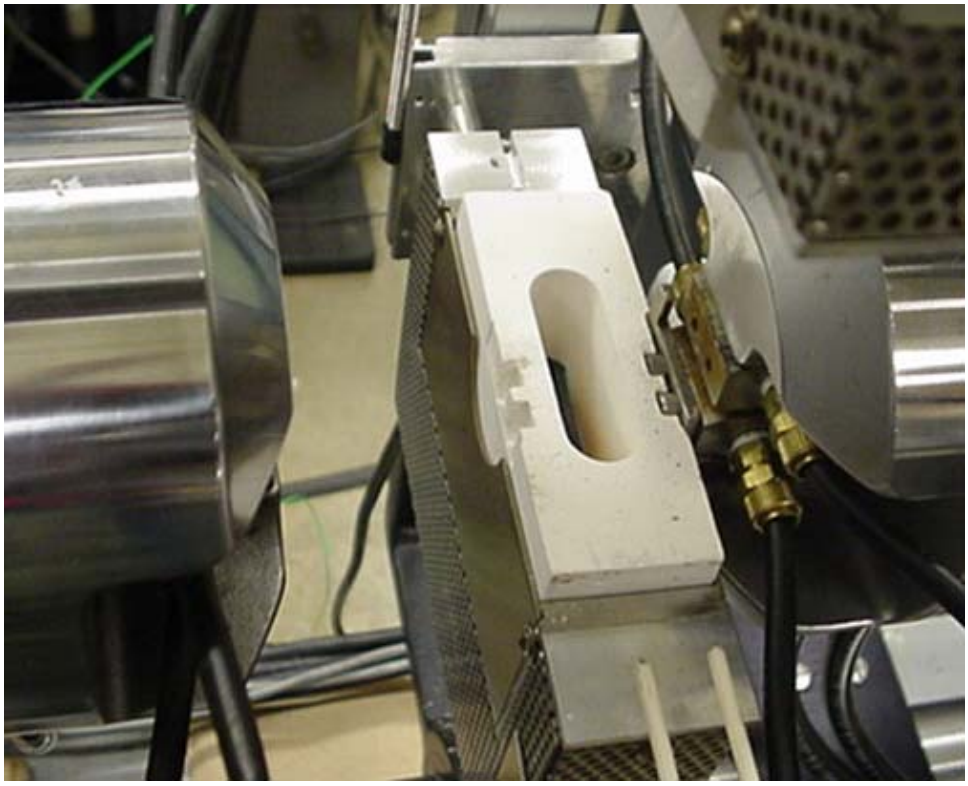

Figure 3-4. Amteco Furnace Used in Experiments

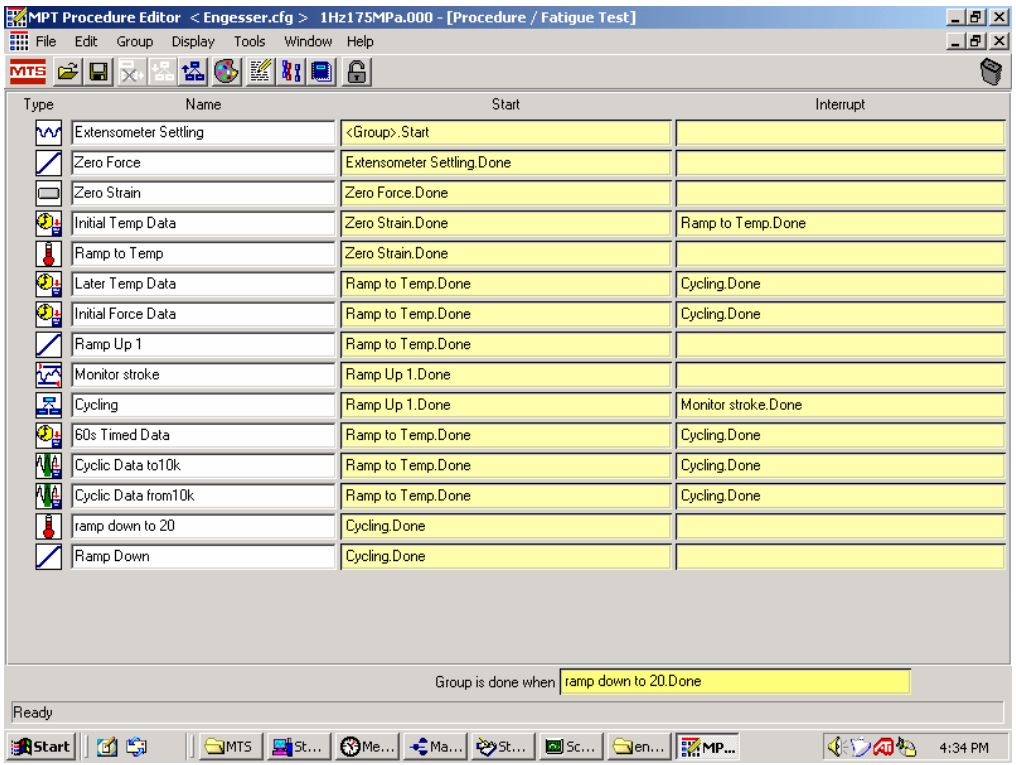

Figure 3-5. MTS TestStar IV Software (MPT Portion)

3.3 Test Procedures

3.3.1 Specimen and Equipment Preparation.

The samples were measured and wrapped with steel mesh before testing started. The height and width of the gage section were measured using a Fowler Precision Dial Caliper. This cross sectional area was used to calculate the stress on the specimen by taking the measured load during the test and dividing it by the cross sectional area. After the measurements of the specimens were recorded, steel mesh was then wrapped around the tab portions of the C/SiC composite. This was done to aid in the prevention of slipping and crushing when the specimens were being gripped and loaded.

The target specimen temperature for all of the tests was 550°C. Therefore, the furnace chamber temperature had to be calibrated to the actual temperature of the sample. To accomplish this, a thermocouple was glued on the top middle portion of a dummy specimen. This thermocouple was located 39 mm from each end of the sample. Two thermocouples were also glued on the bottom right and bottom left of the same dummy specimen. These thermocouples were located 34 mm from each end of the specimen. The glue used to attach the thermocouples to the specimen was Omega CC High Temperature Cement. The furnace was then heated until the middle thermocouple was stable at 550°C. The temperature of the furnace at this point was 554°C. Figure 3-6 shows the results from this calibration process.

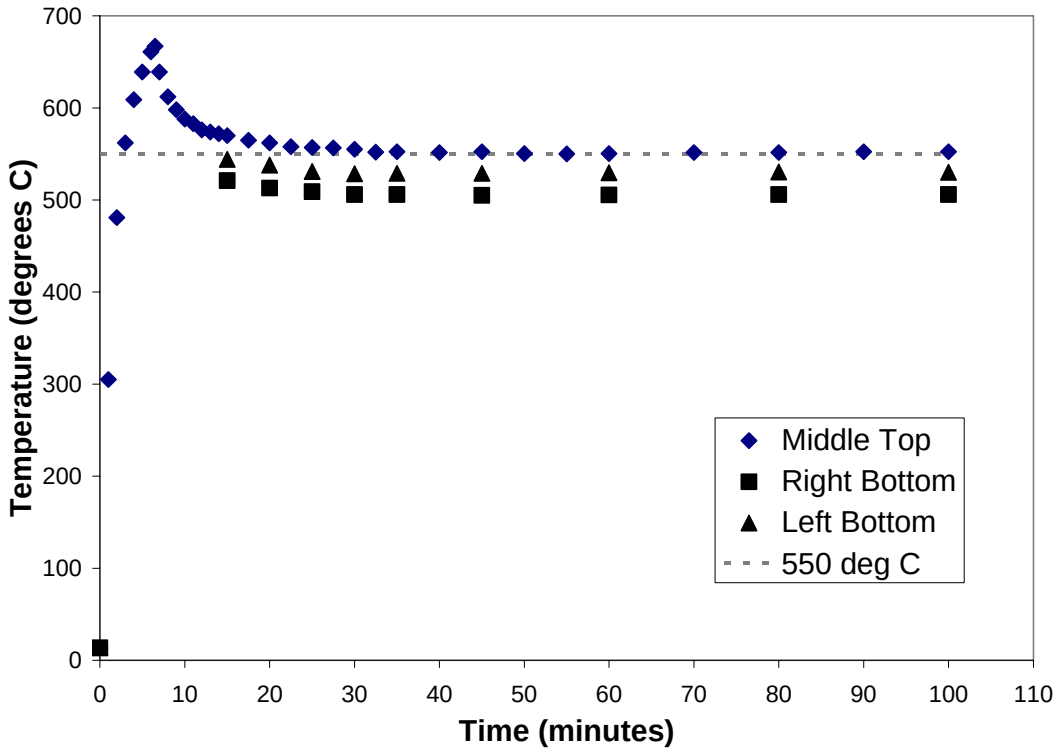

Figure 3-6. Oven Set at 554°C - Middle Thermocouple on Top of Sample

The dummy specimen was then flipped over so that the middle thermocouple was located at the bottom of the sample. When the bottom middle thermocouple was stable at 550°C, the temperature of the furnace was 565°C. Figure 3-7 shows this process.

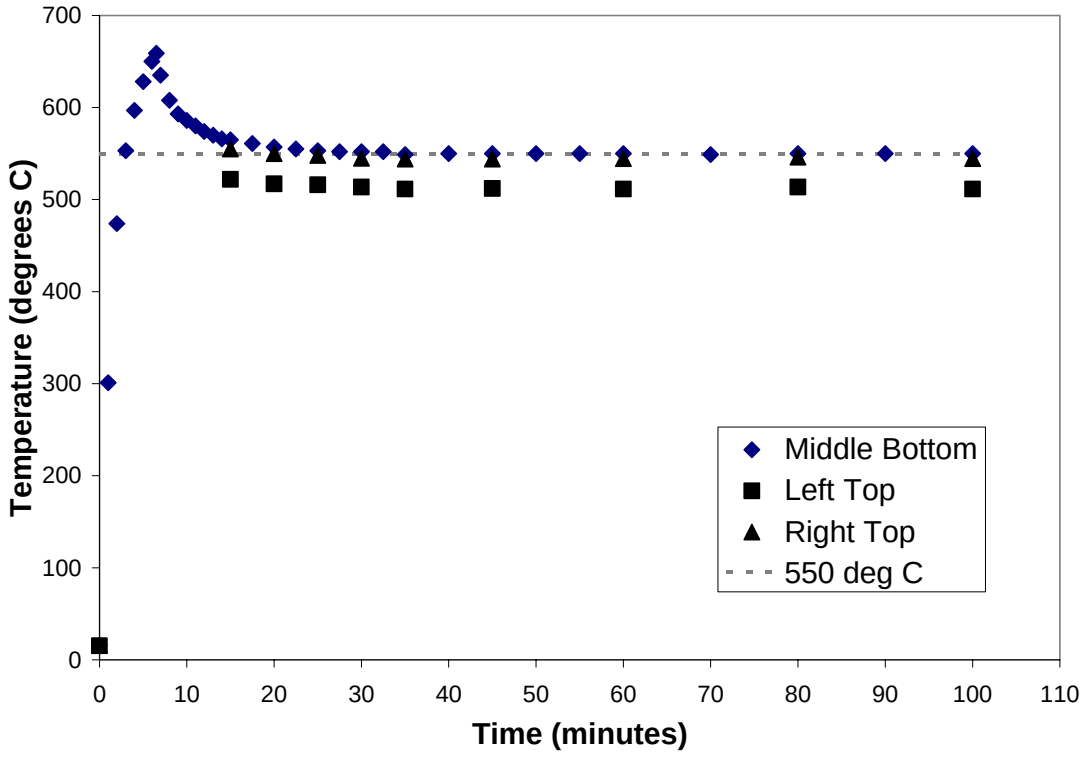

Figure 3-7. Oven Set at 565°C - Middle Thermocouple on Bottom of Sample

In order to get the entire middle portion of the specimen's temperature closest to 550°C, a furnace temperature of 559°C was chosen. The furnace temperature of 559°C was then tested with both the middle thermocouple on the top and bottom. At a furnace temperature of 559°C, the approximate temperatures of the top middle, top left, and top right after 30 minutes of heating were 559°C, 506°C, and 538°C

respectively. The temperatures of the bottom middle, bottom left, and bottom right after 30 minutes of heating were 542°C, 537°C, and 512 °C respectively. The furnace was then set at 559°C throughout the experiment. Graphs of the top and bottom specimen temperatures at a furnace temperature of 559°C can be seen in Figures 3-8, 3-9, and 3-10.

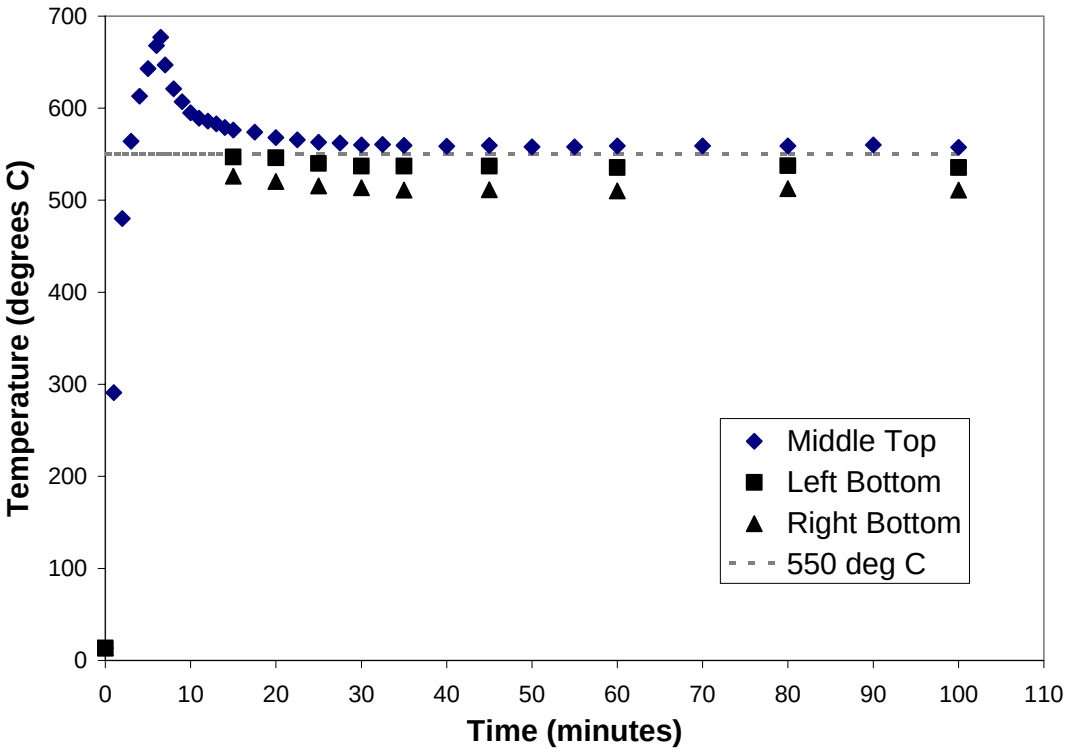

Figure 3-8. Oven Set at 559°C – Middle Thermocouple on Top

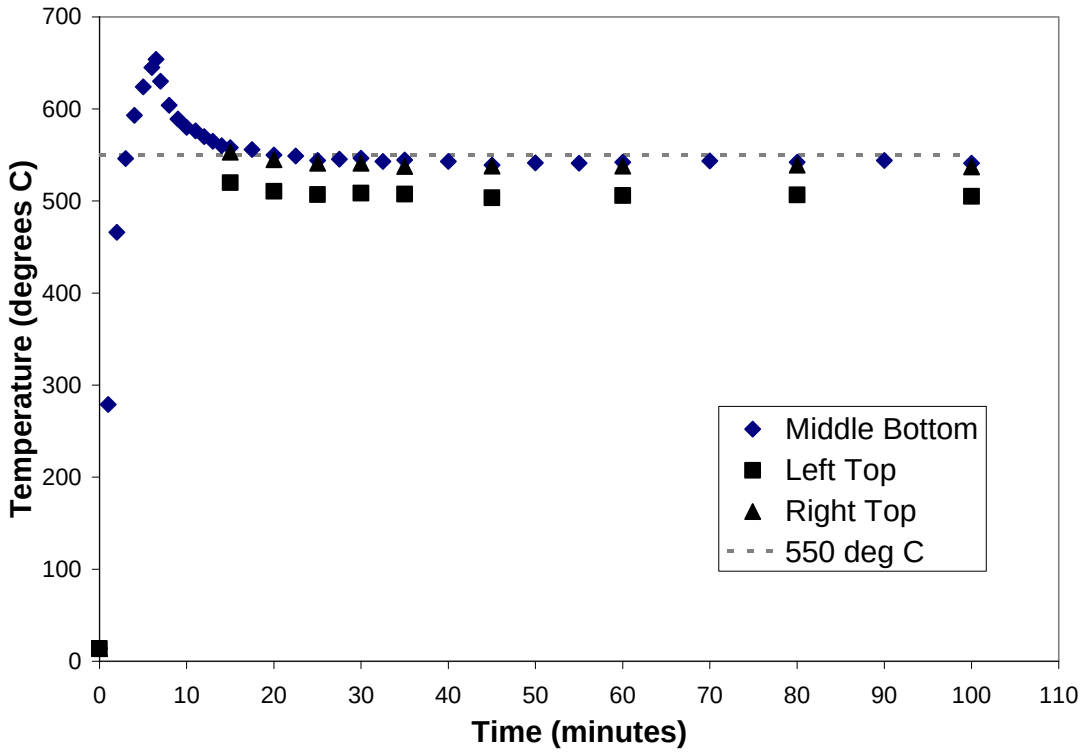

Figure 3-9. Oven Set at 559°C – Middle Thermocouple on Bottom

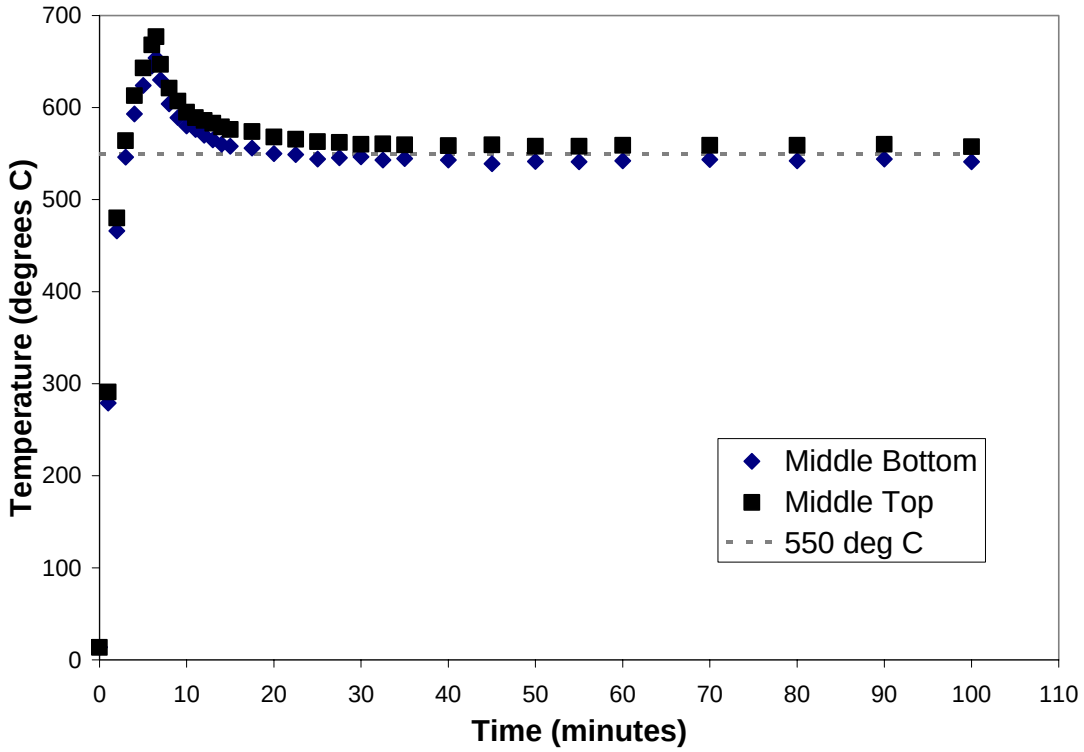

Figure 3-10. Oven Set at 559°C – Combination Graph Showing Middle Thermocouple Temperatures at Top and Bottom of Sample

3.3.2 Testing.

All of the tests were conducted at approximately 550°C in air under standard laboratory conditions. Before a test was started, the C/SiC specimen was mounted in the servo hydraulic machine. One end of the specimen was mounted in stroke control, while the other end was mounted in load control. This assured that the specimen was at zero load during the heating process. The specimen was then heated to 550°C (furnace was at 559°C). This heating process took approximately 7 minutes. The specimen's temperature was then allowed to stabilize for another 23 minutes, which brought the total initial heating time to 30 minutes. After the 30

minutes, the longitudinal thermal expansion (α) was calculated from the following equation:

$$\alpha = \frac{\varepsilon_T}{\Delta T} \quad (1)$$

where ε_T is the thermal strain and ΔT is the change from room temperature to 550°C. The average longitudinal thermal expansion for C/SiC was found to be 2.47×10^{-6}/°C. The strain was then reset to zero, and the various tests were started. Tests performed in this research included monotonic tension tests, creep-rupture, fatigue, and combinations of creep-rupture and fatigue. Data acquisition was recorded at various time intervals for the monotonic tension and creep-rupture tests, and it was recorded in logarithmic intervals for the fatigue and combination (creep-rupture and fatigue) tests. Furnace temperature, displacement, voltage (converted to strain), and load were the data that was recorded by the computer software.

3.3.2.1 Monotonic Tension Tests.

There was one monotonic tension test performed on C/SiC during this research effort. This test was performed in stroke control with a displacement rate of .05 mm/sec.

3.3.2.2 Creep-Rupture Tests.

There were 3 creep-rupture tests performed on C/SiC. They were performed in load control at stresses of 105 MPa, 175 MPa, and 350 MPa. The creep load was reached by a ramping rate of 10 MPa/s.

3.3.2.3 Fatigue Tests.

There were 9 fatigue tests performed on C/SiC during the study. They were performed at 0.1 Hz, 1 Hz, and 10 Hz. In addition, 8 fatigue tests at 375 Hz were performed at the Air Force Research Lab Materials Directorate at Wright-Patterson AFB and are included in this study. The fatigue tests were conducted in load control with an R-ratio (minimum load/maximum load) of 0.05 and a triangular waveform. The maximum load during the fatigue tests varied from 105 MPa to 500 MPa.

3.3.2.4 Combination (Creep-Rupture and Fatigue) or Creep-Fatigue Tests.

There were 3 combination tests performed on the C/SiC composite. These tests were fatigue tests with a specified hold time at the maximum stress. The hold time was 5 seconds for the 1 Hz test at 175 MPa. For the two 0.1 Hz tests conducted at 175 MPa and 105 MPa the hold time was 50 seconds. These combination tests were also conducted in load control with an R-ratio (minimum load/maximum load) of 0.05 and a triangular waveform. Figure 3-11 shows example segments of the waveform from these 3 tests.

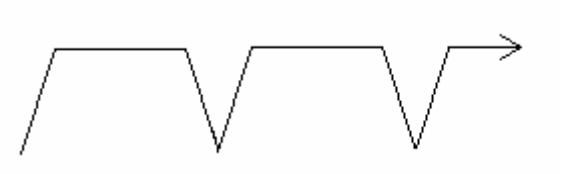

Figure 3-11. Example Waveform for Combination (Creep-Fatigue) Tests

3.3.3 Test Matrix.

Table 1 is a summary of the tests performed on the C/SiC composite in this study.

Table 3-1. Test Matrix

Specimen Number	Test Temperature (°C)	Type of Loading	Maximum Stress (MPa)	R Ratio
02-317	550	Monotonic	487	N/A
02-314	550	Creep	105	N/A
02-303	550	Creep	175	N/A
02-326	550	Creep	350	N/A
02-315	550	0.1 Hz	105	0.05
02-312	550	0.1 Hz	175	0.05
02-318	550	0.1 Hz	275	0.05
02-325	550	0.1 Hz	350	0.05
02-310	550	1 Hz	175	0.05
02-320	550	10 Hz	105	0.05
02-327	550	10 Hz	175	0.05
02-319	550	10 Hz	275	0.05
02-321	550	10 Hz	350	0.05
02-316	550	0.1 Hz - hold 50s	105	0.05
02-313	550	0.1 Hz - hold 50s	175	0.05
02-311	550	1 Hz - hold 5s	175	0.05
02-302	550	Invalid	Invalid	N/A
*02-304	550	375 Hz	175	0.05
*02-307	550	375 Hz	275	0.05
*02-269	550	375 Hz	325	0.05
*02-272	550	375 Hz	375	0.05
*02-272	550	375 Hz	400	0.05
*02-271	550	375 Hz	425	0.05
*02-305	550	375 Hz	500	0.05
*02-306	550	375 Hz	500	0.05

* Test Performed at AF Research Lab Materials Directorate, WPAFB

3.4 Post-Failure Analysis

The post failure analysis consisted of cutting the specimens, mounting them, polishing, and finally analyzing them under an optical microscope and a Scanning Electron Microscope (SEM).

3.4.1 Cutting.

The specimens were cut so that the cross sectional area of the fracture surface could be analyzed. Careful attention was used so that the longitudinal fibers were perpendicular to the cutting blade. Cutting was accomplished with a Buehler ISOMET 1000 cutting machine and a Buehler Series 15LC diamond wafering blade. The speed of the saw was set at 350 rpm. Figure 3-12 shows where the cuts were made on the specimens.

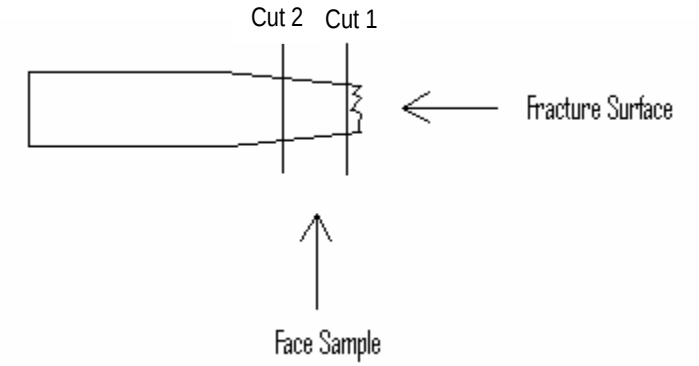

Figure 3-12. Specimen Cuts Made Before Mounting

3.4.2 Mounting.

After the specimens were cut, the face sample (Figure 3-12) of each specimen was mounted in a 3.175 cm (1.25 inch) diameter Simplimet 2000 mounting press.

The mounting compound was a phenolic powder called Buehler Kunductomet II. The mounting process consisted of a pressure of 29 MPa (4200 psi) and a temperature of 150°C. The total heating time was 6 minutes and the cool-down time was 3 minutes. Mounted specimens were then infiltrated with a Caldofix Epoxy.

3.4.3 Polishing.

All of the specimens were polished on a Phoenix 4000 at 150 rpm. The first step in polishing the mounted specimens was to rough polish them. This was done with 600 grit SiC sand paper and a force of 7 lbs for 6 minutes. Specimens were then polished for 18 minutes using Buehler Texmet 2000 pad, 6 µm diamond suspension, and a force of 0.5 lbs. The next step consisted of a Buehler Texmet 1000 pad, 1 µm diamond suspension, and a force of 0.3 lbs. The specimen was polished for 42 minutes in this segment. Lastly, the final polishing step was conducted for 10 minutes and consisted of a Buehler Microcloth pad, Mastermet suspension, and a force of 0.2 lbs. The times of the polishing steps are approximate because each specimen was a little different. Table 3-2 shows the polishing procedure steps.

Table 3-2. Polishing Procedure

Surface	Abrasive Type/Size	Time (min)	Force (lbs)
Carbimet	SiC 600 grit	6	7
Texmet 2000	6 µm diamond	18	0.5
Texmet 1000	1 µm diamond	42	0.3
Microcloth	Mastermet	10	0.2

3.4.4 Microscopic Analysis.

Upon completion of polishing, the specimens were analyzed with 2 different optical microscopes. They were the Zeiss Stemi SV 11 and the Nikon EPIHOT. Pictures were taken of the specimens at different magnification levels. These micrographs can be seen in Section 4.6 of this report.

The fracture surfaces seen in Figure 3-12 were also analyzed using a Scanning Electron Microscope (SEM). The SEM was a Quanta 200 HV. These micrographs can be seen in Section 4.7 of this report.

IV. Results and Discussion

This chapter begins by discussing the monotonic tension test that was accomplished. It then follows with a discussion of the creep-rupture tests. Next, the fatigue test data is explained. The combination (creep-rupture and fatigue) tests are then compared to the actual creep-rupture and fatigue data. After this, combined results of all the tests are briefly mentioned. Lastly, the microscopic analysis of the C/SiC samples is discussed.

4.1 Monotonic Tension Test

The Ultimate Tensile Strength (UTS) at 550°C measured from the monotonic tension test was observed to be 487 MPa. This value is comparable to the room temperature UTSs observed in other studies. For example, Staehler et al. (14) observed the UTS at room temperature to be 493 MPa, while Shuler et al. (26) and Effinger et al. (23) reported 420 MPa and 530 MPa respectively. As a result, an elevated temperature of 550°C has very little effect on the UTS of a C/SiC composite. At 550°C the monotonic strain at failure in this study was observed to be 0.92%. Staehler et al. (14) reported a strain at failure for a monotonic tension test at room temperature to be 1.2% to 1.3%.

The stress-strain curve from the monotonic tension test conducted in this study is shown in Figure 4-1. This figure shows that there is neither a linear elastic region nor a distinct knee in the stress-strain curve for the 550°C monotonic tension data. The 550ºC curve is also consistent with the room temperature stress-strain curve in Figure 4-1.

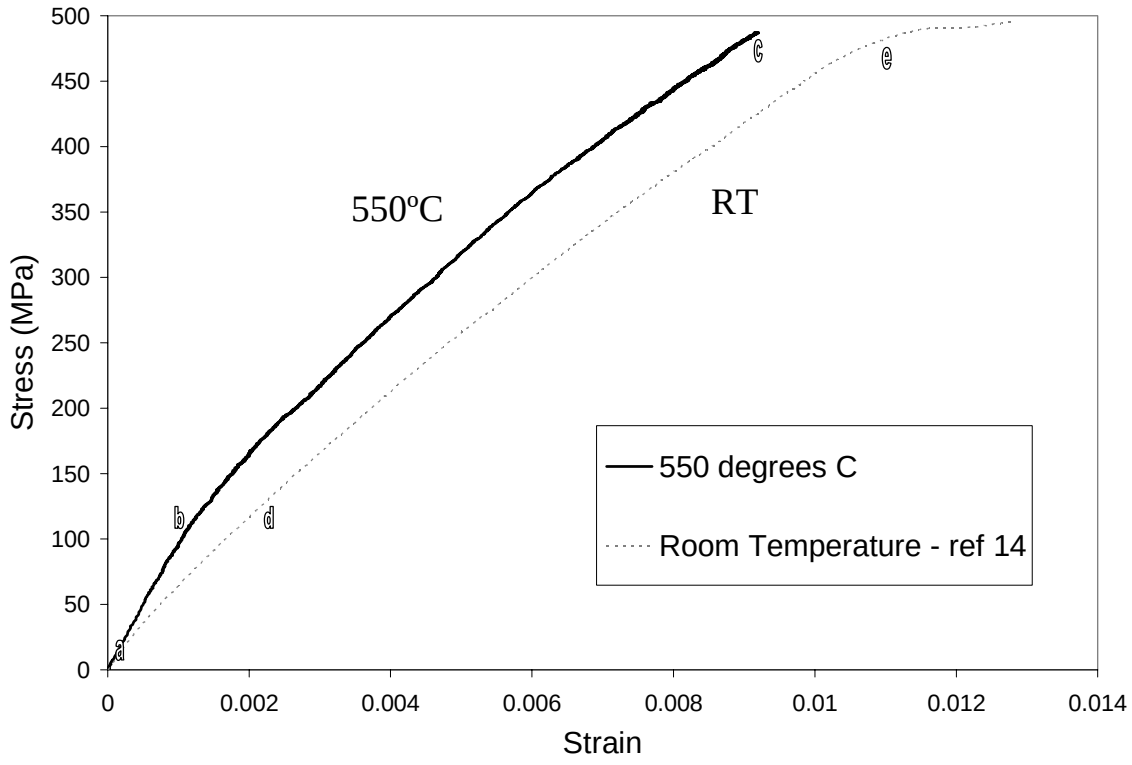

Figure 4-1. Stress-Strain Curve for Monotonic Tension Test at 550°C

When a straight line is fit to the 550°C stress-strain curve from point (a) to (b) and then from point (b) to (c), the Modulus of Elasticity is found to be 96.6 GPa and 46.0 GPa respectively. Staehler's (14) modulus of elasticity at room temperature from point (a) to (d) and from (d) to (e) is 61.4 GPa and 41.3 GPa respectively. The high initial modulus value for the 550°C data is due to the steep slope at the beginning of the stress-strain curve. This steep slope could be caused by the expansion of the composite during the initial heating time. This would then cause the composite not to expand or stretch as much during initial monotonic tension loading. However, the stress-strain curves are very similar and almost parallel each other after the initial loading period.

There is similarity in the UTS, the strain at failure, and the modulus of elasticity of a 550°C and a room temperature monotonic tensile test. The values at 550°C are very close to those of room temperature. Therefore, an elevated temperature of 550°C has very little or no effect on the UTS, the strain at failure, and the modulus of elasticity when monotonic tension loading is applied at a displacement rate of 0.05 mm/second. However, if the displacement rate were lowered significantly then oxidation of the carbon fibers within the C/SiC composite might have an effect on the results. The oxygen in the air would have more time to creep into the matrix cracks and oxidize with the carbon fibers. Oxidation would then cause the UTS and the strain at failure to lower.

4.2 Creep-Rupture Tests

The three creep-rupture tests in this study were accomplished at 105 MPa, 175 MPa, and 350 MPa. Table 4-1, Figure 4-2, and Figure 4-3 summarize the creep-rupture tests performed and also some creep-rupture tests performed by Verilli et al. (2).

Table 4-1. Creep-Rupture Results

Specimen Number	Stress (MPa)	Type of Loading	Temperature (°C)	Time to Failure (hours)	Strain at Failure (%)	Modulus during Loading (GPa)
02-314	105	Creep	550	10.59	0.20	96.1
02-303	175	Creep	550	1.68	0.51	66.4
02-326	350	Creep	550	0.43	1.02	57.3
Verrilli	70	Creep	550	24.23	N/A	N/A
Verrilli	105	Creep	550	18.28	N/A	N/A
Verrilli	175	Creep	550	1.53	N/A	N/A

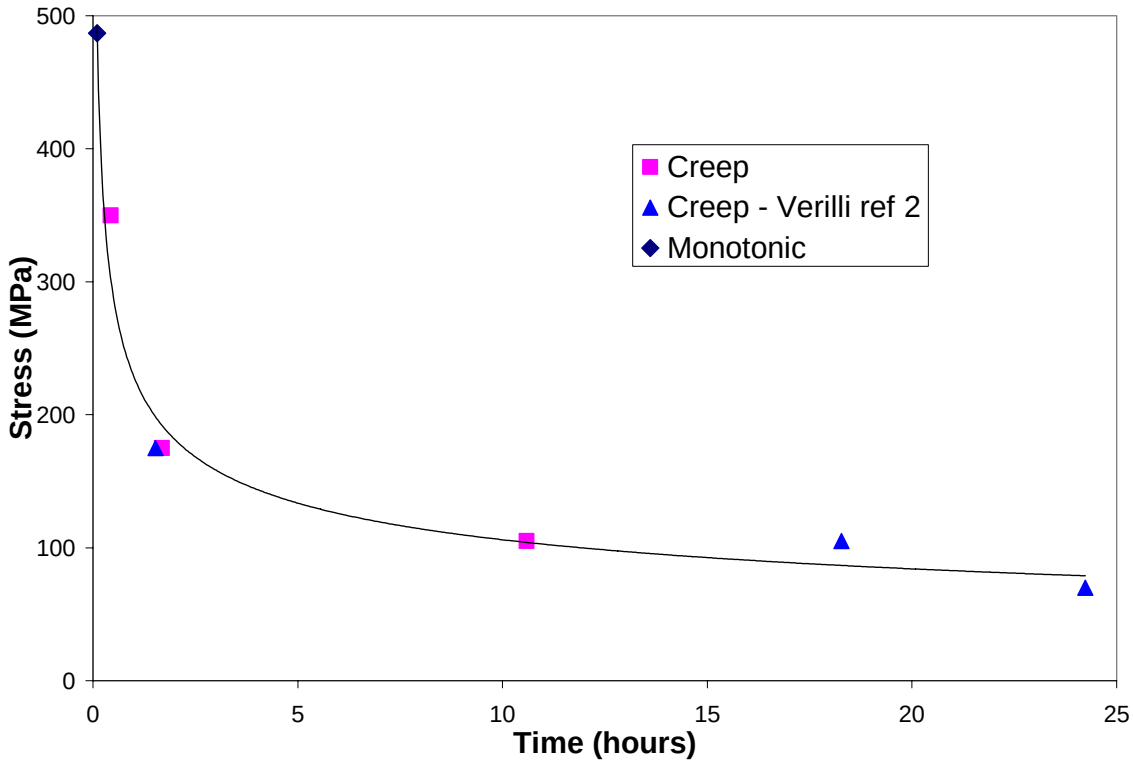

Figure 4-2. Maximum Stress vs. Time to Failure of Creep-Rupture Tests

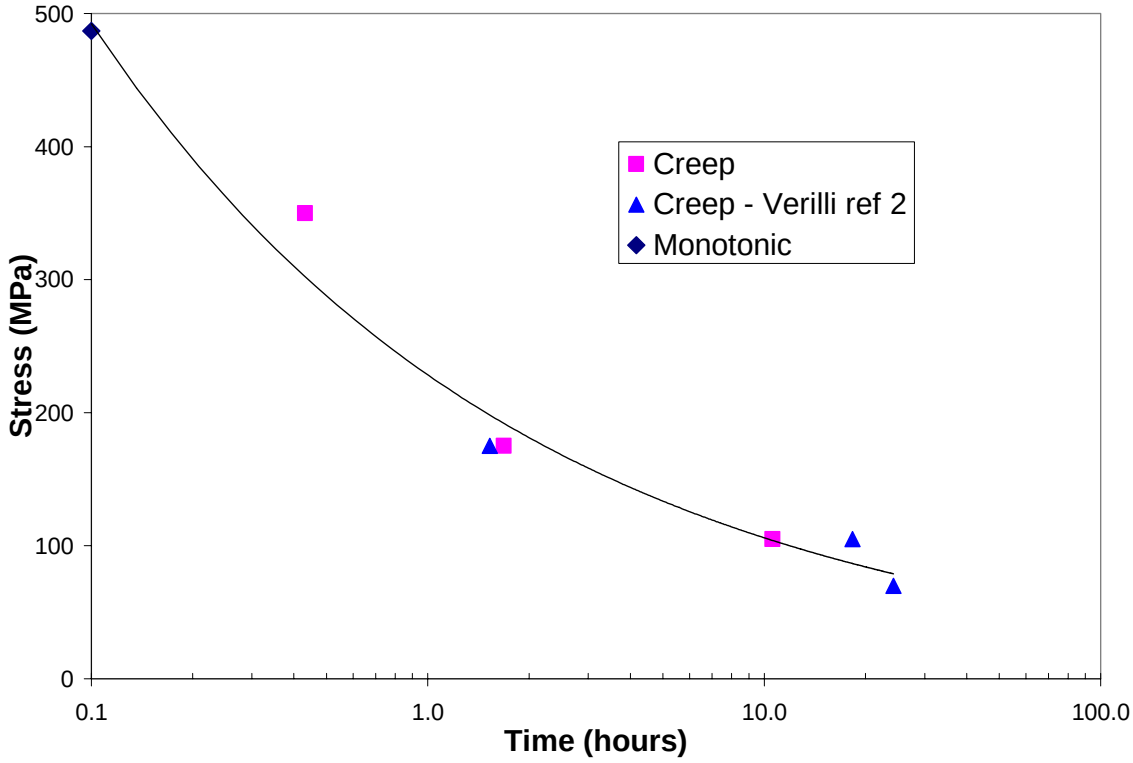

Figure 4-3. Maximum Stress vs. Time to Failure of Creep-Rupture Tests (log scale)

As can be seen from Table 4-2, creep-rupture lives of the specimens in this research effort were less than 11 hours at 105 MPa despite the fact that the UTS of C/SiC is around 500 MPa. The short life of the specimens is due to the oxidation of the carbon fibers within the C/SiC composite. This carbon fiber oxidation effect will be discussed in sections 4.6 and 4.7. In Figure 4-2 and Figure 4-3 there is practically no difference in the data of this study and Verilli's (2), rather the data from both studies fall within a reasonable scatter band. The slight variation in the results could be attributed to different seal coating methods, slight differences in manufacturing techniques, or the large plate-to-plate variations of the manufactured C/SiC material (6-447). The variation could also occur because of differences in experimental techniques. However, it appears as though the results of the 3 creep-rupture tests performed in this study and the 3 performed in Verilli's (2) study are statistically similar enough to add the same trend lines to the data in Figure 4-2 and Figure 4-3.

Figure 4-4 shows the strain as a function of time for the 3 creep-rupture tests. It is interesting to note that as the creep-rupture stress is decreased, the strain at failure also decreases. The higher stress tests are able to elongate more than the lower stress tests. Once again, this is caused by oxidation of the carbon fibers. The longer the specimen is stressed, the more time oxygen has to react with the carbon fibers within the composite. Thus we see the 105 MPa creep-rupture test lasting 10.59 hours and only elongating 0.20%, while the 350 MPa creep test lasts only 0.43 hours and elongates 1.02%. Oxidation of the carbon fibers is also evident when comparing the strain the C/SiC underwent after reaching the creep-rupture stress. The 105 MPa sample only

elongated 0.09% after reaching 105 MPa, while the 175 MPa and 350 MPa samples elongated 0.25% and 0.41% respectively after reaching 175 MPa and 350 MPa.

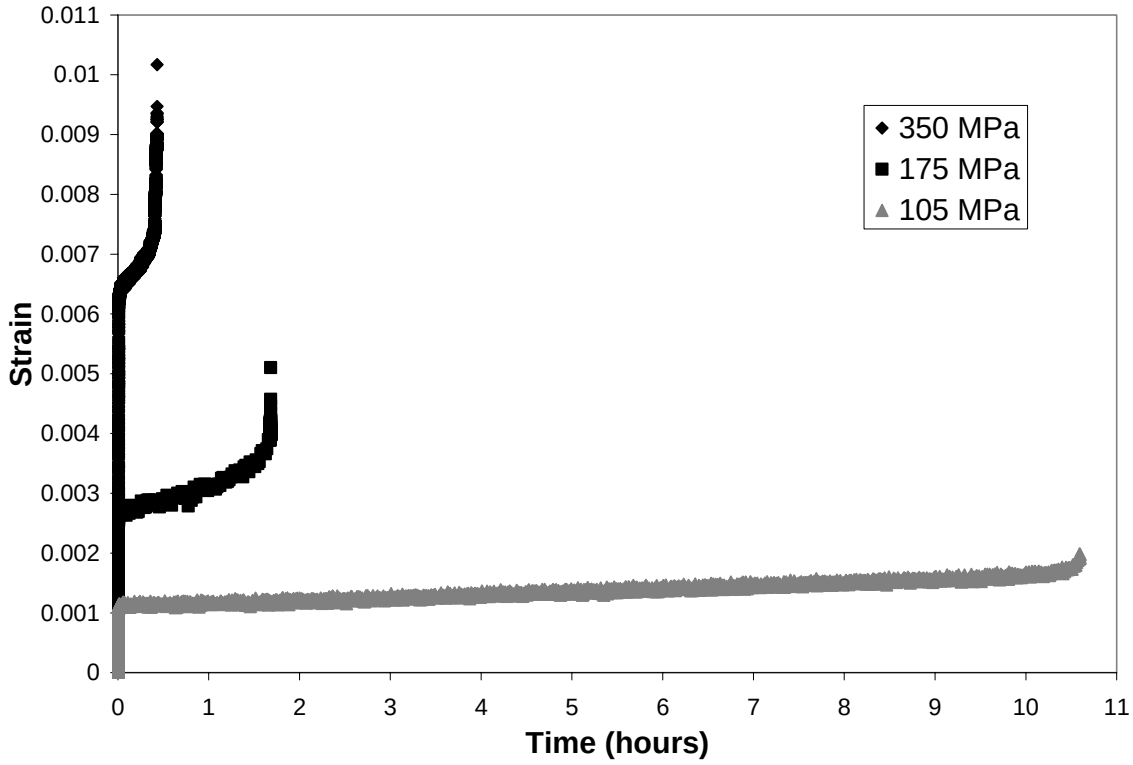

Figure 4-4. Strain vs. Time for the Three Creep-Rupture Tests

A rough estimate of the modulus of elasticity can also be determined during the initial loading to the creep stress. This rough estimate is simply the secant modulus of the data in Figure 4-5. Figure 4-5 displays the stress-strain curve during the 10 MPa/second loading period for the creep-rupture stresses of 350 MPa, 175 MPa, and 105 MPa.

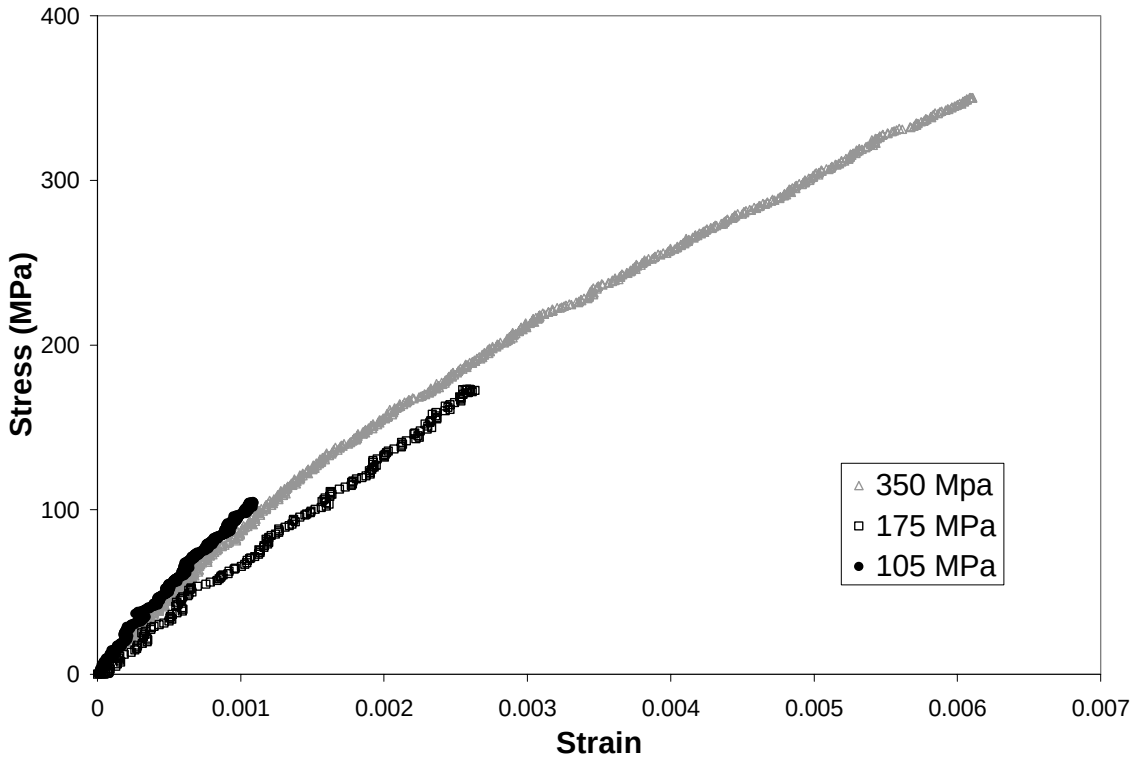

Figure 4-5. Stress vs. Strain - During Initial Ramp Period for Three Creep-Rupture Tests

The secant modulus values estimated from the initial loading to creep stress were 57.3 GPa, 66.4 GPa, and 96.1 GPa for the creep loads of 350 MPa, 175 MPa, and 105 MPa respectively. These values are consistent with the monotonic test shown in Figure 4-1. They fall between the two modulus values of 96.6 GPa and 46.0 GPa representing the modulus values from point (a) to point (b) and from (b) to (c) in Figure 4-1. They are also similar to the secant modulus values of the monotonic test at various loads. The secant modulus values obtained from the monotonic test in Figure 4-1 at loads of 350 MPa, 175 MPa, and 105 MPa were 61.8 GPa, 81.2 GPa, and 97.0 GPa respectively. The stress-strain curves of the creep-rupture tests and the monotonic test begin similarly, but they do not reach the part where the monotonic tension stress-strain curve begins to

flatten out. The 175 MPa and 105 MPa creep tests have higher modulus values than the 350 MPa creep test because they don't go to a high enough stress. The 175 MPa and the 105 MPa stress-strain curves stop at the steeper portion of the stress-strain curve for C/SiC shown in Figure 4-1.

4.3 Fatigue Tests

The seventeen fatigue tests conducted in this study were accomplished at 0.1 Hz, 1 Hz, 10 Hz, and 375 Hz. Strain could not be measured during the 10 Hz and 375 Hz tests. Table 4-2 summarizes the fatigue test results as well as three low cycle fatigue tests accomplished by Verilli et al. (2) at 0.033 Hz.

Maximum stress versus cycles to failure (S-N) curves were developed from the data of the fatigue results performed in this experiment and Verrilli's (2) low cycle fatigue tests. The S-N curves shown in Figure 4-6(a) and Figure 4-6(b) are expressed as the applied maximum stress versus cycles to failure for the five different frequencies. Figure 4-6(a) displays the data conducted in this research effort, and Figure 4-6(b) adds Verilli's (2) data. The S-N curves of the data in this study are very consistent. Verilli's 0.033 Hz curve in Figure 4-6(b) is either inconsistent with the other S-N curves or there is a limiting effect of frequency on fatigue behavior. Further, the variation in the results from the present study and Verilli's (2) study could be attributed to different seal coating methods, slight differences in manufacturing techniques, or the large plate-to-plate variations of the manufactured C/SiC material (6-447).

Table 4-2. Fatigue Test Results

Specimen Number	Max Stress (Mpa)	Frequency (Hz)	Temperature (°C)	Time to Failure (hrs)	Cycles to Failure	Strain at Failure (%)
02-315	105	0.1	550	13.09	4,701	0.43%
02-312	175	0.1	550	3.77	1,353	0.55%
02-318	275	0.1	550	1.45	522	0.66%
02-325	350	0.1	550	0.59	212	0.82%
02-310	175	1	550	3.13	10,977	0.52%
02-320	105	10	550	19.84	575,607	N/A
02-327	175	10	550	4.62	136,163	N/A
02-319	275	10	550	0.87	24,873	N/A
02-321	350	10	550	0.22	6,376	N/A
*02-304	175	375	550	55.75	75,265,164	N/A
*02-307	275	375	550	11.57	15,624,760	N/A
*02-269	325	375	550	1.07	1,450,276	N/A
*02-272	375	375	550	0.14	188,132	N/A
*02-272	400	375	550	0.24	318,880	N/A
*02-271	425	375	550	0.23	313,976	N/A
*02-305	500	375	550	0.13	179,448	N/A
*02-306	500	375	550	0.005	11,152	N/A
Verilli	70	0.033	550	32.33	3,924	N/A
Verilli	105	0.033	550	34.03	4,015	N/A
Verilli	175	0.033	550	16.83	1,980	N/A

* Test Performed at AF Research Lab Materials Directorate, WPAFB

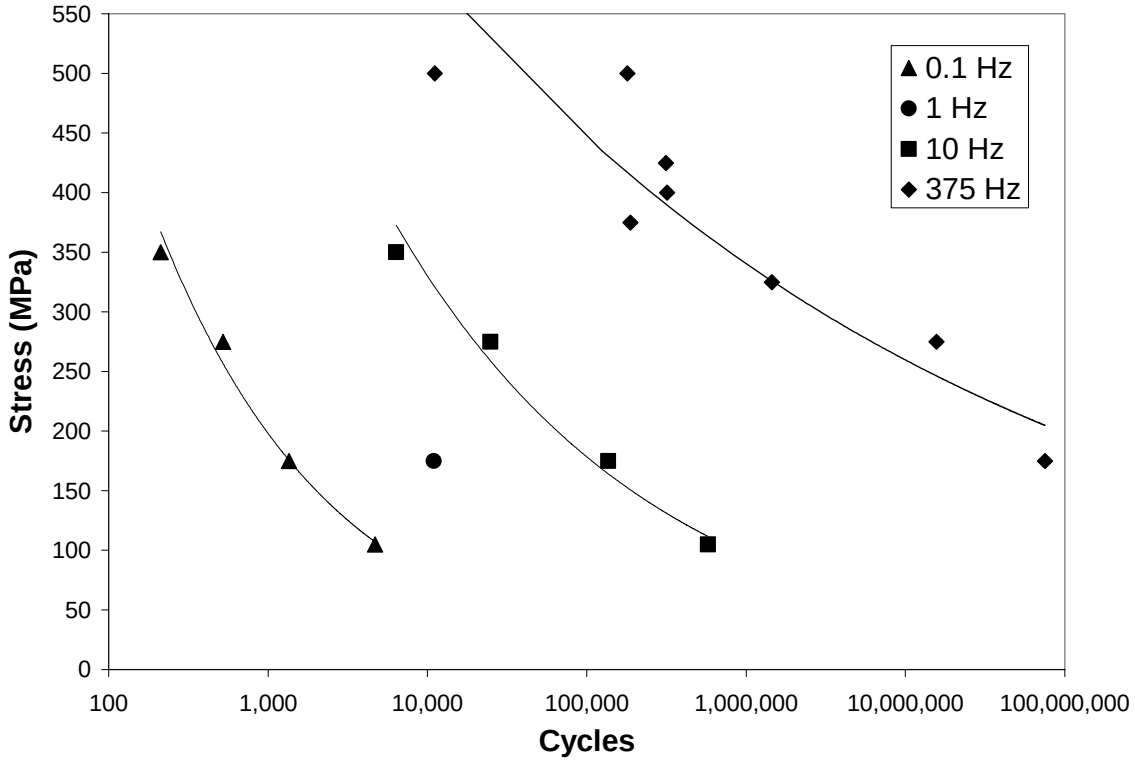

Figure 4-6(a). S-N Curve for Fatigue Tests at 550°C

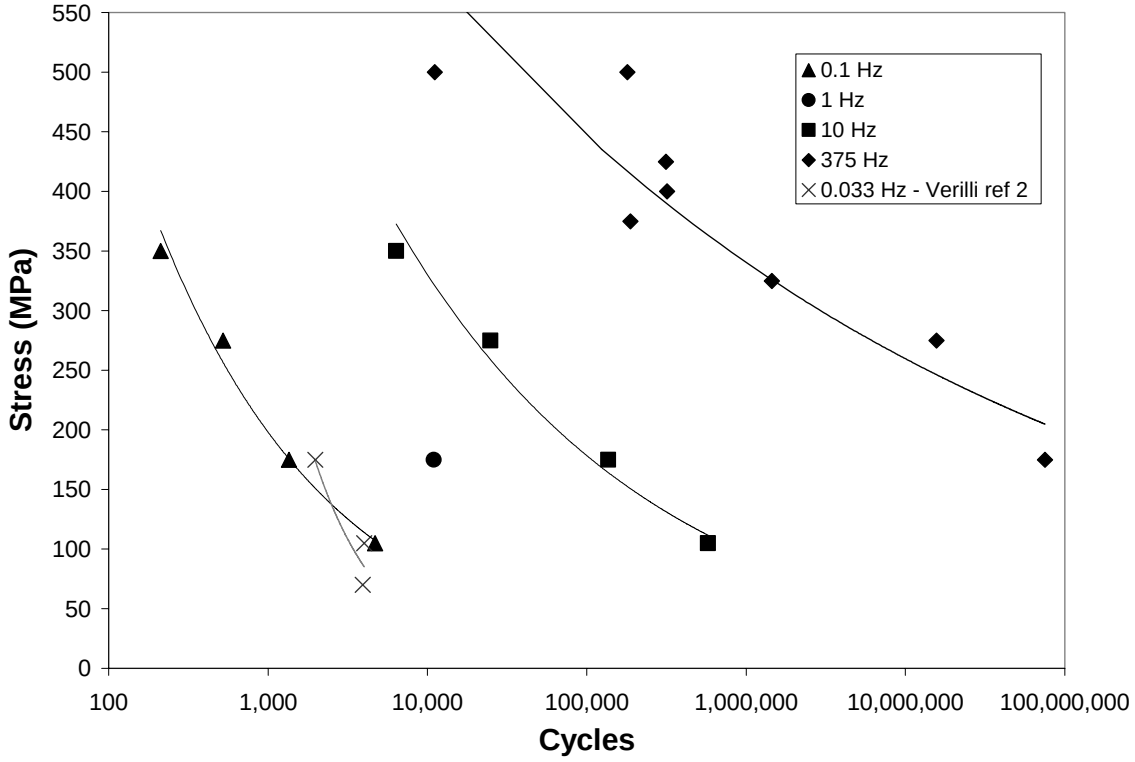

Figure 4-6(b). S-N Curve for Fatigue Tests at 550ºC – Verilli's(2) data added

The S-N curves in Figure 4-6(a) and Figure 4-6(b) indicate that there is an increase in cycles to failure as the frequency is increased at 550°C. For instance, at a maximum applied stress of 175 MPa, the cycles to failure of 0.1 Hz and 375 Hz are 1353 and 75,265,164 cycles respectively. This is the opposite of the room temperature results reported by Staehler et al.(14). In their research, they found that there was a reduction in cycles to failure as frequency is increased at room temperature. The difference in results is due to the oxidation of the carbon fibers in the C/SiC composite at 550°C. At lower frequencies, air is allowed to penetrate the matrix cracks and react with the carbon fibers.

According to Verilli et al. (2), life of the C/SiC composite is more dependent on time at the elevated temperature rather than number of cycles at elevated temperature because of oxidation. Thus a plot of maximum applied stress versus time to failure is given in Figure 4-7 and Figure 4-8 for the given frequencies.

In Figure 4-7 and Figure 4-8 we see that at the higher applied stresses greater than 350 MPa, frequency of fatigue does not play a role in composite life. The data converges at high fatigue stresses. However, at fatigue stresses lower than 350 MPa, the slopes of the frequency data (0.1 Hz, 10 Hz, and 375 Hz) in Figure 4-8 are decreasing as the frequency increases and the higher the frequency data have greater values than the lower frequency data. In short, at 175 MPa, the 375 Hz sample has a longer time life than the 10 Hz sample, and the 10 Hz sample has a longer time life than the 0.1 Hz sample. This is very interesting because it means that oxidation of the carbon fibers within the composite is reduced when frequency of fatigue is increased. At high frequencies, C/SiC composites have longer fatigue lives and time lives than at low frequencies. This phenomenon is hard to explain and could occur because of a number of different reasons.

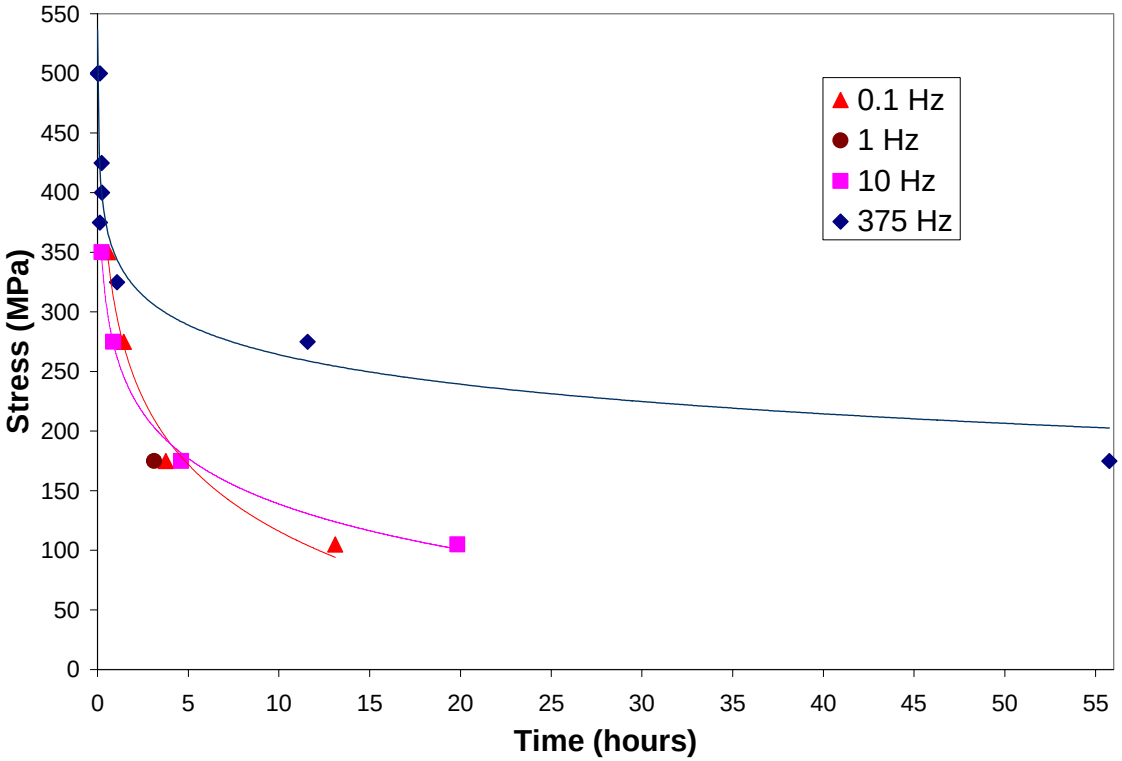

Figure 4-7. Maximum Stress vs. Time to Failure for Fatigue Tests

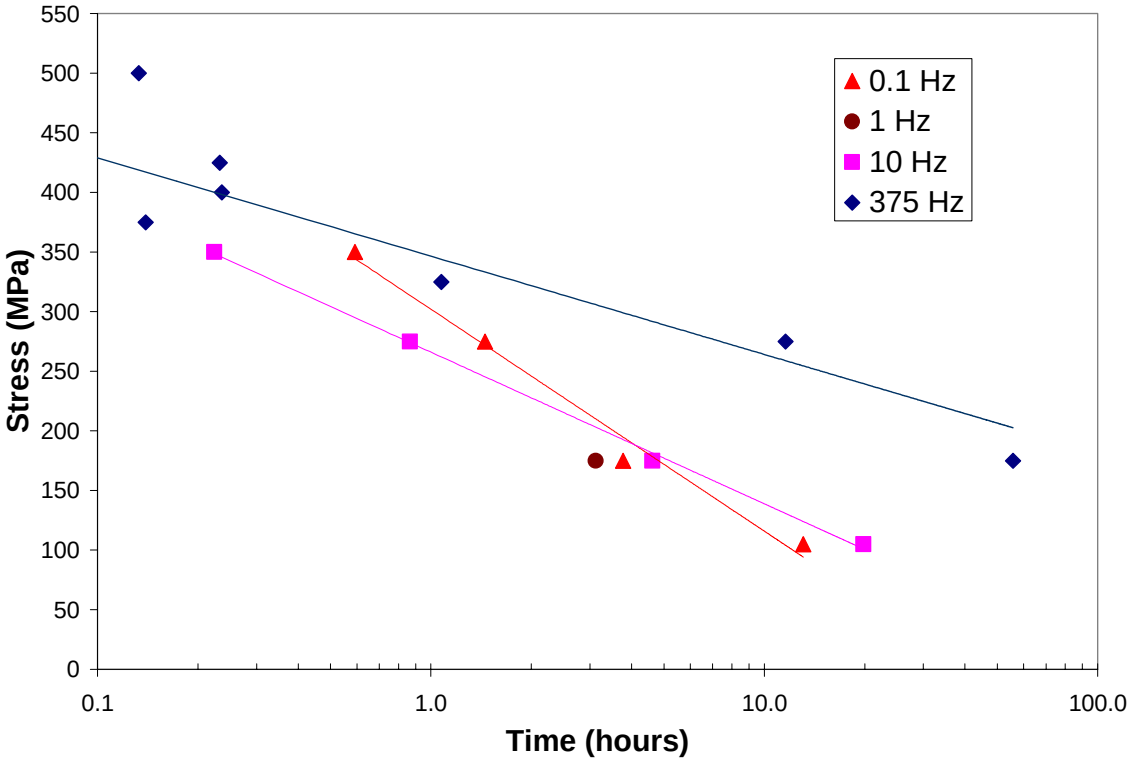

Figure 4-8. Maximum Stress vs. Time to Failure for Fatigue Tests – Log Scale

One possible explanation is that because of the high frequency, there is a lot of internal friction between the fibers and the matrix. This internal friction causes an increase in surface temperature and the internal temperature of the composite (14:10). It is possible that the internal temperature could increase enough that oxidation would be inhibited. The micro-cracks within the matrix begin to close as the temperature of the sample approaches the approximate processing temperature of 1100°C (4:8). At this processing temperature, the thermal expansion of the carbon fibers and the SiC matrix are matched, which in turn causes the crack edges to come together and stop the seeping of oxygen into the composite. Another explanation is the possible formation of a silica scale (SiO_2) within the C/SiC composite. This growth of silica scale occurs as the SiC matrix oxidizes. The silica scale helps to fill in matrix cracks, which seal off the fibers from the outside air (4:8). The presence of oxidation within C/SiC is drastically reduced when this formation occurs.

Stress-strain loops were recorded for the 0.1 Hz and 1 Hz tests. Examples of the stress-strain loops are given for 0.1 Hz (105 MPa), 1 Hz (175 MPa), and 0.1 Hz (350 MPa) in Figures 4-9, 4-10, and 4-11 respectively. Hysteresis can be seen in all of the stress-strain loops. According to Staehler et al. (14), this hysteresis during a fatigue test is caused by friction between the fibers and the matrix along a debonded surface. The weak bond between the carbon fibers and the SiC matrix is considered beneficial under monotonic tensile loading conditions, but has a negative effect during cyclic loading (14:4-5). The negative effect is due to the internal frictional sliding and heating between the fiber and the matrix. Figures 4-9, 4-10, and 4-11 also show that the most dramatic changes in the stress-strain loops occur during the first few cycles and the last few cycles

of the fatigue loading. Dramatic changes in the first few cycles occur because the C/SiC composite begins to experience fiber debonding and an increase in matrix cracks. The changes in the stress-strain loops during the last few cycles occur because the composite is beginning to show signs of failure.

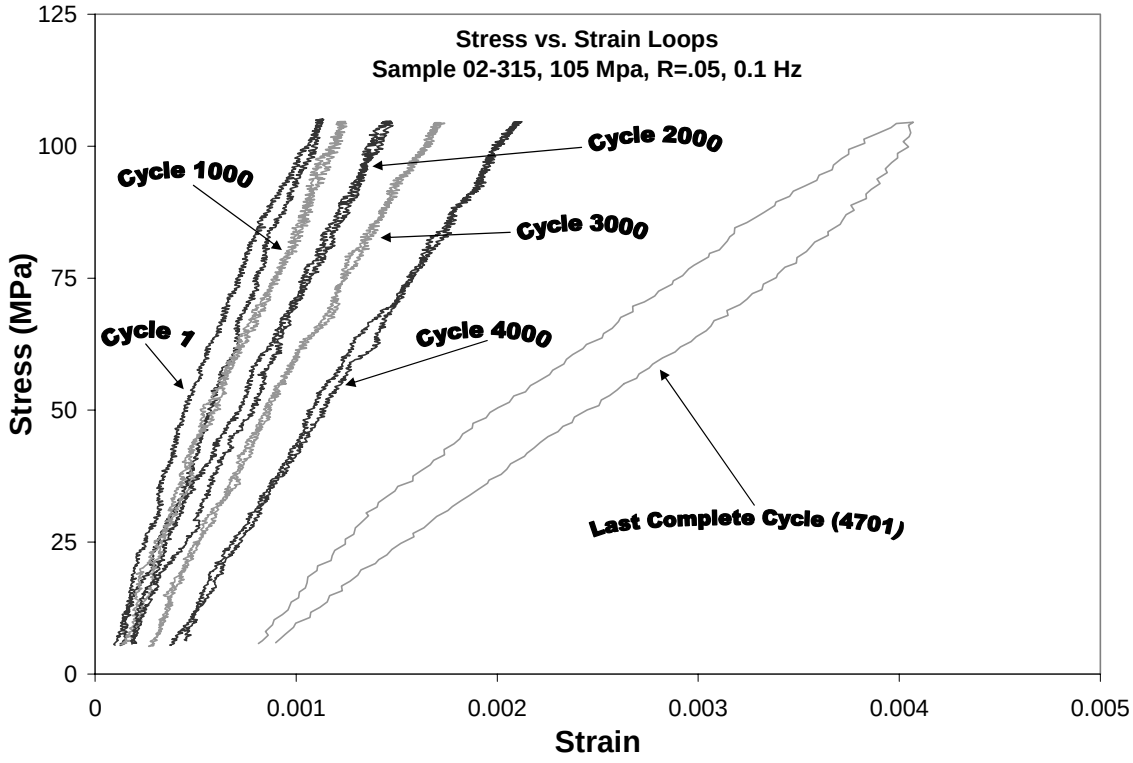

Figure 4-9. Stress-Strain Loop (0.1 Hz, 105 MPa)

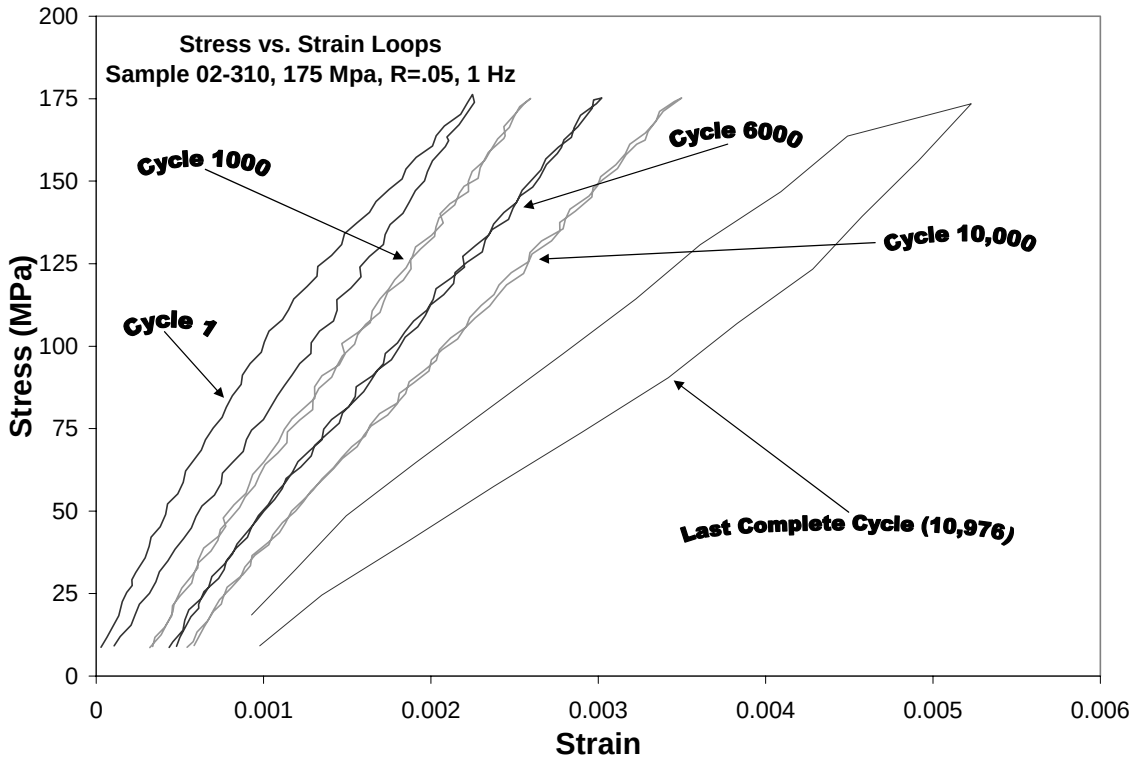

Figure 4-10. Stress-Strain Loop (1 Hz, 175 MPa)

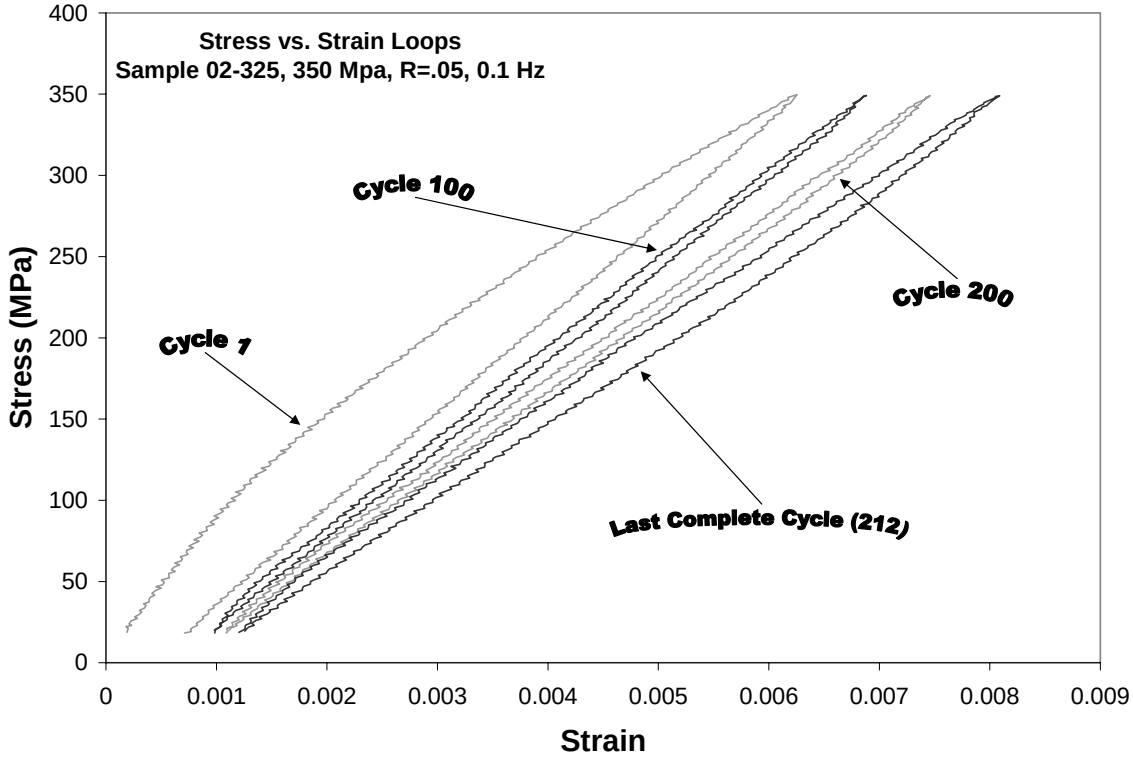

Figure 4-11. Stress-Strain Loop (0.1 Hz, 350 MPa)

The stress-strain loops can also be used to determine the maximum strain during each cycle. This data is plotted so that damage progression can be observed throughout the life of the C/SiC composite. Figure 4-12 and Figure 4-13 show this damage progression by plotting the maximum cycle strain versus cycles and time.

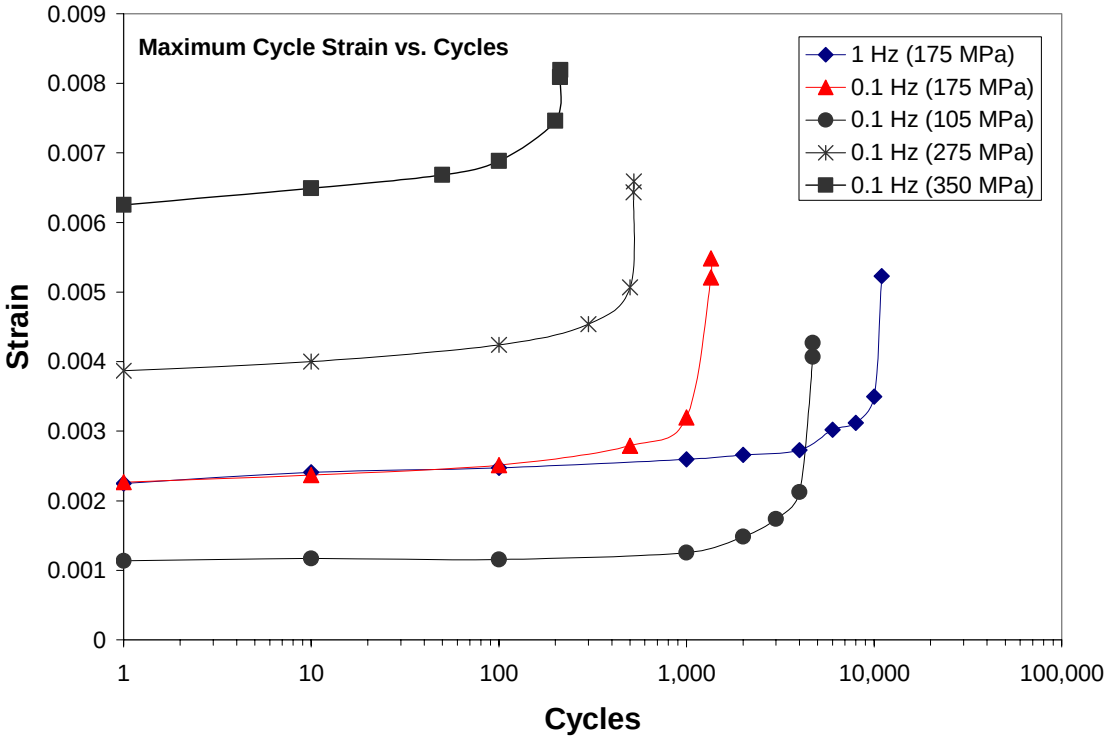

Figure 4-12. Maximum Cycle Strain vs. Cycles at 550°C

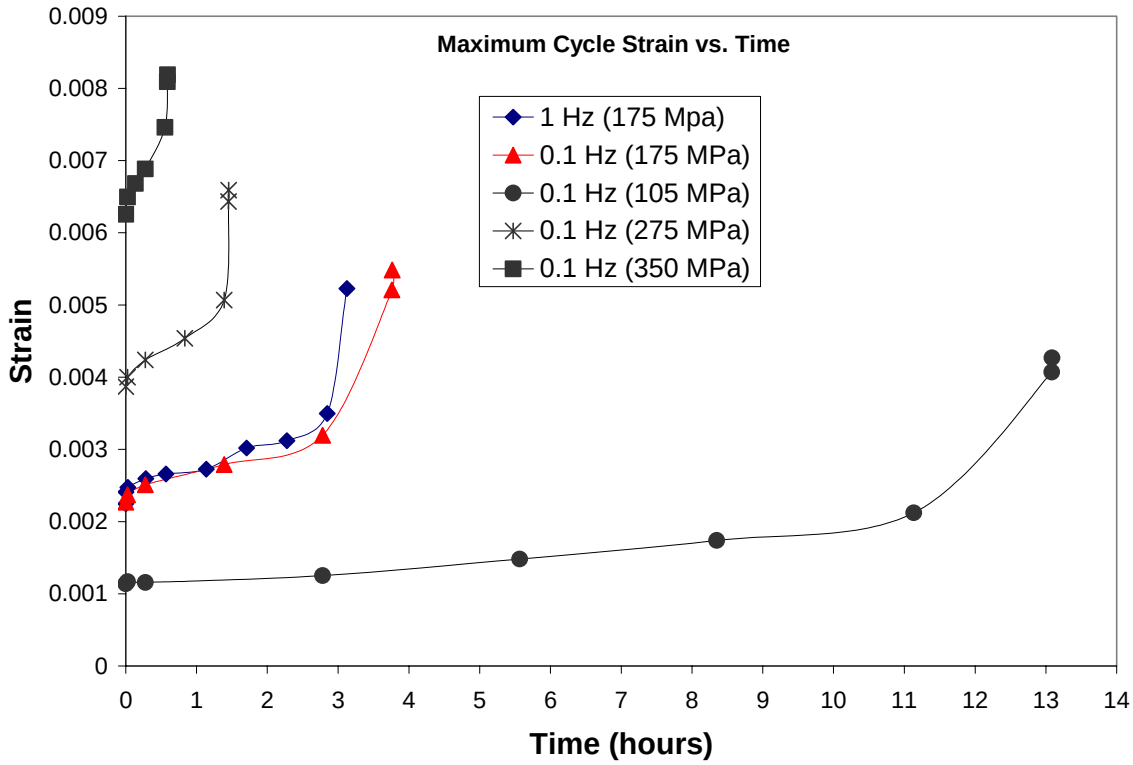

Figure 4-13. Maximum Cycle Strain vs. Time at 550°C

Figure 4-12 and 4-13 demonstrate that the strain of the C/SiC composites appears to be independent of frequency. The sample tested at 1 Hz data and 175 MPa lasted 3.13 hours and had a strain at failure of 0.52%. The sample tested at 0.1 Hz and 175 MPa lasted 3.77 hours and had a strain at failure of 0.55%. These values are very comparable. The data of the 1 Hz and 0.1 Hz samples displayed in Figure 4-13 also shows that curves of these two samples are very similar. However, when looking at the cycles to failure, there is great disparity. The 1 Hz sample failed at 10,977 cycles, whereas, the 0.1 Hz sample failed at 1353 cycles. This disparity is shown in Figure 4-12. Therefore, the maximum cycle strain is not dependent on cycles, but more dependent on the time the sample is exposed to the temperature of 550°C.

The difference in maximum cycle strain from the first cycle to the last cycle can also be calculated from Figure 4-12. For the 0.1 Hz tests conducted at 350 MPa, 275 MPa, 175 MPa, and 105 MPa the differences were 0.19%, 0.27%, 0.32% and 0.31% respectively. This upward trend is due to C/SiC becoming less stiff as the carbon fibers are oxidized. This stiffness can be determined from the secant modulus data described next.

Modulus of Elasticity values can be estimated from the stress-strain loops by computing the secant modulus. This provides information about the degradation of C/SiC during cycling. The secant modulus data can then be plotted as a function of cycles, time, and life fraction. These graphs are shown in Figures 4-14, 4-15, and 4-16. The three secant modulus graphs (Figure 4-14, Figure 4-15, and Figure 4-16) definitely show that there is a degradation in modulus values as the composite undergoes fatigue loading. Rapid degradation occurs after 100 cycles for the 0.1 Hz samples and after 1000 cycles for the 1 Hz sample as seen in Figure 4-14. As expected, secant modulus values of the low stress fatigue samples (105 MPa and 175 MPa) have higher modulus values than the high stress fatigue samples (275 MPa and 350 MPa) during the beginning of fatigue loading. However, at the end of their fatigue lives, the low stress fatigue samples have lower modulus values than the high stress fatigue samples. For example, during sample life secant modulus is reduced from 96.6 GPa to 24.6 GPa for the 0.1 Hz (105 MPa) sample and from only 96.6 GPa to 42.7 GPa for the 0.1 Hz (350 MPa) sample. This can be seen in Figure 4-14, 4-15, and 4-16. It occurs because at low stress fatigue (105 MPa and 175 MPa), the samples are equally stiff at the beginning of loading. As time goes on, oxidation occurs which makes the composite less stiff. Thus the modulus of elasticity

begins to drop rapidly. The high stressed fatigue samples (275 MPa and 350 MPa) maintain their original stiffness because oxidation does not occur to a great extent within these samples. Thus, modulus degradation is less in the high stressed fatigue samples and more in the low stressed fatigue samples.

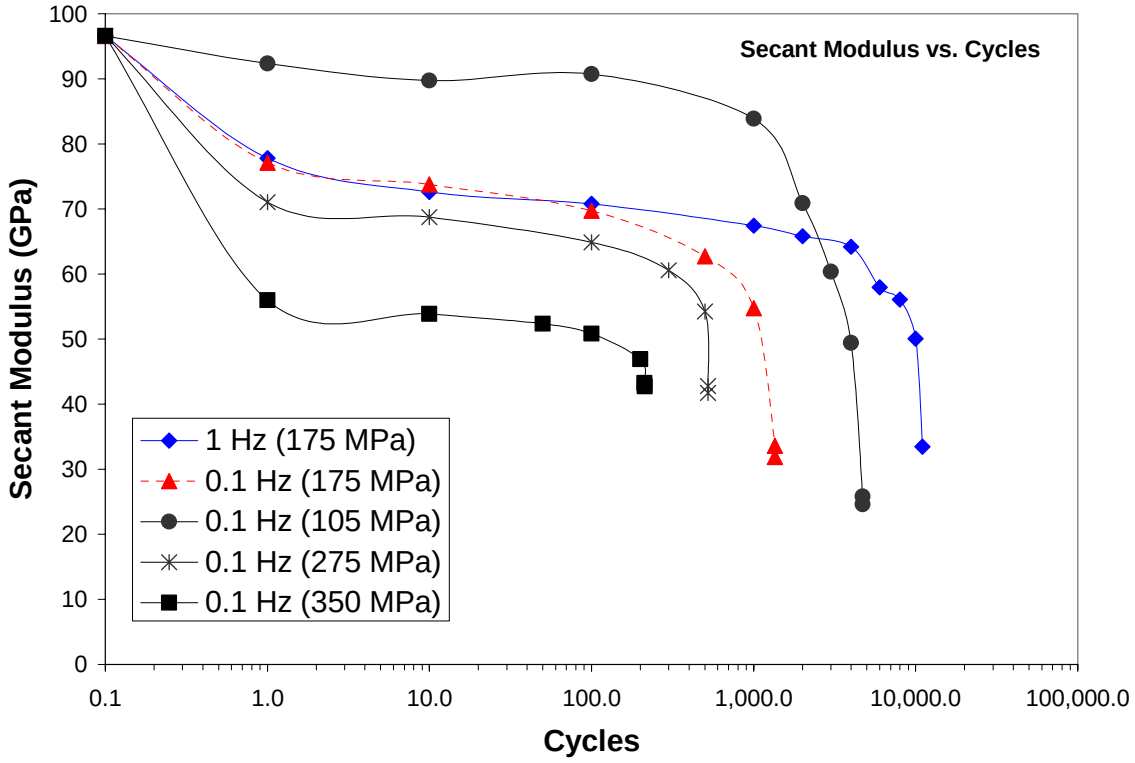

Figure 4-14. Secant Modulus vs. Cycles at 550°C

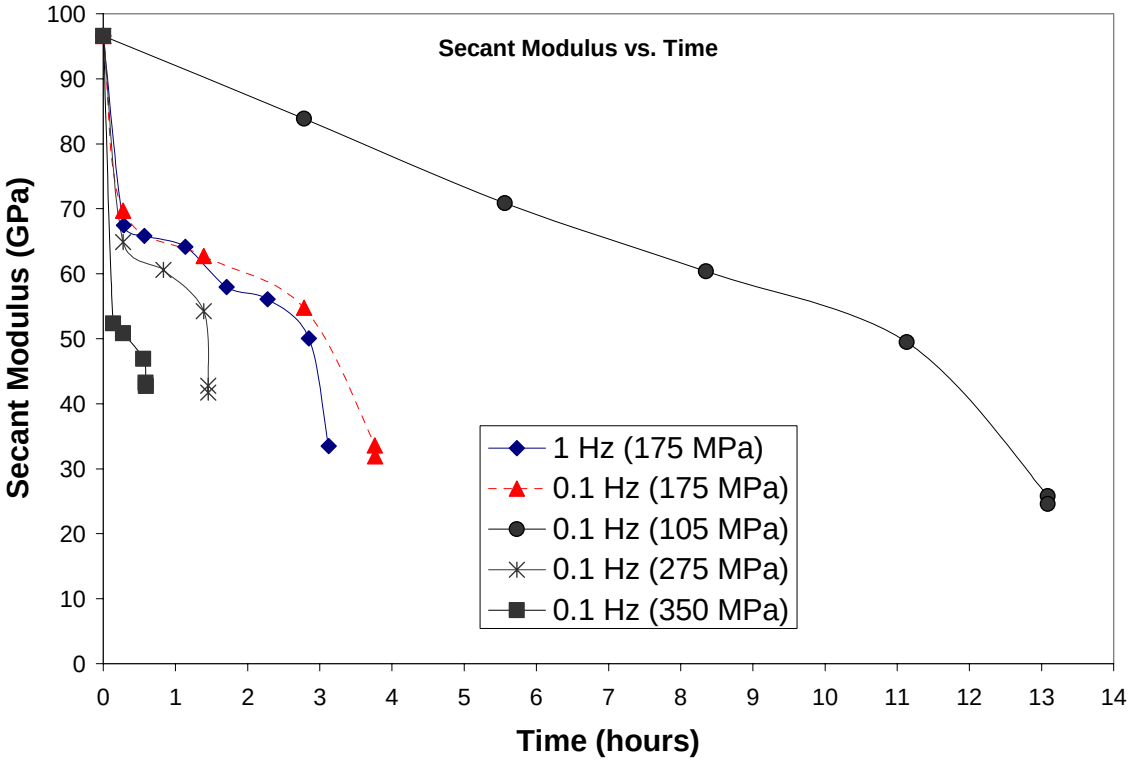

Figure 4-15. Secant Modulus vs. Time at 550°C

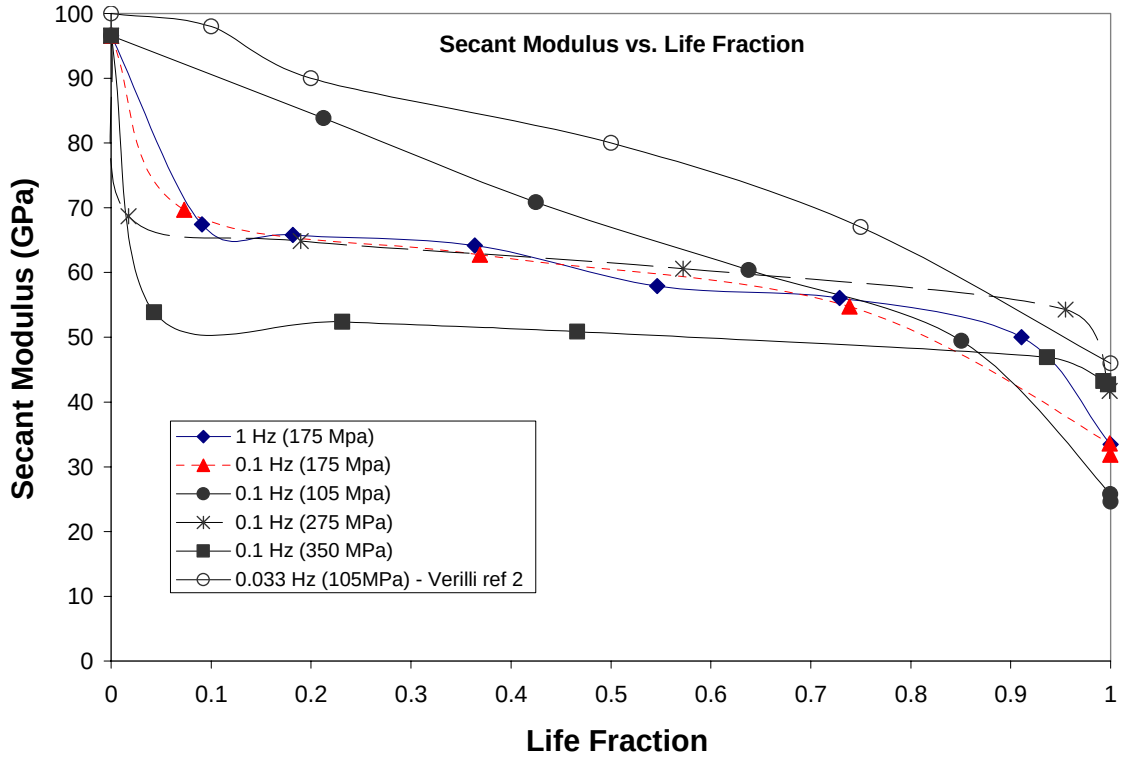

Figure 4-16. Secant Modulus vs. Life Fraction at 550°C

4.4 Combination (Creep-Rupture and Fatigue) Tests

The three combination tests were performed to compare the differences between creep-rupture tests and fatigue tests. Recall from chapter 3 that these combination tests were fatigue tests with a specified hold time at the maximum stress. The hold time was 5 seconds for the 1 Hz test at 175 MPa. For the two 0.1 Hz tests conducted at 175 MPa and 105 MPa the hold time was 50 seconds. Three similar fatigue tests and two creep-rupture tests were compared to the three combination tests. Table 4-3 displays the results of the combination tests, the creep-rupture, and the fatigue tests that were compared.

Table 4-3. Combination (Creep-Rupture and Fatigue) Test Results

Specimen Number	Max Stress (Mpa)	Type of Loading	Frequency (Hz)	Hold Time (sec)	Time to Failure (hrs)	Cycles to Failure	Strain at Failure (%)
02-316	105	Combo	0.1	50	8.68	521	0.54%
02-313	175	Combo	0.1	50	2.31	139	0.49%
02-311	175	Combo	1	5	2.01	1203	0.70%
02-315	105	Fatigue	0.1	0	13.09	4701	0.43%
02-312	175	Fatigue	0.1	0	3.77	1,353	0.55%
02-310	175	Fatigue	1	0	3.13	10,977	0.52%
02-314	105	Creep	N/A	until failure	10.59	1	0.20%
02-303	175	Creep	N/A	until failure	1.68	1	0.51%

A straightforward way to compare the combination, creep-rupture, and fatigue data in Table 4-3 is to display a plot of maximum stress versus time to failure. The plot of this data is given in Figure 4-17(a) for the given tests. A bar graph also displays the same data in Figure 4-17(b).

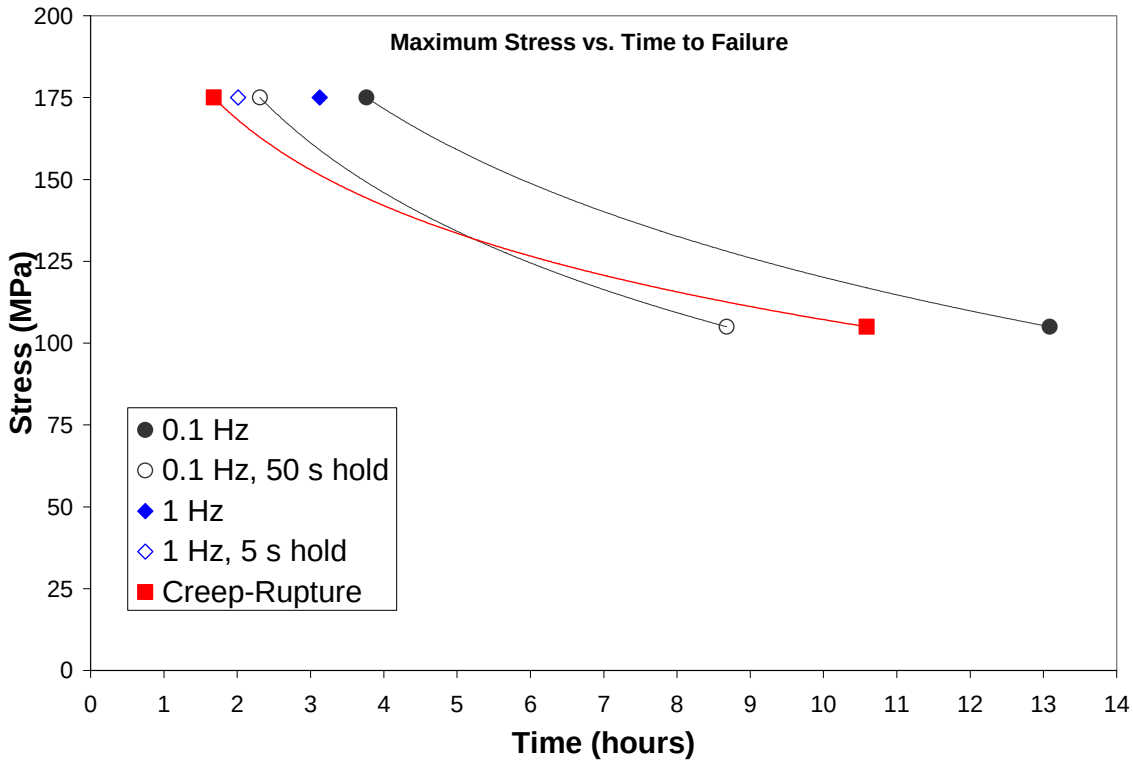

Figure 4-17(a). Maximum Stress vs. Time to Failure of the Tests in Table 4.3

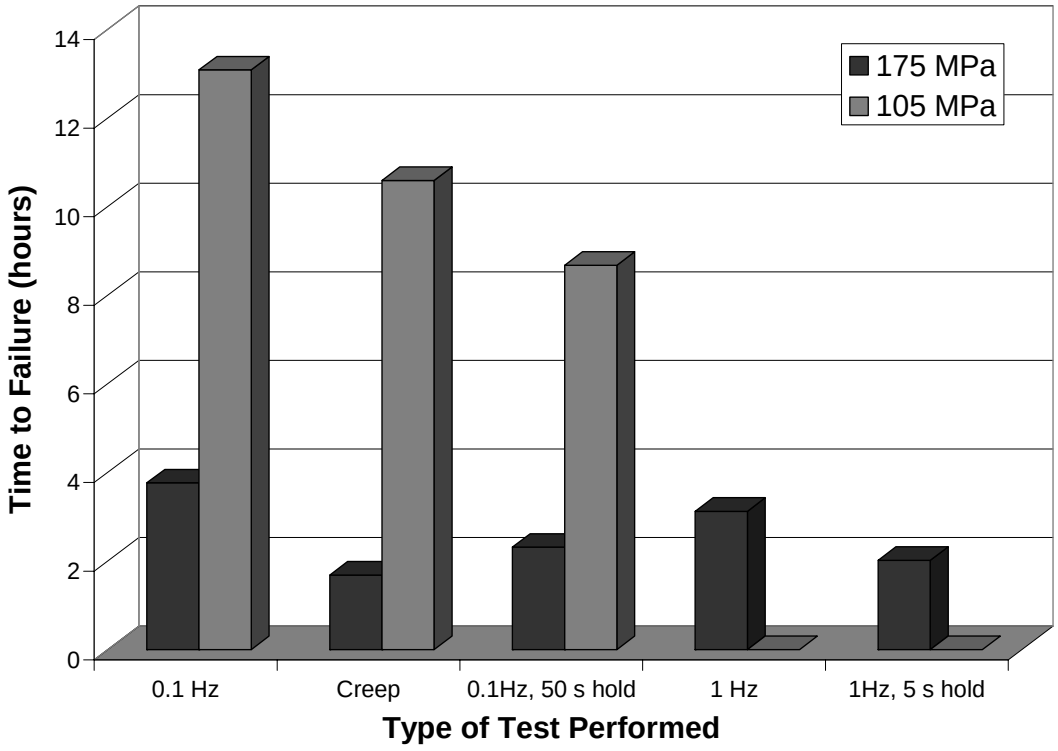

Figure 4-17(b). Bar Graph Displaying Time to Failure of the Tests in Table 4.3

The creep-rupture data in Figure 4-17(a) and Figure 4-17(b) is very interesting. At 175 MPa, the creep-rupture test is the first to fail at 1.68 hours. However, at 105 MPa the creep-rupture life of 10.59 hours falls in between the 0.1 Hz life and the 0.1 Hz (50 second hold) life. It was expected that the creep-rupture sample would be the first to fail at 105 MPa. This data could be explained by experimental variation or it could demonstrate that at low stresses oxidation is not the sole damage mechanism of C/SiC. Fatigue cycle damage does play a role in the overall failure of the composite. If more combination, creep-rupture, and fatigue tests were accomplished at even lower stresses, the primary damage mechanism might become fatigue cycle damage. It is possible that at lower stresses (less than 100 MPa) the creep-rupture tests don't open the matrix cracks enough to allow air to seep into the composite and damage the internal carbon fibers. Oxidation would only occur on the surface if the matrix cracks weren't opened. This would then leave fatigue cycle damage as the primary damage mechanism at low stresses.

An S-N curve was made from the data of the combination tests and the comparative fatigue tests performed in this experiment. The S-N curve shown in Figure 4-18 is expressed as the applied maximum stress versus cycles to failure. Figure 4-18 demonstrates that the primary damage mechanism of the combination tests was indeed oxidation. This is true because the S-N curve of the combination tests for the 0.1 Hz data falls to the left of the S-N fatigue curve. The one data point of the 1 Hz (5 second hold) at 175 MPa also falls to the left of the 1 Hz (175 MPa) data point. This means that when the sample is held for the 5 seconds (1 Hz) or 50 seconds (0.1 Hz) there is more oxidation of the carbon fibers than when undergoing regular fatigue. This occurs because the matrix cracks are held open longer during the combination tests, which allows more

oxygen to enter the C/SiC composite. However, as stated earlier, oxidation is not the sole damage mechanism of C/SiC. There is some fatigue cycle damage that also plays a role in the overall failure of the composite.

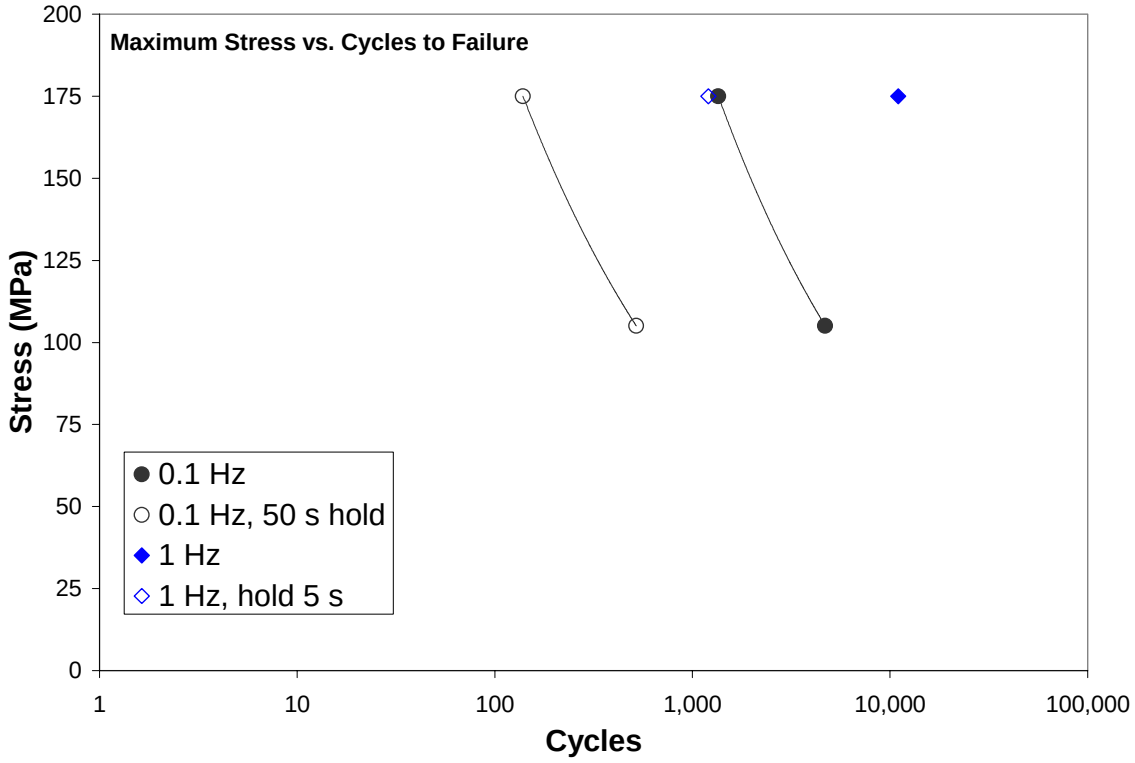

Figure 4-18. S-N Curves of Combination Results and Comparative Fatigue Results

Secant modulus degradation also occurred within the combination tests. Figure 4-19 displays this degradation as a function of life fraction, and is quite similar to Figure 4-16. Degradation of the secant modulus is very evident in the combination tests. The modulus degradation was more evident in the 0.1 Hz (105 MPa) combination sample. It degraded from 96.6 GPa to 19.4 GPa, while the 0.1 Hz (175 MPa) combination sample degraded from 96.6 GPa to 25.1 GPa. This occurs because oxidation makes the composite less stiff

with time. The 0.1 Hz (105 MPa) combination sample and the 0.1 Hz (105 MPa) sample last longer as seen from Figure 4-17. Therefore, they degrade more than the higher stressed samples.

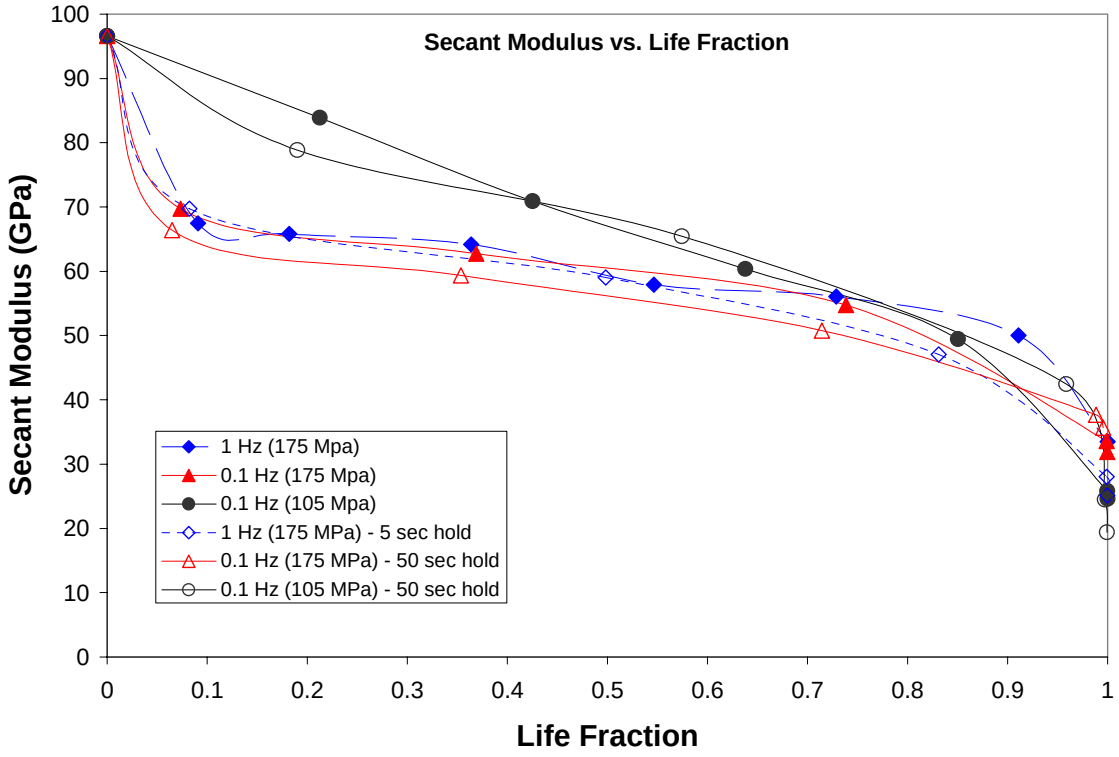

Figure 4-19. Secant Modulus vs. Life Fraction – Combination Tests

The combination test sample strain throughout the life of the composite was also observed. It can be compared to similar fatigue data and is shown in Figure 4-20. The maximum cycle strain data for the combination tests is very similar to that of the fatigue data in Figure 4-20. The data curves look almost identical except for the fact that the combination tests fail before the fatigue tests. One interesting note, however, is that one would expect the combination tests to have a lower strain at failure than the fatigue tests.

This would be expected because the creep-rupture tests at 105 MPa and 175 MPa have lower strain at failure values than the fatigue tests at these same stresses. The strain at failure data for these two creep-rupture tests is shown in Figure 4-20 as well.

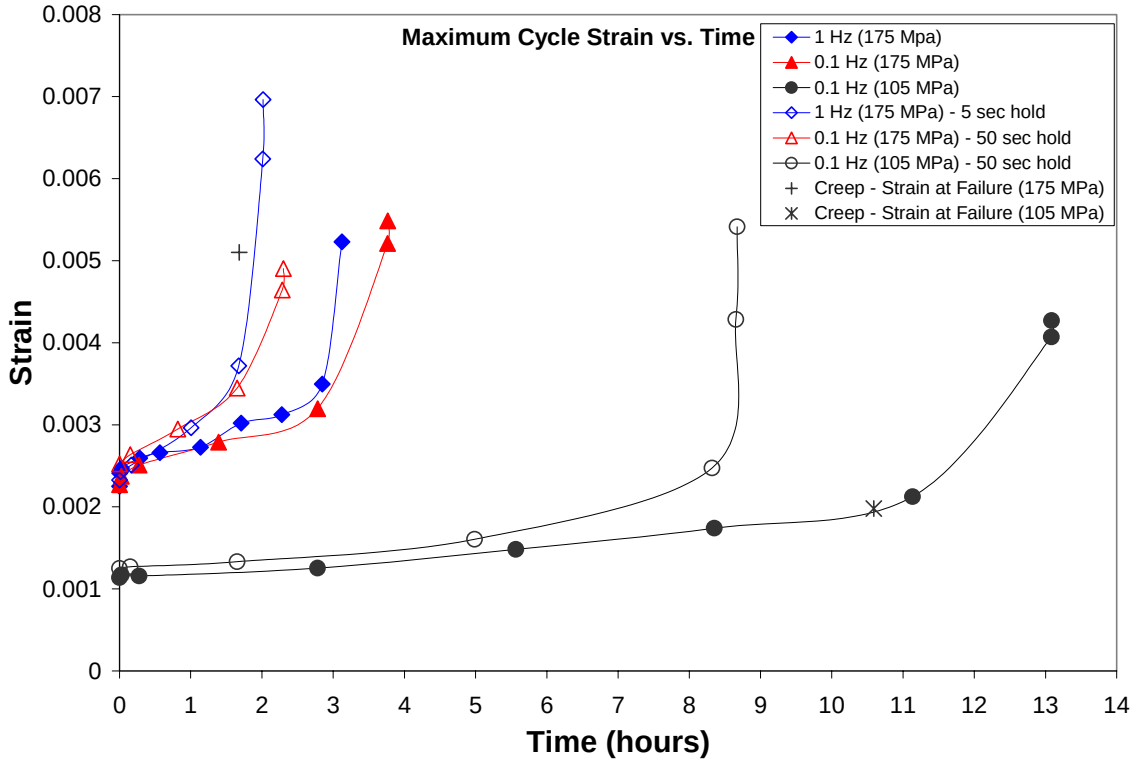

Figure 4-20. Maximum Cycle Strain vs. Time – Combination Tests

4.5 Combined Results

The most straightforward way to combine all of the test results is to display a graph of maximum applied stress versus time to failure. This plot will compare the times to failure of all of the creep-rupture, fatigue, and combination tests at once. Figure 4-21 and 4-22 display this data.

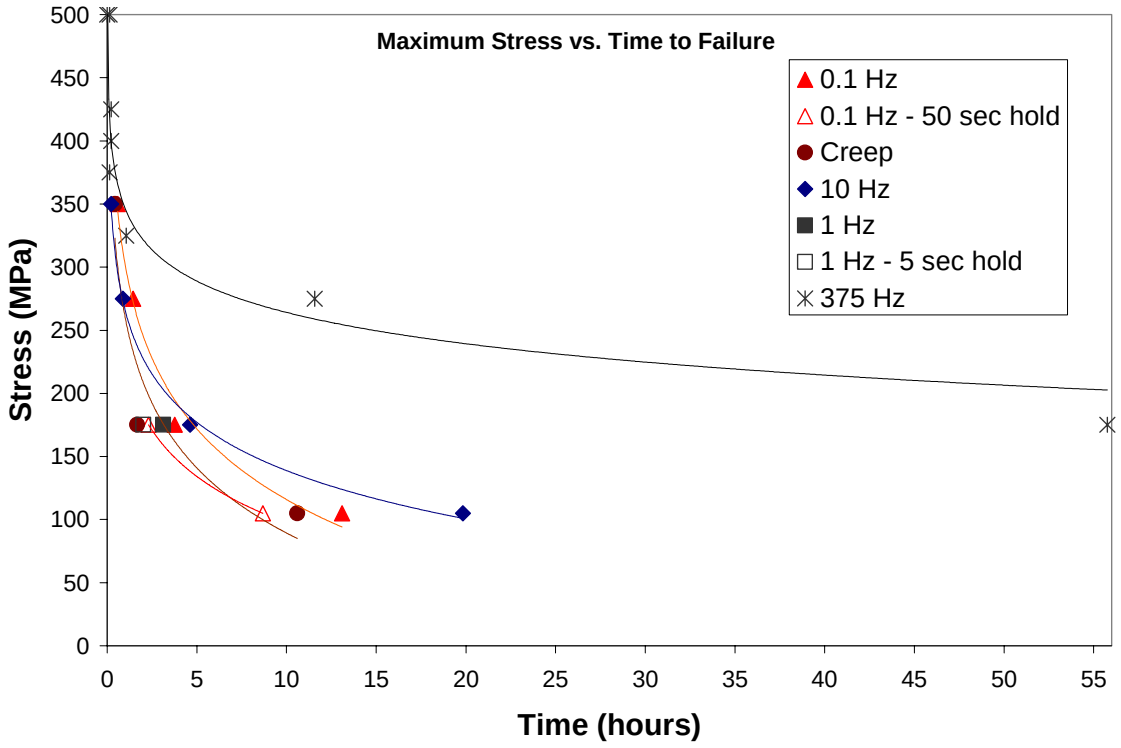

Figure 4-21. Maximum Stress vs. Time to Failure (All Tests)

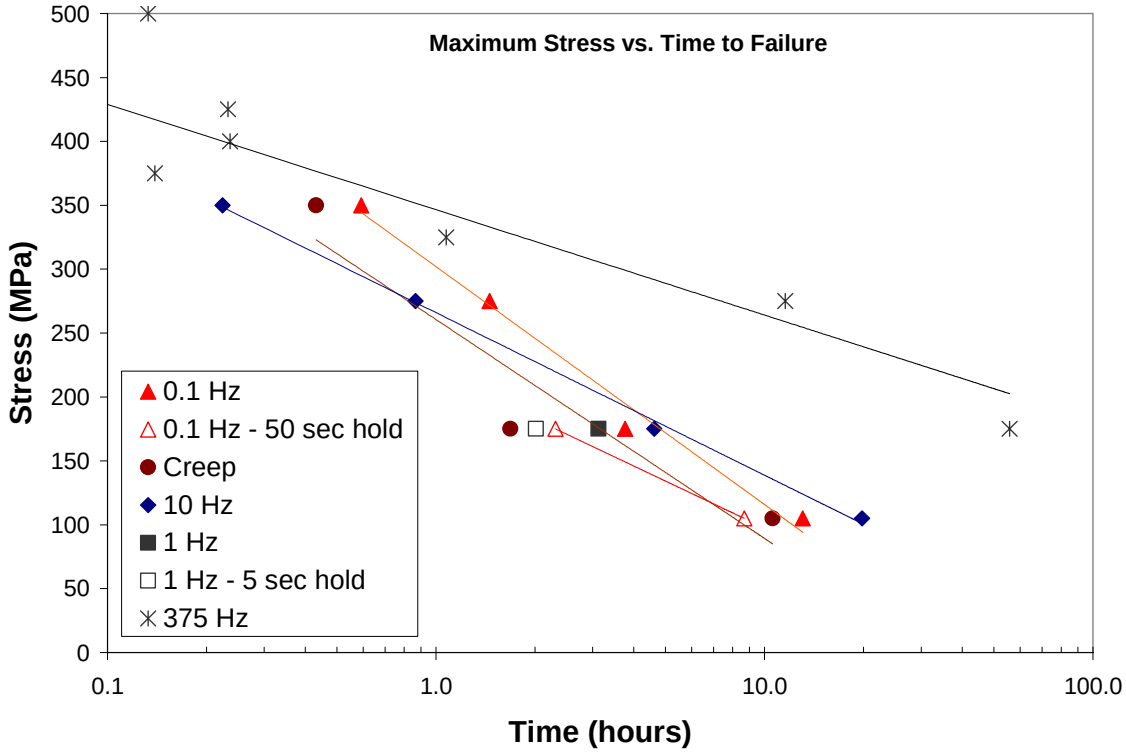

Figure 4-22. Maximum Stress vs. Time to Failure (All Tests) – log scale

Figure 4-21 and Figure 4-22 verify what was stated in Section 4.3. The longer composite lives belong to the high frequency fatigued samples. This is not what occurred in Staehler's (14) study at room temperature for C/SiC, and it is not the behavior observed in most materials at room temperature. It doesn't seem rational that a 375 Hz (175 MPa) fatigued sample will have a longer time to failure than a 1 Hz (175 MPa) fatigued sample. This observation means that oxidation of the carbon fibers within the composite is reduced when frequency of fatigue is increased. This could occur because the internal temperature from fiber matrix friction could reach the composite processing temperature of 1100ºC when frequency of fatigue is high. At this processing temperature, the thermal expansion of the carbon fibers and the SiC matrix are matched, which in turn causes the crack edges to come together and stop the seeping of oxygen into the composite. Another explanation is the possible formation of a silica scale (SiO_2) within the C/SiC composite. This growth of silica scale occurs as the SiC matrix oxidizes. The silica scale helps to fill in matrix cracks, which seal off the fibers from the outside air (4:8). The presence of oxidation within C/SiC is drastically reduced when this formation occurs. The following two sections on microscopic analysis and scanning electron microscopic analysis will illustrate the effects that high frequency fatigue has on carbon fiber oxidation and micro-crack closing.

4.6 Microscopic Analysis

Comparisons of the fracture surfaces and the polished fracture surfaces of various samples were analyzed. Table 4-4 summarizes the details of the samples that are displayed in this section.

Table 4-4. Samples Displayed in Micrographs

Specimen Number	Max Stress (Mpa)	Type of Loading	Frequency (Hz)	Time to Failure (hrs)	Cycles to Failure
02-317	487	Monotonic	N/A	0.01	1
02-314	105	Creep	N/A	10.59	1
02-326	350	Creep	N/A	0.43	1
02-315	105	Fatigue	0.1	13.09	4,701
02-325	350	Fatigue	0.1	0.59	212
02-320	105	Fatigue	10	19.84	575,607
02-321	350	Fatigue	10	0.22	6,376
02-304	175	Fatigue	375	55.75	75,265,164
02-271	425	Fatigue	375	0.23	313,976

The fracture surfaces of the creep-rupture and the fatigue specimens are displayed in Figures 4-23 and 4-24. These two figures demonstrate that there are no distinctive features on the fracture surface which can be attributed to test frequency or type of loading. Staehler et al. (14) also noted the lack of distinguishing features between different frequencies at room temperature. In order to get a clearer picture of the damage that is occurring within the C/SiC composite, the polished face samples of the fracture surfaces need to be analyzed more closely.

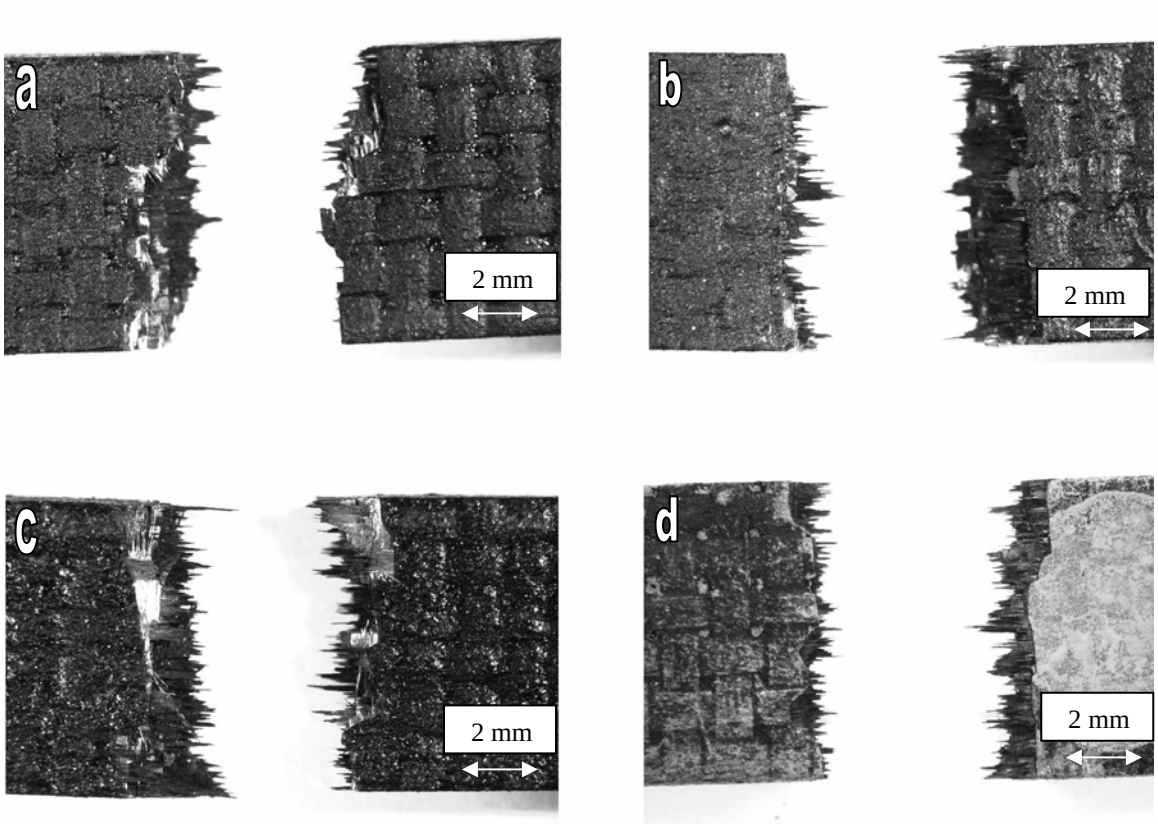

Figure 4-23. Micrographs contrasting features between specimens fractured at (a) 105 MPa - Creep-Rupture (b) 105 MPa - 0.1 Hz (c) 105 MPa - 10 Hz, and (d) 175 MPa -375 Hz.

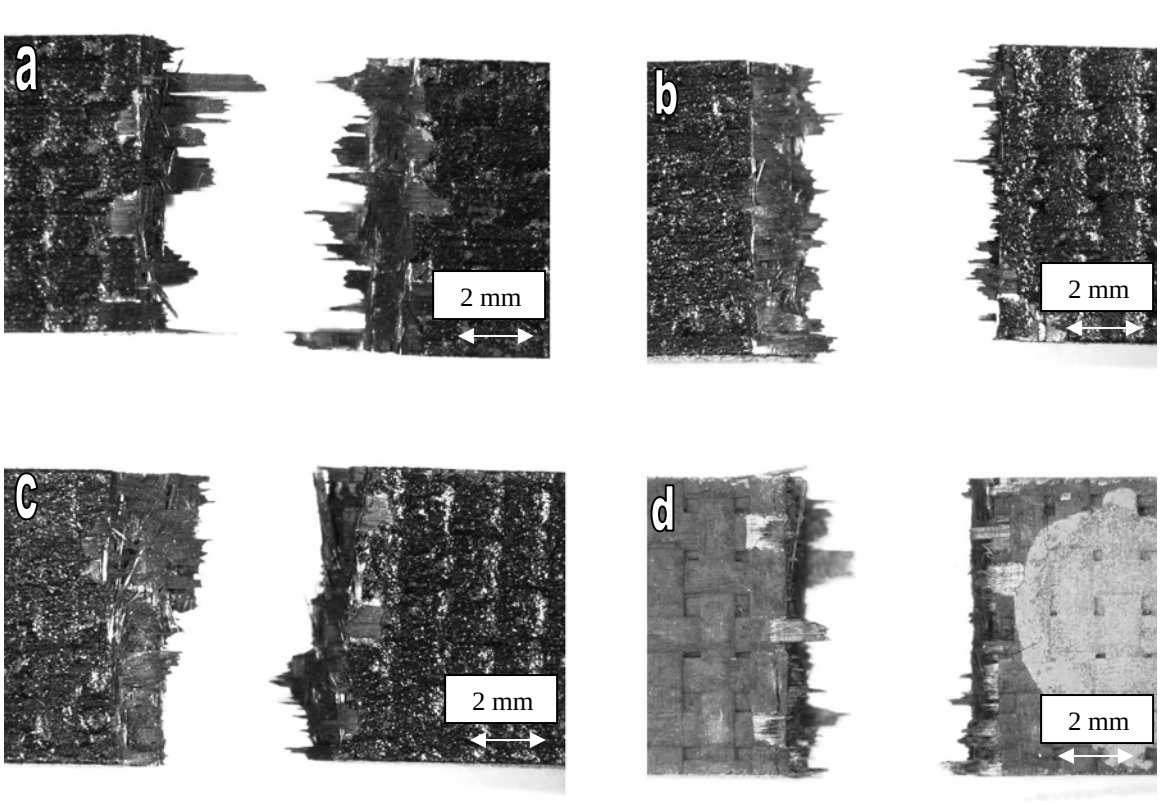

Figure 4-24. Micrographs contrasting features between specimens fractured at (a) 350 MPa - Creep-Rupture (b) 350 MPa - 0.1 Hz (c) 350 MPa - 10 Hz, and (d) 425 MPa - 375 Hz.

The polished samples are the cross-sections that are cut from the fracture surfaces. This procedure was explained in chapter 3.4.1. Figure 4-25 through Figure 4-33 are micrographs of the nine samples listed in Table 4-4. The load direction is perpendicular to all of these images. Each figure displays the entire cross-section of the sample. These detailed pictures were obtained by combining 12 separate area micrographs of the cross-section. In each figure, part (a) is the entire 12 portioned cross-section, part (b), (c), and (d) are enhanced portions of the other micrographs designated by a boxed area.

Verilli et al. (2) stated “Oxidation of the fibers is the dominant damage mode at 550°C”. Section 4.3 of this research effort also explained how oxidation is probably reduced as frequency of fatigue is increased at stresses lower than 350 MPa. Therefore, oxidation of the carbon fibers within C/SiC needs to be evaluated in Figures 4-25 thru Figure 4-33. Figure 4-25 displays the cross-sectional area of sample 02-317. This sample was tested under monotonic loading conditions. It was exposed during loading to an elevated temperature of 550°C for the least amount of time (20 seconds), hence, oxidation of the carbon fibers in sample 02-317 did not occur to a great extent. Samples that displayed the next lowest amounts of oxidation within them were samples 02-321 (10 Hz, 350 MPa, 0.22 hours), 02-326 (Creep-Rupture, 350 MPa, 0.43 hours), and 02-325 (0.1 Hz, 350 MPa, 0.59 hours) shown in Figures 4-26, 4-27, and 4-28 respectively. These four samples showed small amounts of oxidation. Large amounts of oxidation can be seen in samples 02-314 (Creep-Rupture, 105 MPa, 10.59 hours), 02-315 (0.1 Hz, 105 MPa, 13.09 hours), and 02-320 (10 Hz, 105 MPa, 19.84 hours) shown in Figures 4-29, 4-30, and 4-31 respectively. These three figures show where entire tows have oxidized and are missing. The edges of these samples also display large amounts of oxidation.

The assumption that oxidation is entirely time dependent could be assumed by looking at the seven figures listed above. However, sample 02-304, (375 Hz, 175 MPa, 55.75 hours) displayed in Figure 4-32, shows that this is not the case. Low oxidation levels can be seen in samples 02-271 (375 Hz, 425 MPa, 0.23 hours) and 02-304 (375 Hz, 175 MPa, 55.75 hours) shown in Figures 4-32 and 4-33 respectively. Sample 02-304 lasted 55.75 hours, and it is obvious that less oxidation occurred within this specimen than that of samples 02-314 (Creep-Rupture, 105 MPa, 10.59 hours), 02-315 (0.1 Hz, 105

MPa, 13.09 hours), and 02-320 (10 Hz, 105 MPa, 19.84 hours). Sample 02-304 was oxidized less even though it was exposed to an oxidizing environment for a longer period of time.

Figure 4-32 supports the claim that at high frequencies and low stresses, oxidation within C/SiC is inhibited which then increases composite time life and cycle life. Figure 4-6 in section 4.3 and Figures 4-21 and 4-22 in section 4.5 also support this claim. This claim is astonishing because in most materials, the higher the frequency of fatigue the shorter the time life and cycle life of the material. This is also the case with C/SiC at room temperature. Staehler's (14) study showed that 375 Hz fatigued C/SiC composites had shorter time lives and cycle lives than 4 Hz and 40 Hz fatigued composites at room temperature. However, at an elevated temperature of 550°C, this study shows that C/SiC behaves in an opposite fashion. As frequency of fatigue is increased, the time life and cycle life of the C/SiC composite is also increased.

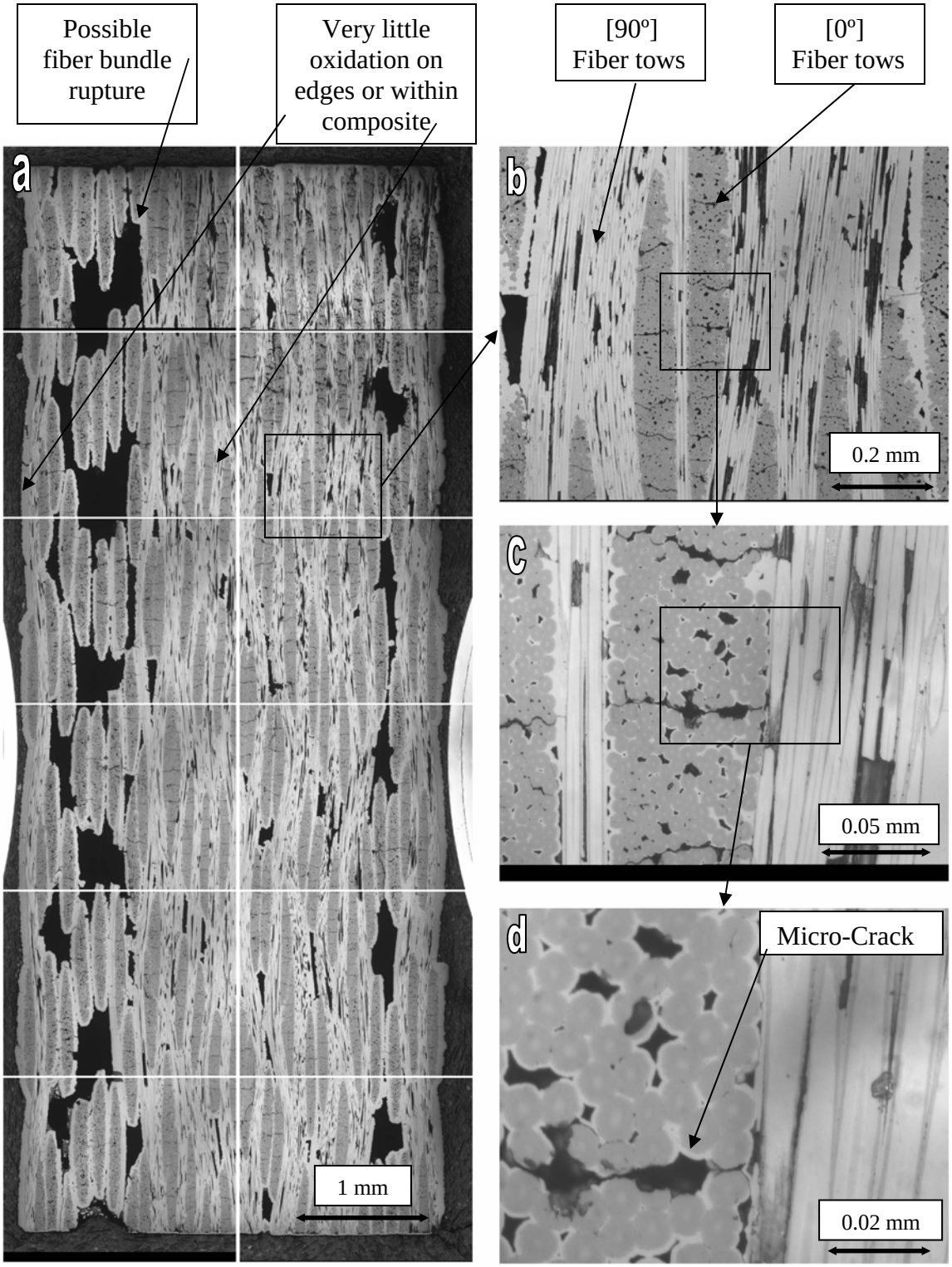

Figure 4-25. Micrographs of polished Sample 02-317 (Monotonic).
Time to failure was 20 seconds. Loading direction is perpendicular to image.
(a) Entire cross-section (b), (c), and (d) Enhanced portions of cross-section

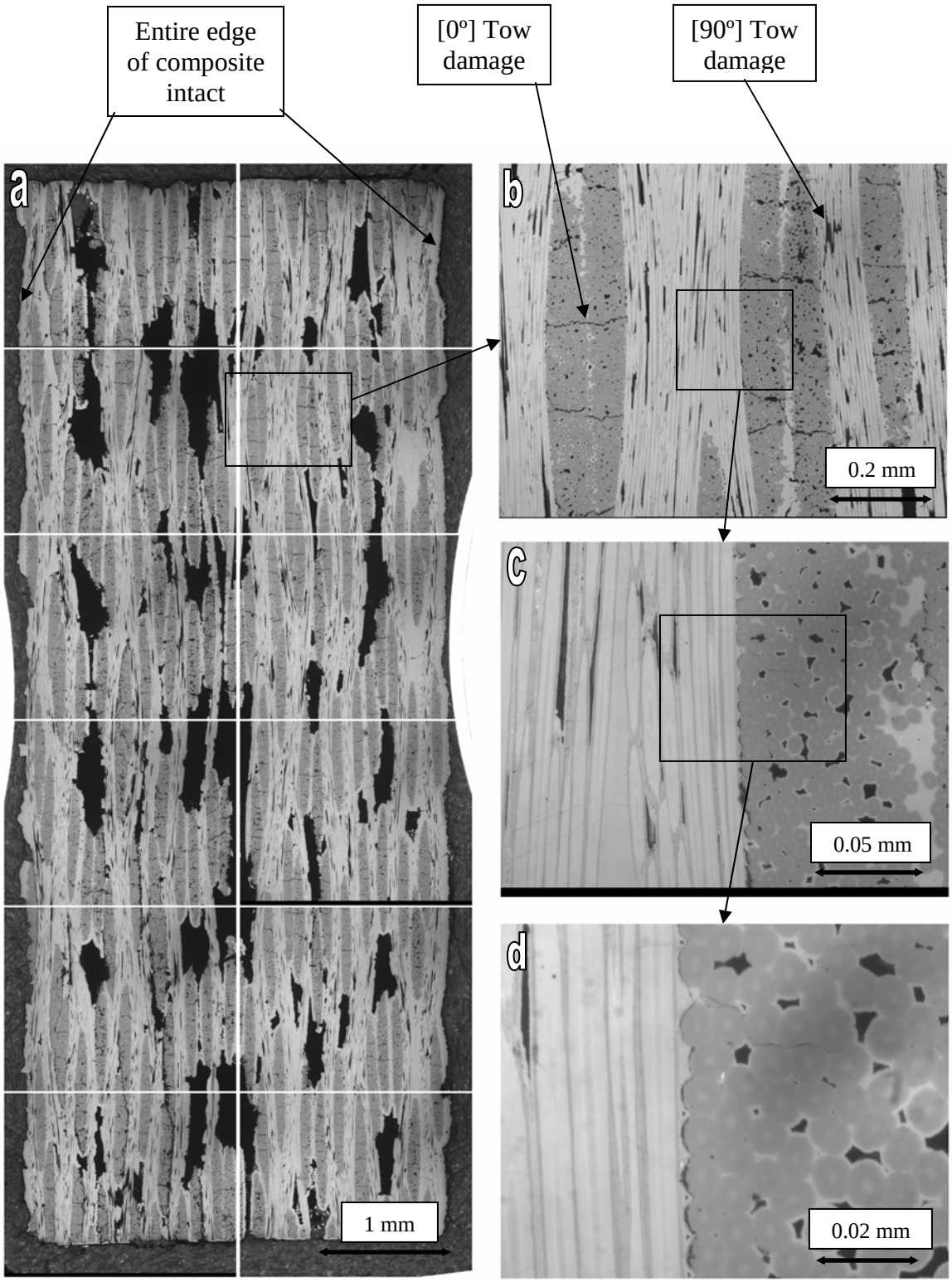

Figure 4-26. Micrographs of polished Sample 02-321 (10 Hz, 350 MPa). Time to failure was 0.22 hours. Loading direction is perpendicular to image. (a) Entire cross-section (b), (c), and (d) Enhanced portions of cross-section

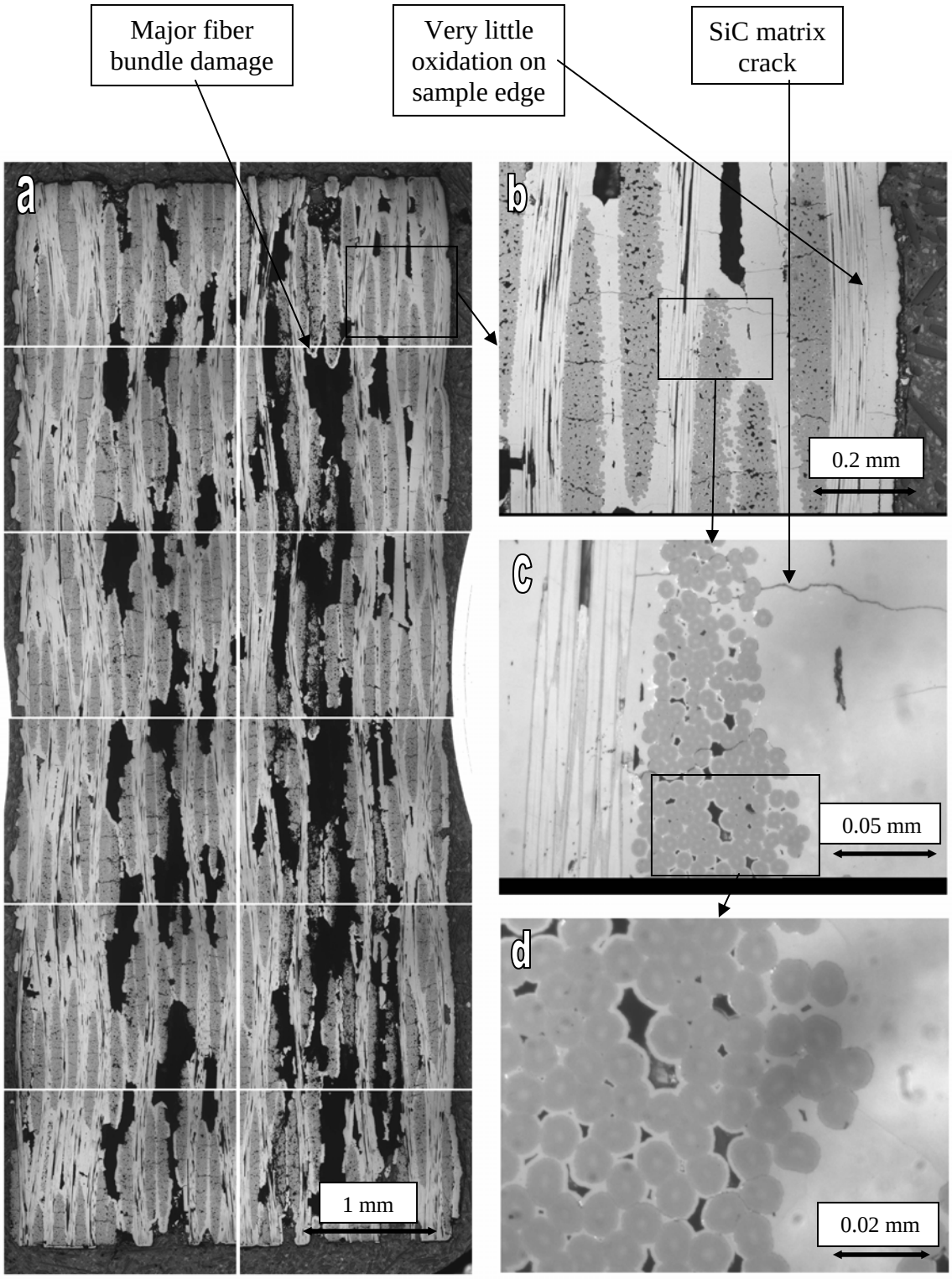

Figure 4-27. Micrographs of polished Sample 02-326 (Creep, 350 MPa). Time to failure was 0.43 hours. Loading direction is perpendicular to image. (a) Entire cross-section (b), (c), and (d) Enhanced portions of cross-section

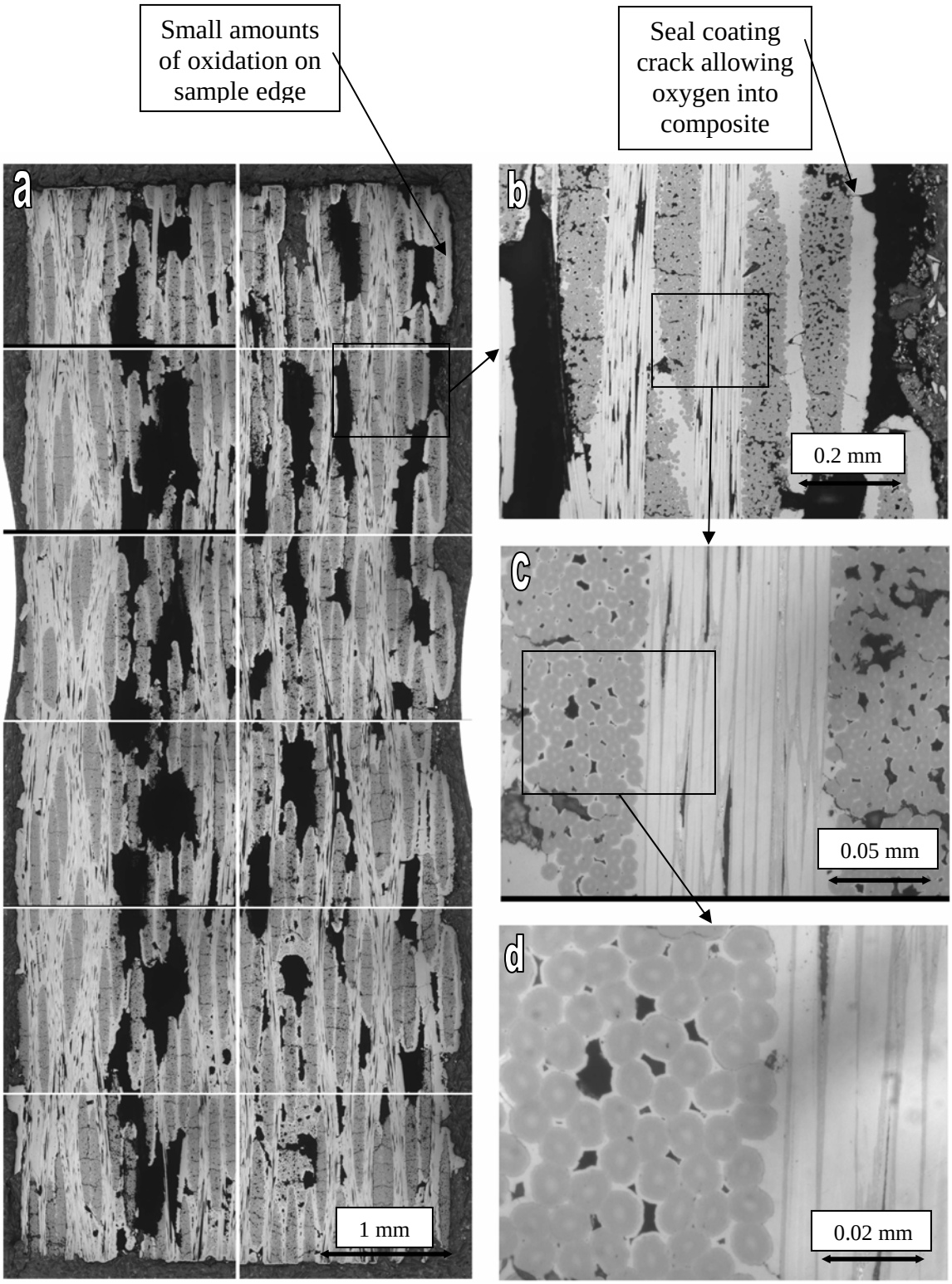

Figure 4-28. Micrographs of polished Sample 02-325 (0.1 Hz, 350 MPa). Time to failure was 0.59 hours. Loading direction is perpendicular to image. (a) Entire cross-section (b), (c), and (d) Enhanced portions of cross-section

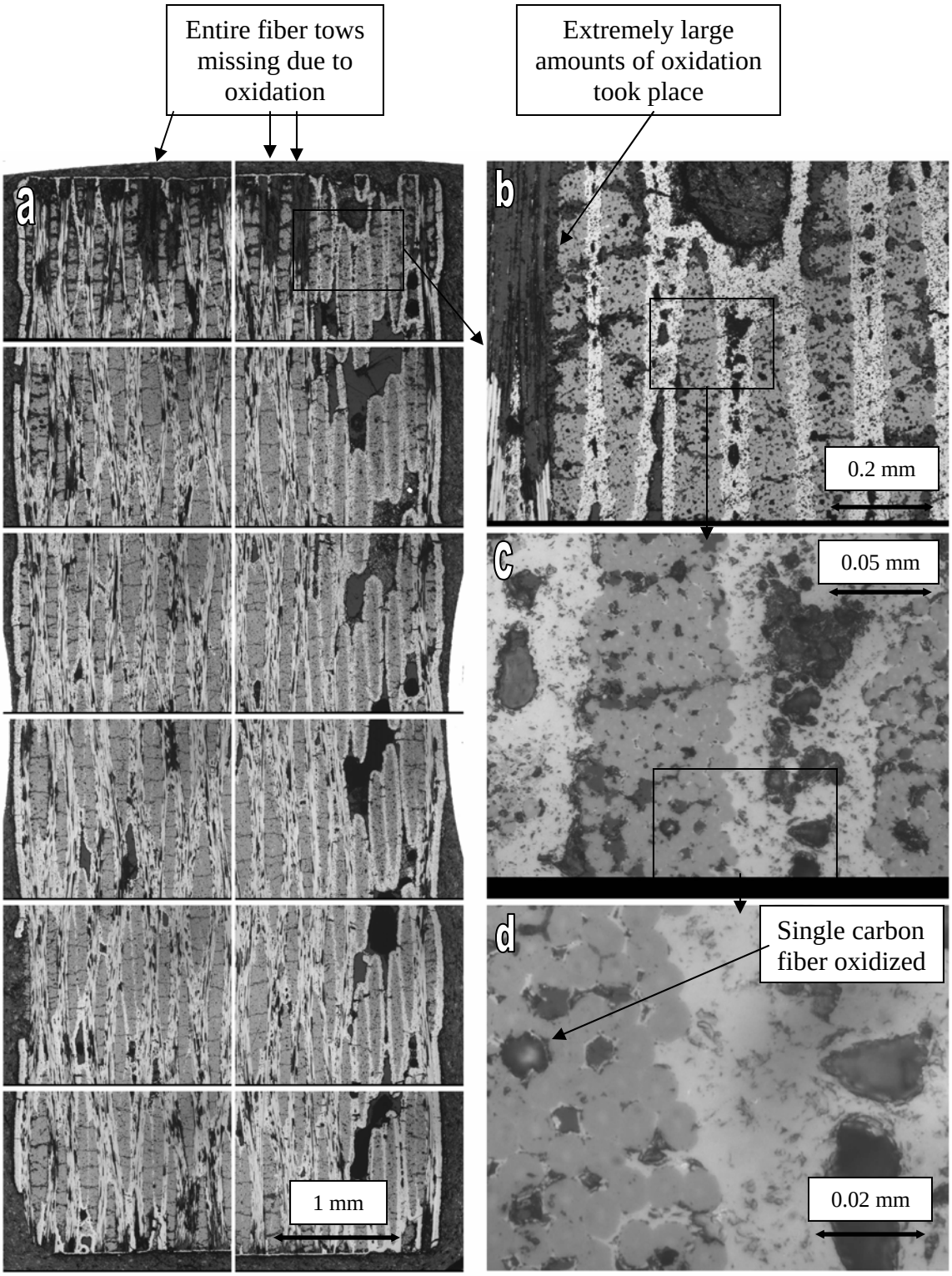

Figure 4-29. Micrographs of polished Sample 02-314 (Creep, 105 MPa). Time to failure was 10.59 hours. Loading direction is perpendicular to image. (a) Entire cross-section (b), (c), and (d) Enhanced portions of cross-section

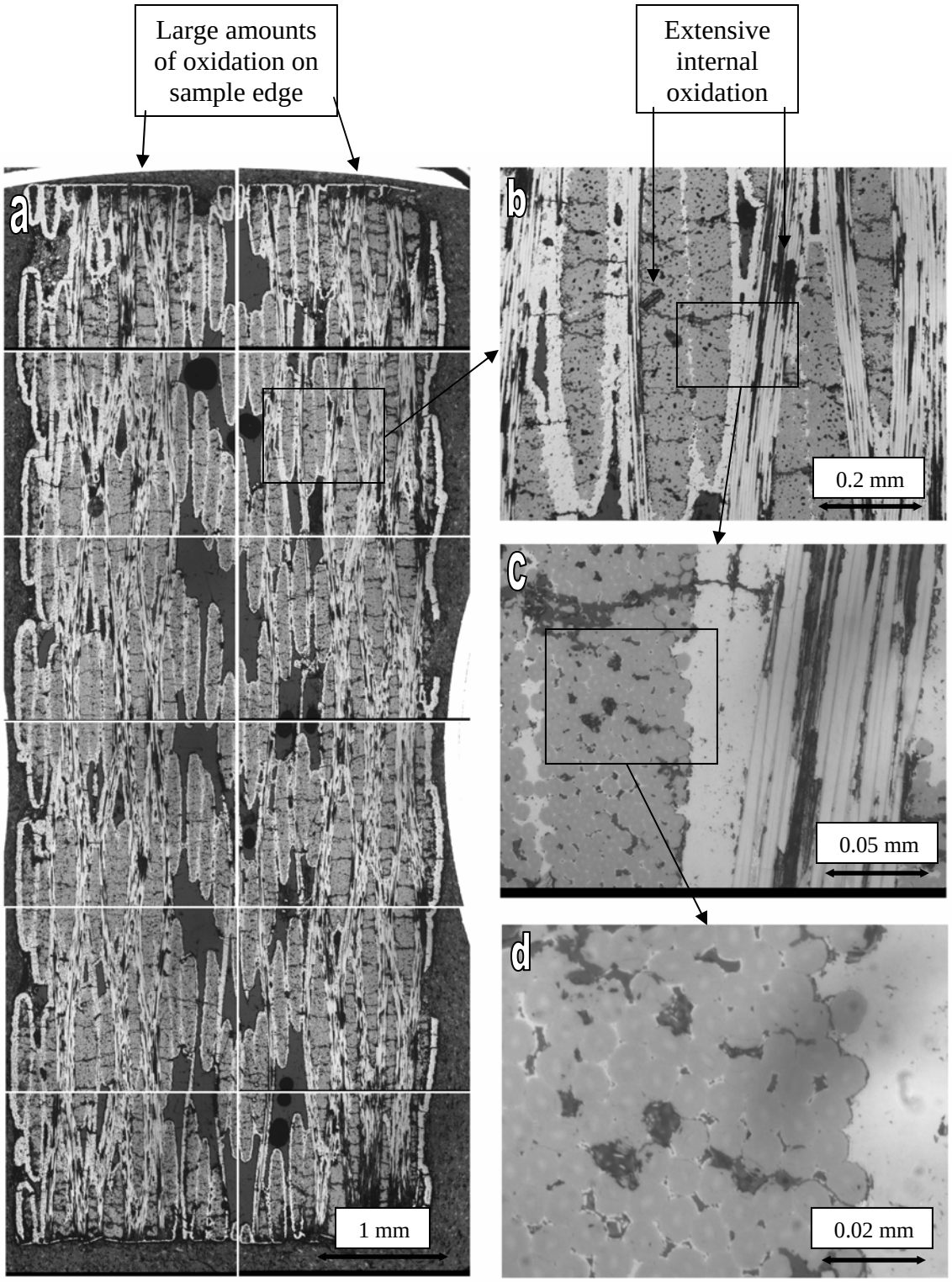

Figure 4-30. Micrographs of polished Sample 02-315 (0.1 Hz, 105 MPa). Time to failure was 13.09 hours. Loading direction is perpendicular to image. (a) Entire cross-section (b), (c), and (d) Enhanced portions of cross-section

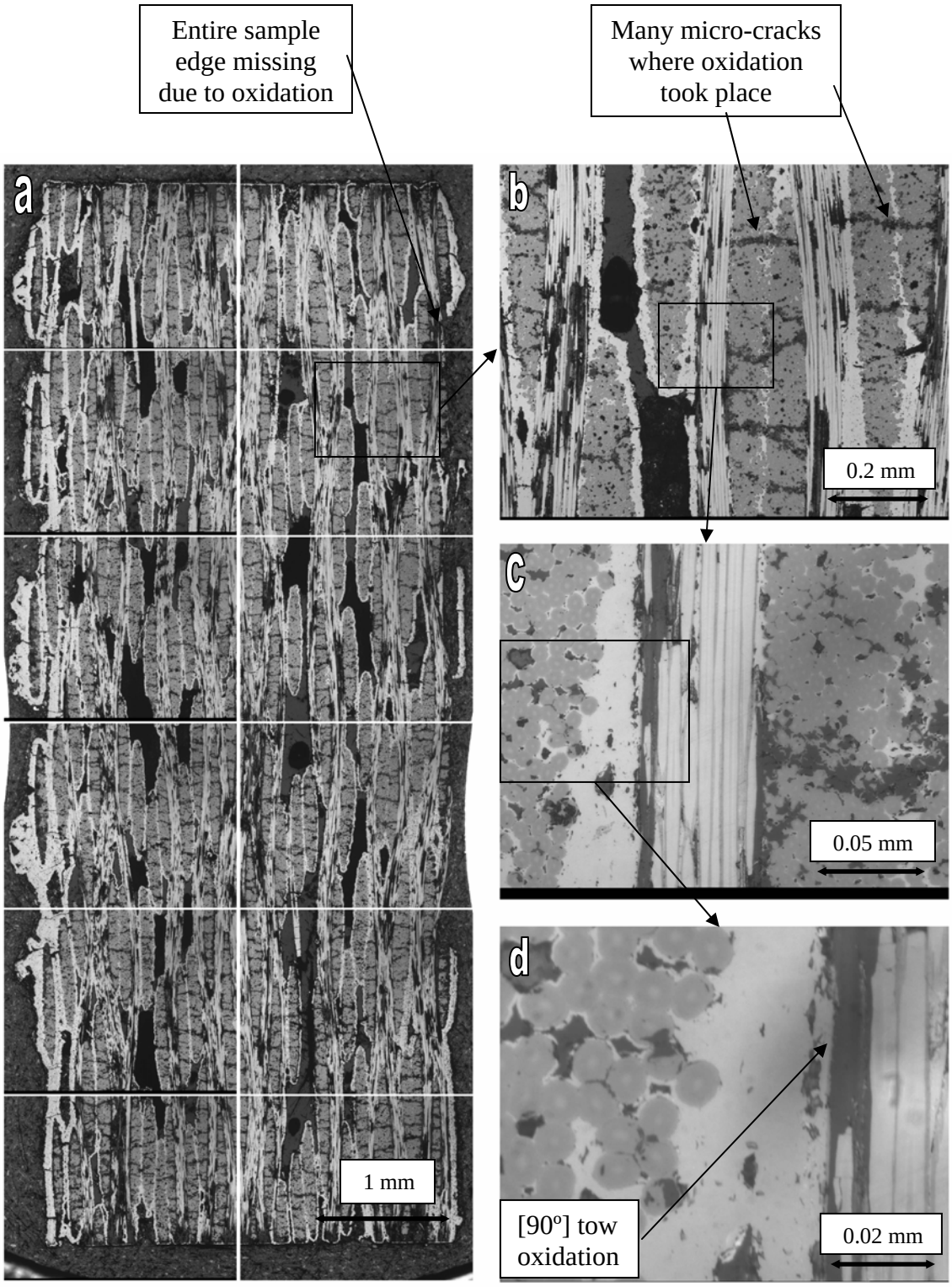

Figure 4-31. Micrographs of polished Sample 02-320 (10 Hz, 105 MPa). Time to failure was 19.84 hours. Loading direction is perpendicular to image. (a) Entire cross-section (b), (c), and (d) Enhanced portions of cross-section

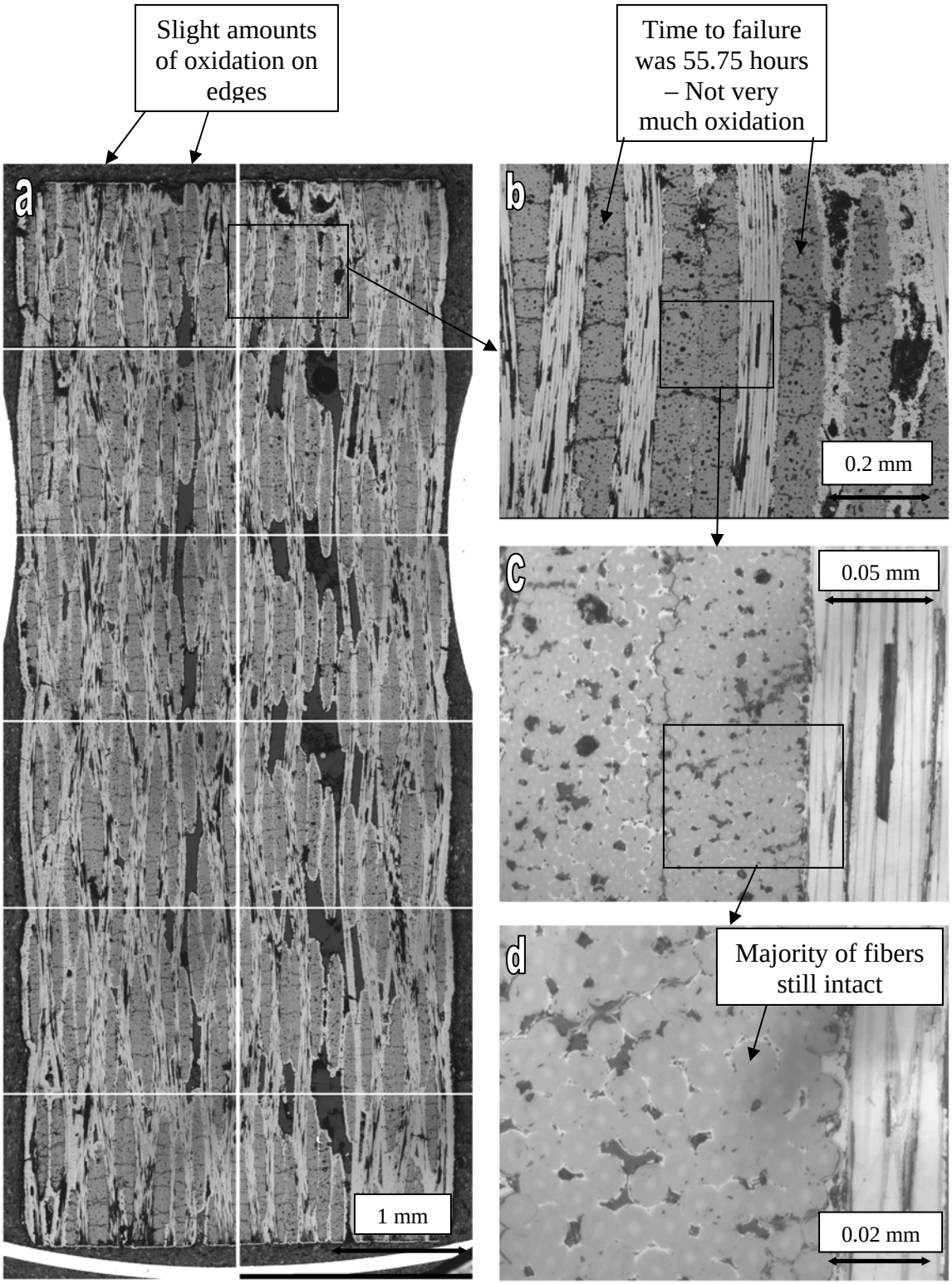

Figure 4-32. Micrographs of polished Sample 02-304 (375 Hz, 175 MPa). Time to failure was 55.75 hours. Loading direction is perpendicular to image. (a) Entire cross-section (b), (c), and (d) Enhanced portions of cross-section

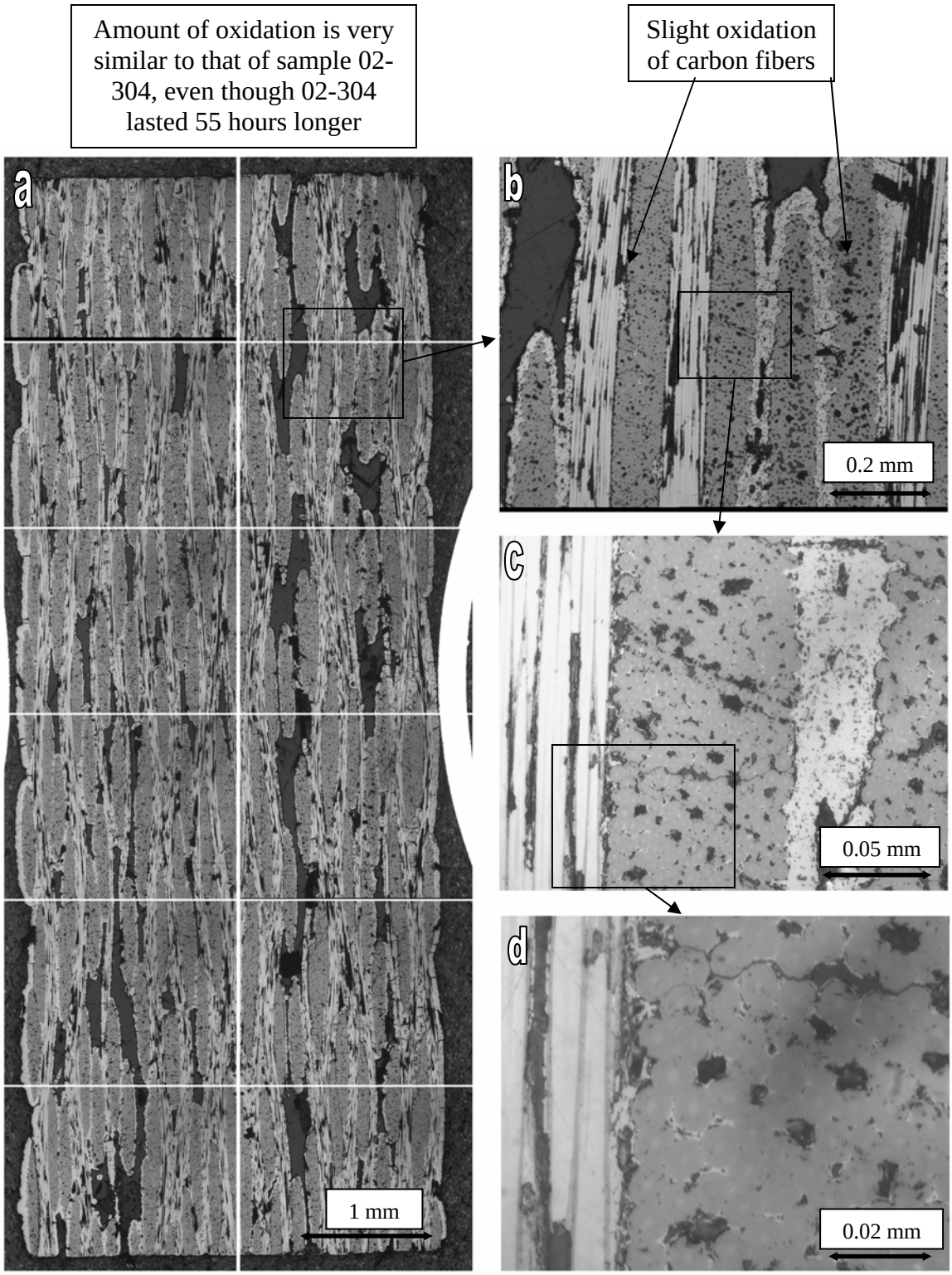

Figure 4-33. Micrographs of polished Sample 02-271 (375 Hz, 425 MPa). Time to failure was 0.23 hours. Loading direction is perpendicular to image. (a) Entire cross-section (b), (c), and (d) Enhanced portions of cross-section

4.7 Scanning Electron Microscopic Analysis

A Scanning Electron Microscope (SEM) was also used to analyze the C/SiC fracture surfaces. Many different areas on the fracture surfaces of the samples were observed in order to investigate the levels of oxidation that occurred within C/SiC. The SEM photographs can be found in Figures 4-34 thru 4-46 and in Appendix A.

4.7.1 Carbon Fiber Oxidation Within the SiC Matrix.

Figures 4-34 thru 4-36 are excellent examples of oxidized [0º] carbon fiber tows within the SiC matrix. Figure 4-34 is a picture of sample 02-310 (175 MPa, 1Hz, 3.13 hours). This figure shows carbon fibers that are well on their way to complete oxidation. There are chunks of carbon already missing from the fibers. In Figure 4-35 there are two carbon fibers that are almost completely oxidized, and many other carbon fibers that are completely missing. This is expected because this picture was taken of sample 02-314 (105 MPa, creep-rupture, 10.59 hours). The long period of time the fibers were exposed to 550ºC allowed them to be oxidized extensively. On the other hand, Figure 4-36 of sample 02-304 (175 MPa, 375 Hz, 55.75 hours) illustrates something extraordinary. This sample lasted 55.75 hours; however, the carbon fibers show less oxidation than either of the previous two figures. This once again demonstrates that high frequency fatigued samples have longer time lives and cycle lives than low frequency fatigued C/SiC samples. They have longer lives because there fibers are not oxidized as thoroughly as fibers that are fatigued at lower frequencies. One possible explanation is that because of the high frequency (375 Hz), there is a lot of internal friction between the fibers and the matrix. This

internal friction causes an increase in the internal temperature of the composite. The micro-cracks within the matrix began to close as the temperature of the sample approaches the approximate processing temperature of 1100°C (4:8). Another explanation is the possible formation of a silica scale (SiO_2) within the C/SiC composite. This growth of silica scale occurs as the SiC matrix oxidizes. The silica scale helps to fill in matrix cracks, which seal off the fibers from the outside air (4:8).

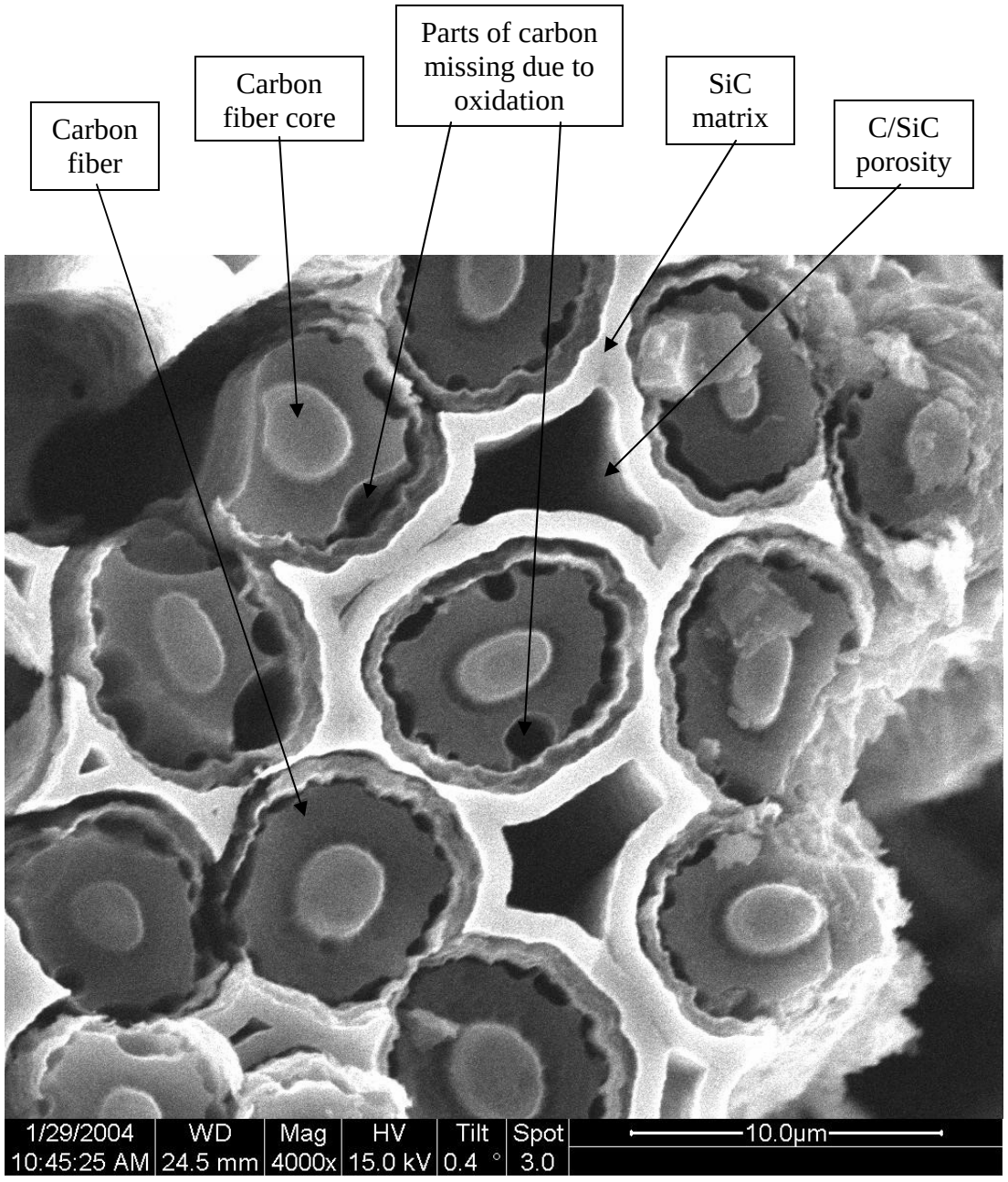

Figure 4-34. Fiber Oxidation Within SiC - Sample 02-310 (175 MPa, 1 Hz, 3.13 hrs.)

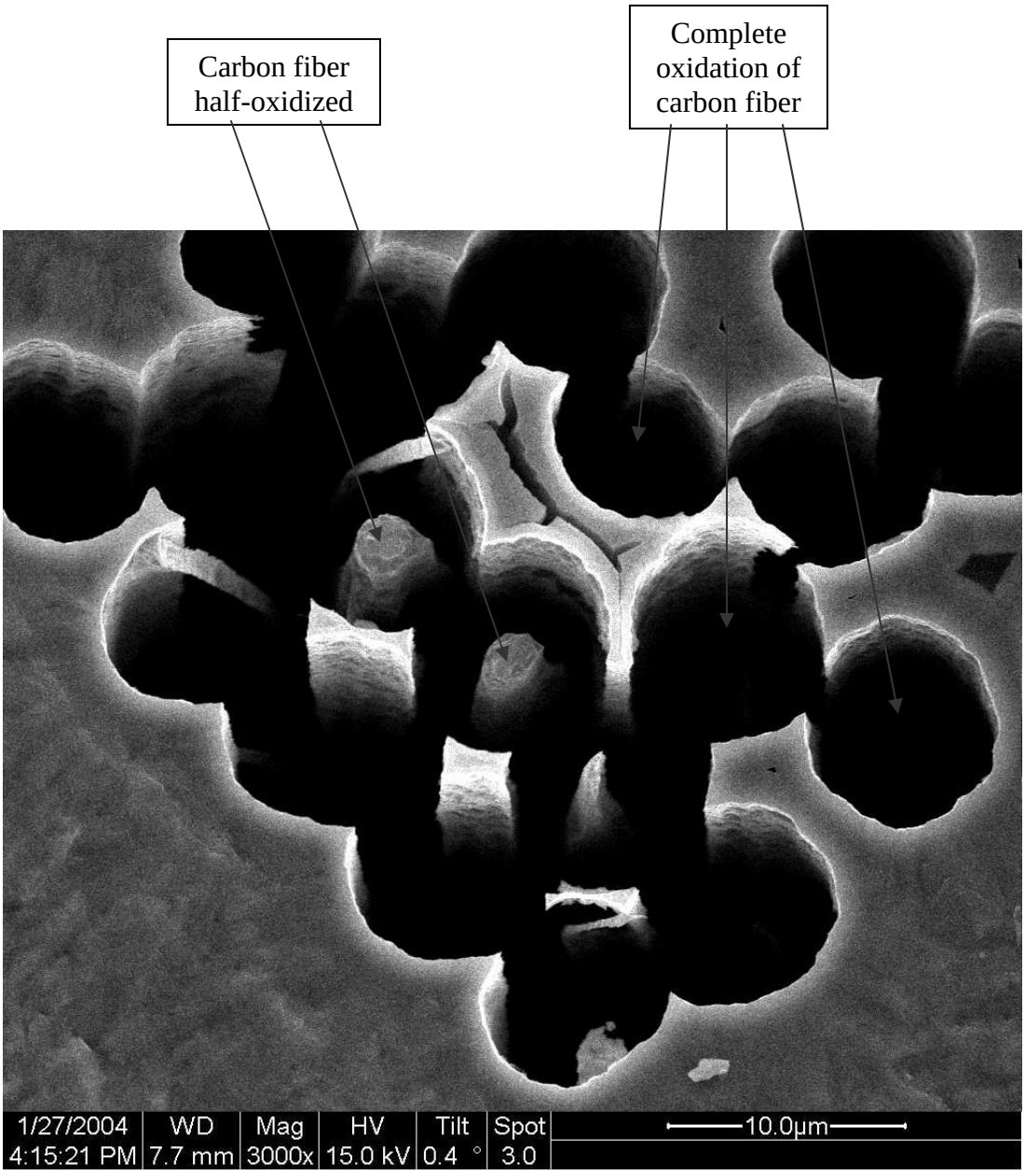

Figure 4-35. Fiber Oxidation Within SiC - Sample 02-314 (105 MPa, Creep, 10.59 hrs.)

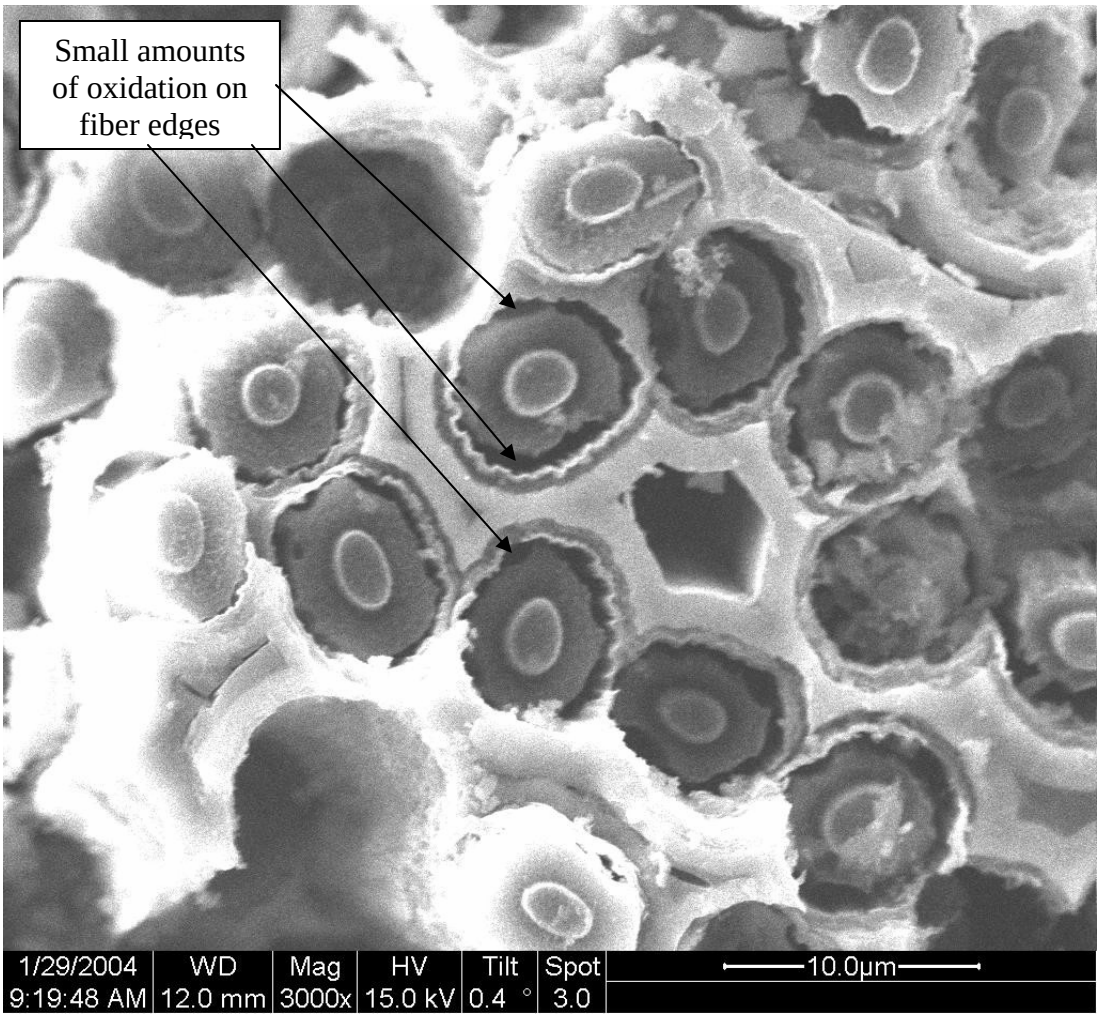

Figure 4-36. Fiber Oxidation Within SiC - Sample 02-304 (175 MPa, 375 Hz, 55.75 hrs.)

4.7.2 Individual Fiber Oxidation.

Examining individual [90º] carbon fibers also demonstrates how much oxidation a C/SiC sample has undergone. Figures 4-37 thru 4-39 are photographs of individual [90º] carbon fibers being oxidized on the fracture surface. An example of a carbon fiber that has undergone a small amount of oxidation is seen in Figure 4-37. This fiber was only oxidized a little because it was exposed to 550ºC for only 0.22 hours. On the other hand, Figure 4-38 shows a fiber that has been oxidized

extensively. This fiber was exposed to 550ºC for 19.84 hours. The fiber has been broken down a great deal, and much of the carbon has already been dissipated. One would expect a fiber that lasted 55.75 hours to look much like the one in Figure 4-38. However, in Figure 4-39 we see a [90º] fiber from sample 02-304 (175 MPa, 375 Hz, 55.75 hours). This fiber shows almost no evidence of oxidation attack on it. Figure 4-39 demonstrates that high frequency fatigued fibers are oxidized less than low frequency fatigued fibers.

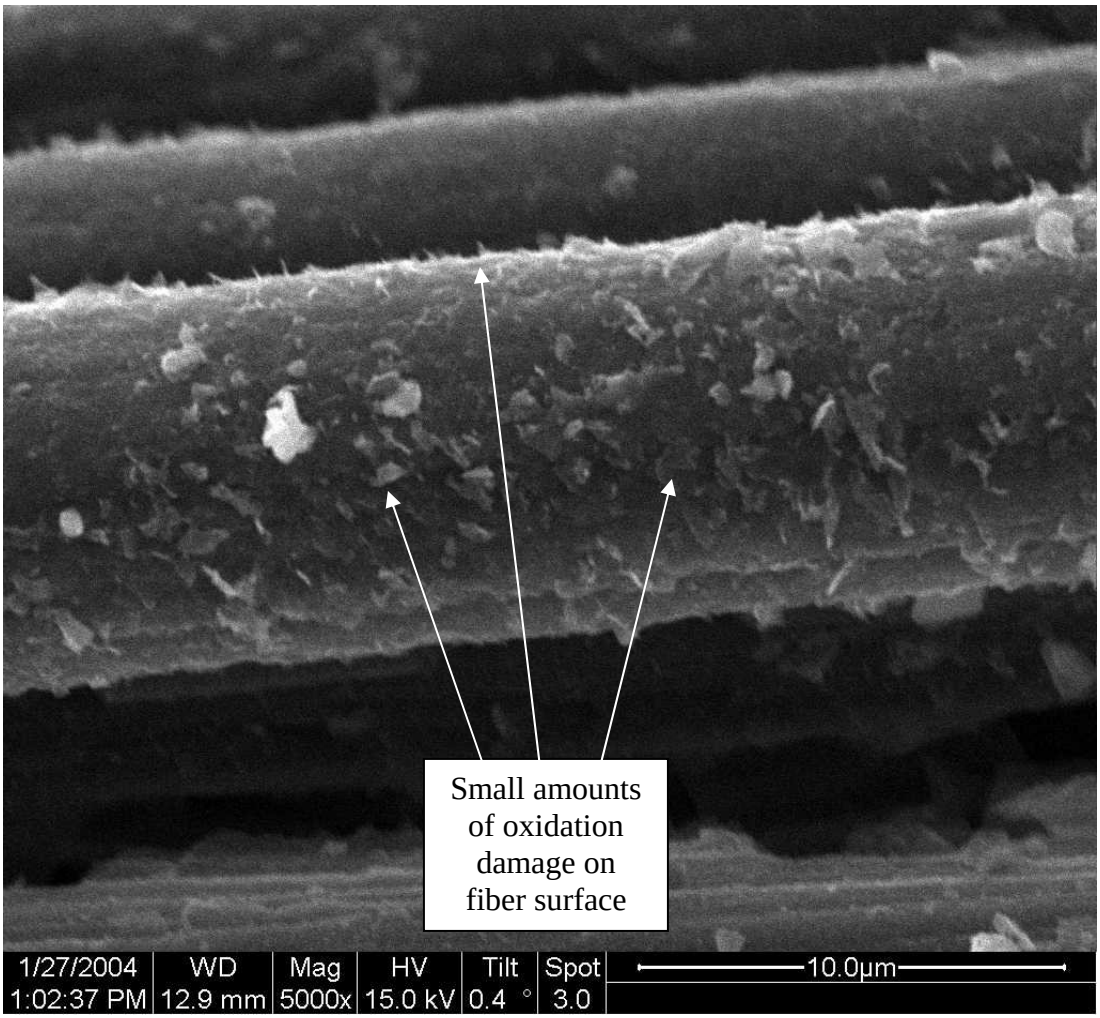

Figure 4-37. Individual Fiber Oxidation - Sample 02-321 (350 MPa, 10 Hz, 0.22 hrs.)

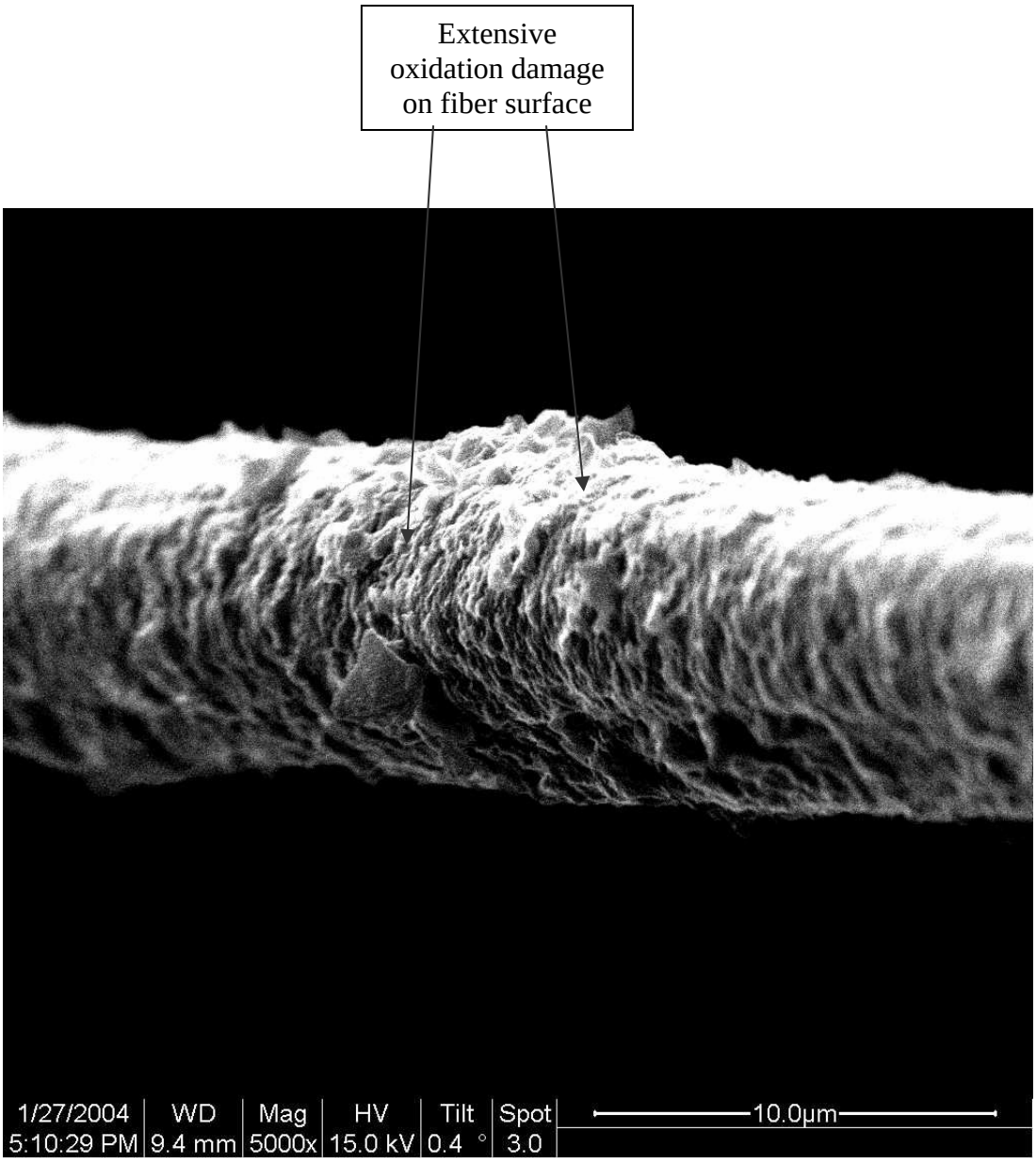

Figure 4-38. Individual Fiber Oxidation - Sample 02-320 (105 MPa, 10 Hz, 19.84 hrs.)

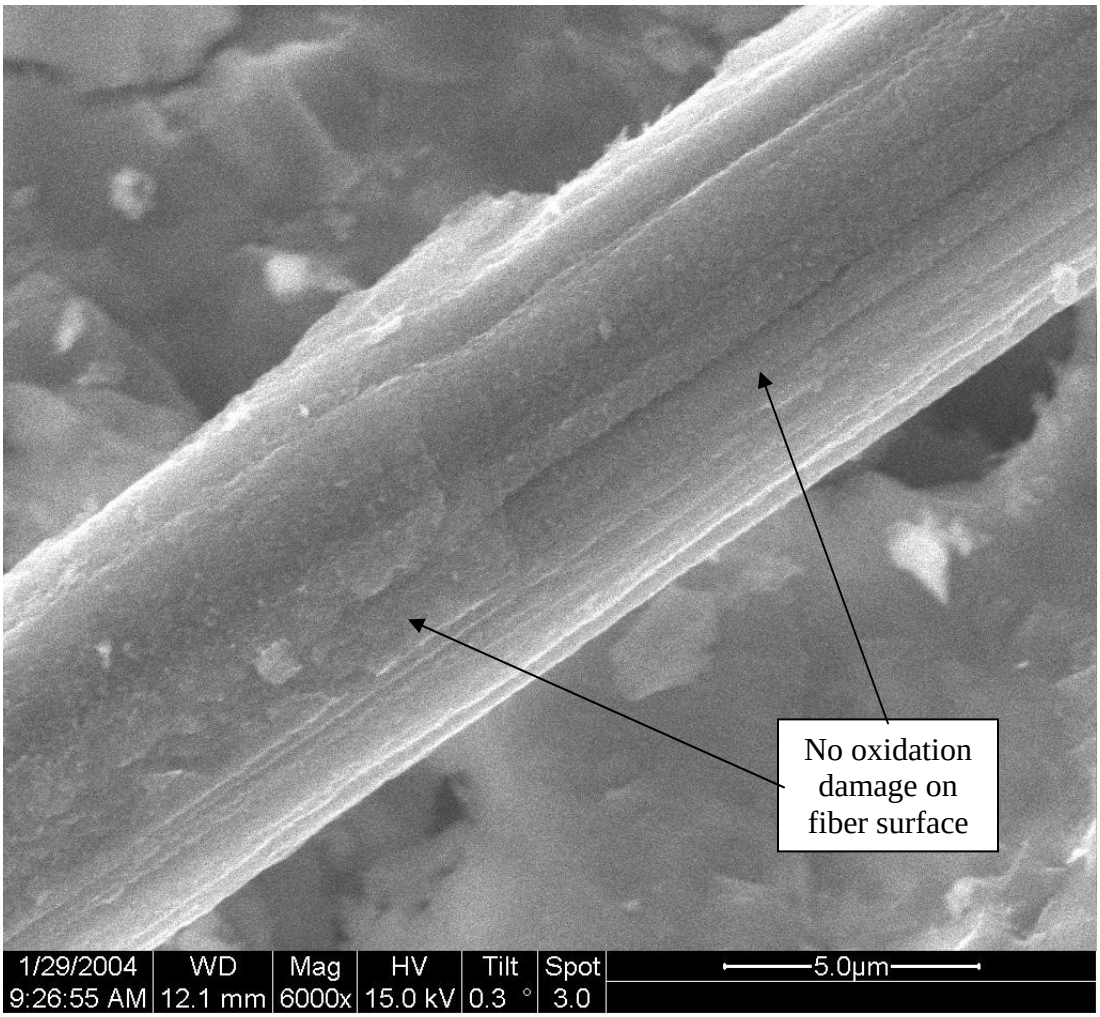

Figure 4-39. Individual Fiber Oxidation - Sample 02-304 (175 MPa, 375 Hz, 55.75 hrs.)

4.7.3 Examination of Fibers on Sample Edges.

The carbon fibers on a sample edge are often the fibers that succumb to oxidation first. Figures 4-40 and 4-41 demonstrate the many carbon fibers that are missing on the sample edges of two different C/SiC specimens. These two specimens underwent a large amount of oxidative attack. There are many carbon fibers that have disappeared due to oxidation effects. Figures 4-42 and 4-43 display the opposite effect. The majority of the fibers are still intact and present within the

samples. These two figures are of sample 02-304 (175 MPa, 375 Hz, 55.75 hours). This once again supports what sections 4.7.2 and 4.7.3 already stated. Oxidation of carbon fibers is reduced in high frequency fatigued C/SiC samples which then increases the fatigue life and time life of C/SiC.

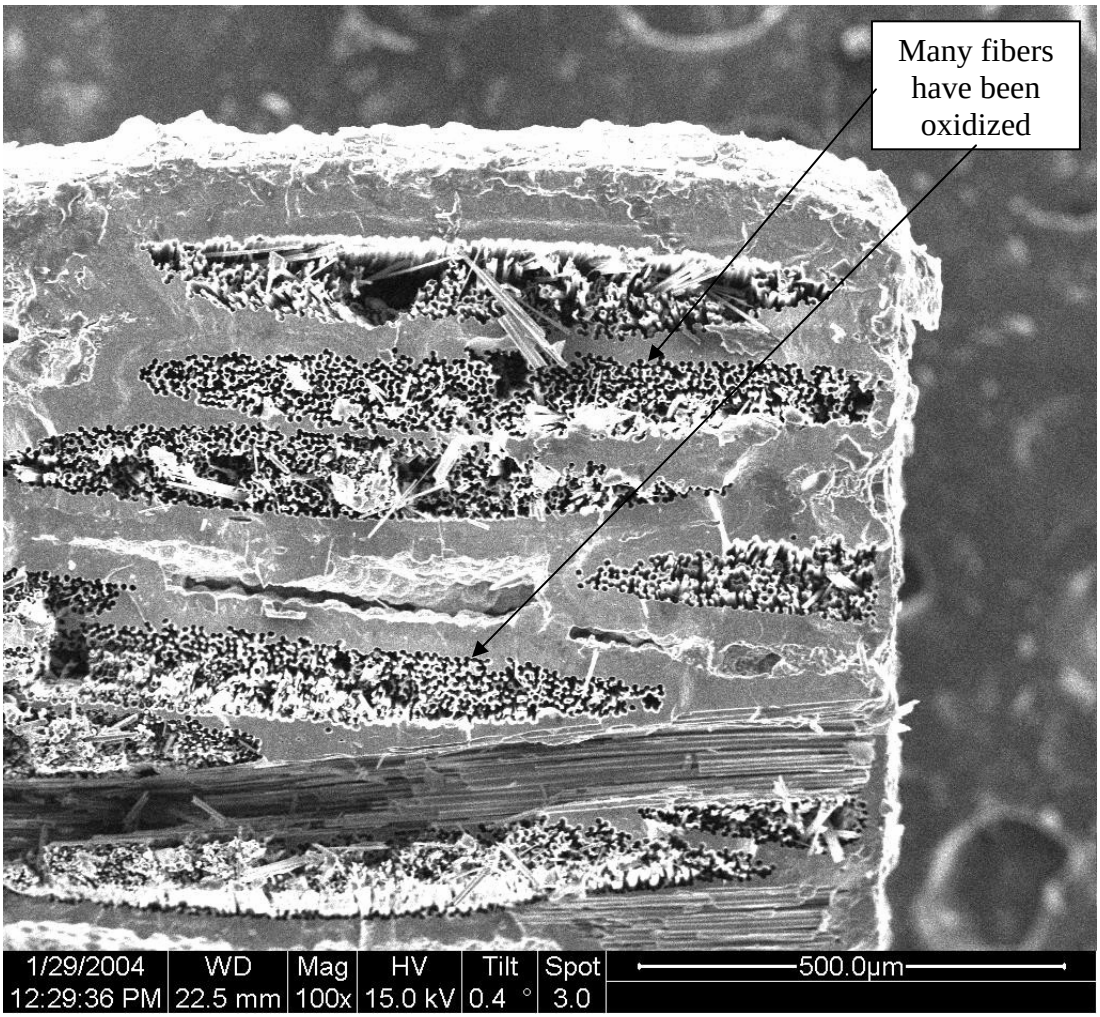

Figure 4-40. Oxidation on C/SiC Edge - Sample 02-314 (105 MPa, Creep, 10.59 hrs.)

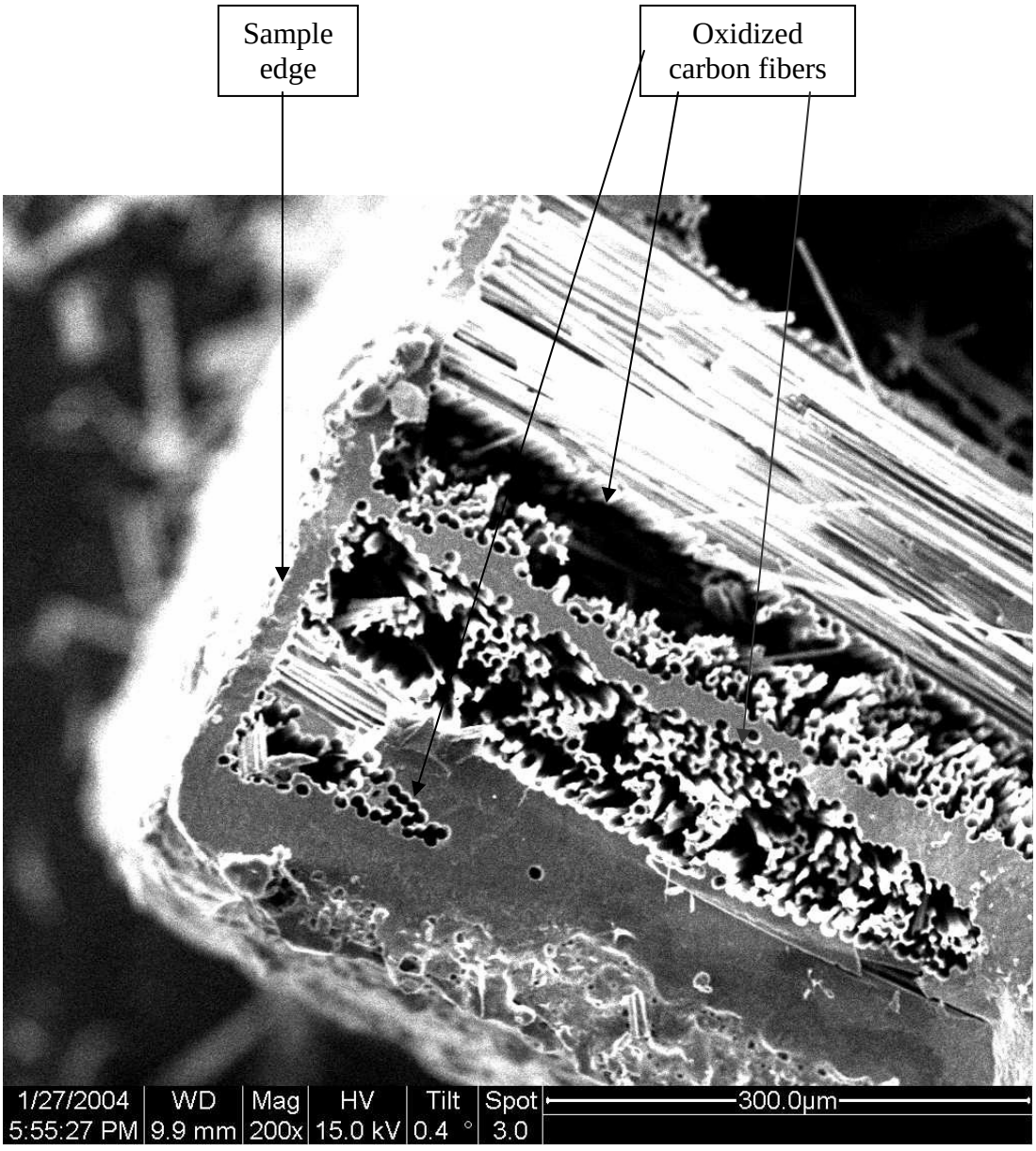

Figure 4-41. Oxidation on C/SiC Edge - Sample 02-315 (105 MPa, 0.1 Hz, 13.09 hrs.)

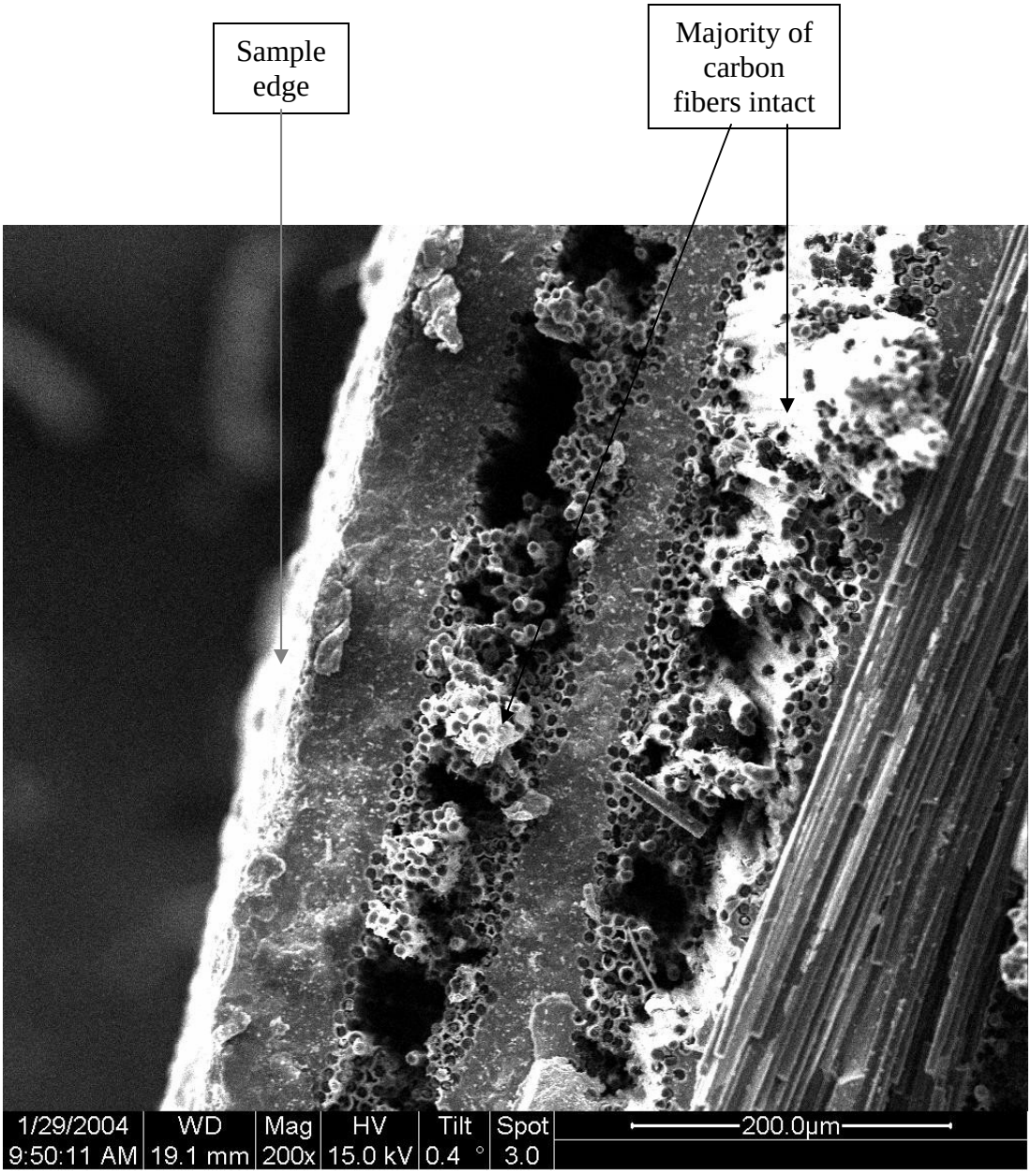

Figure 4-42. Oxidation on C/SiC Edge – Sample 02-304 (175 MPa, 375 Hz, 55.75 hrs.)

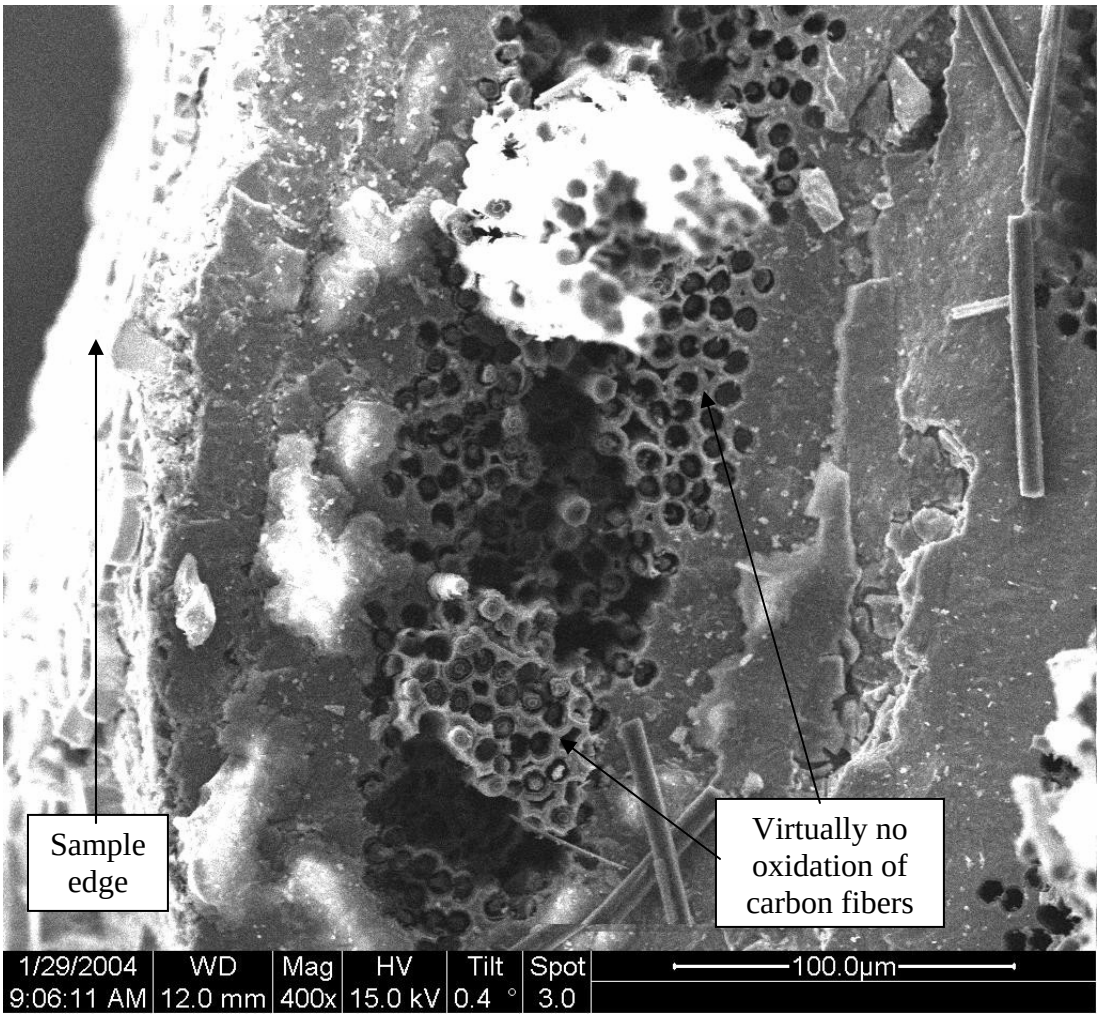

Figure 4-43. Oxidation on C/SiC Edge – Sample 02-304 (175 MPa, 375 Hz, 55.75 hrs.)

4.7.4 Examination of SiC Matrix Cracks.

When C/SiC reaches its processing temperature (approximately 1100ºC), the micro-cracks within the SiC matrix begin to close. At this high temperature, the formation of a silica scale (SiO_2) also helps to fill matrix micro-cracks. Two SiC matrix micro-cracks can be seen in Figure 4-44. These cracks are very open which allowed oxygen to seep into the composite and oxidize the carbon fibers. Evidence of micro-crack closure is seen in Figure 4-45. This figure is a picture of sample 02-

304 (175 MPa, 375 Hz, 55.75 hours). The matrix micro-crack appears to be sealed shut, which most likely stopped the flow of oxygen into the composite. Matrix crack closure within high frequency fatigued specimens would definitely increase C/SiC cycle lives and time lives.

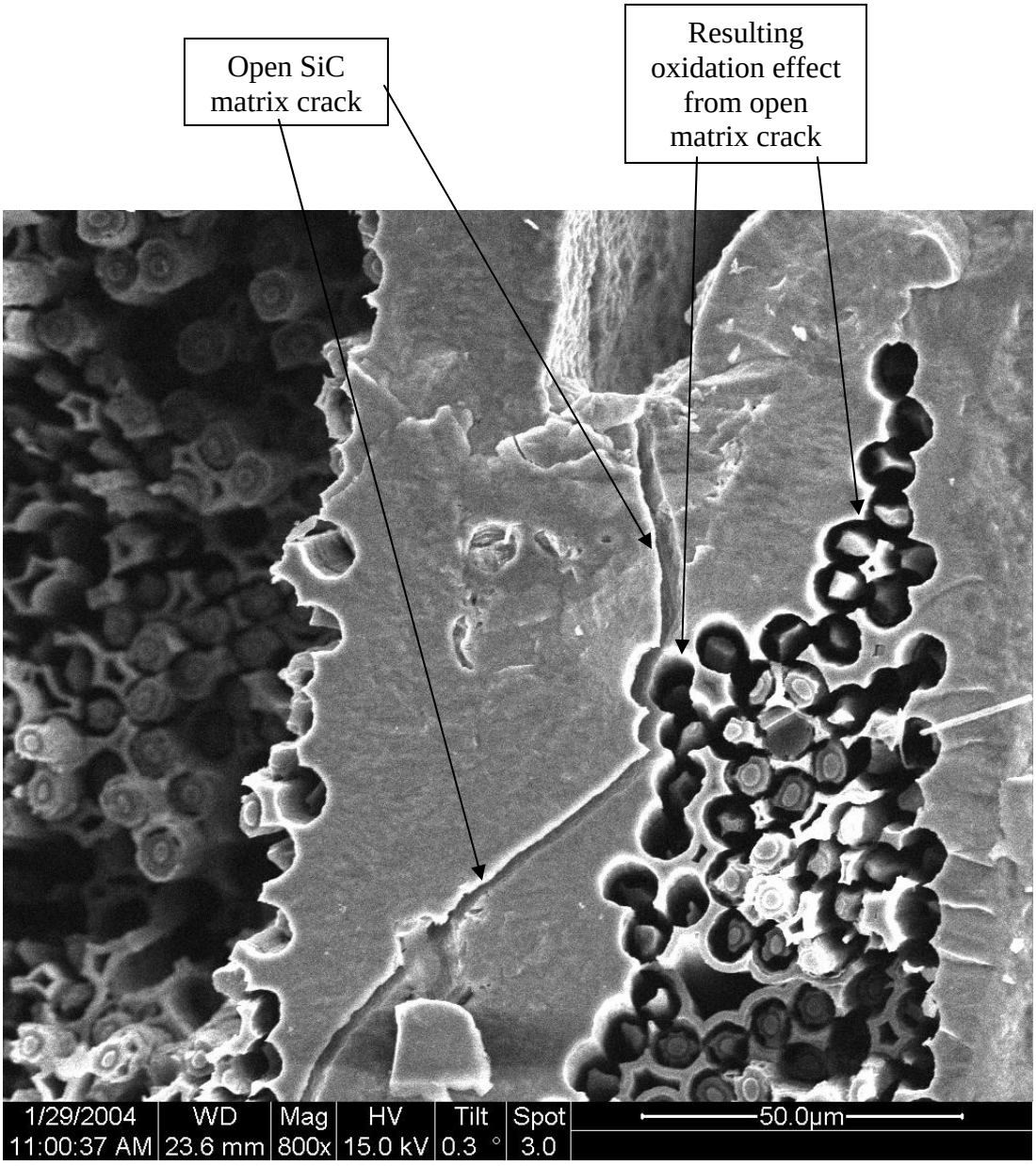

Figure 4-44. SiC Matrix Micro-Cracks - Sample 02-310 (175 MPa, 1 Hz, 3.13 hrs.)

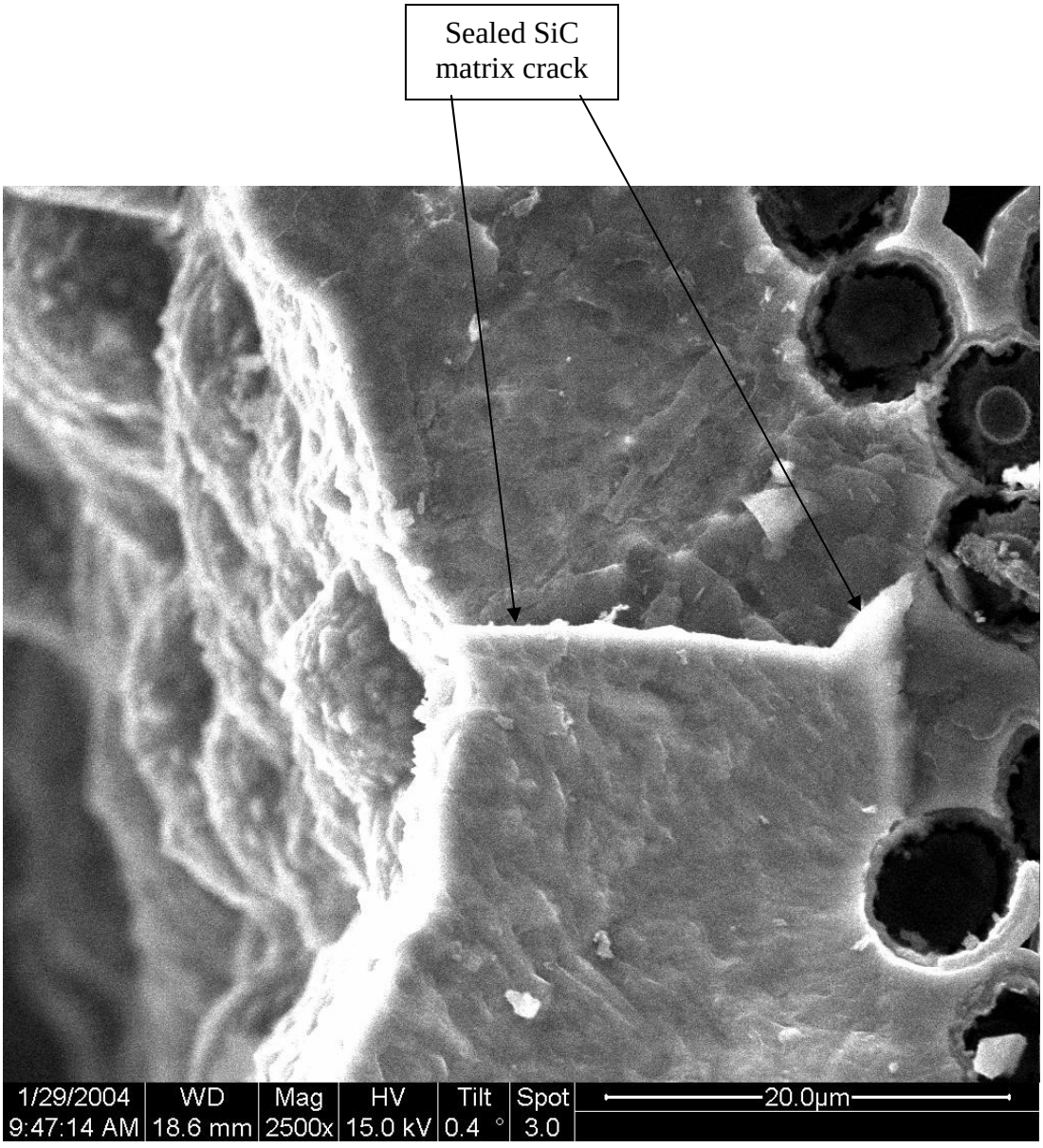

Figure 4-45. SiC Matrix Micro-Crack - Sample 02-304 (175 MPa, 375 Hz, 55.75 hrs.)

V. Conclusions and Recommendations

The main objective of this research effort was to examine the impact that cyclic loading frequency has on the life of a C/SiC composite at an elevated temperature of 550°C. There have been several previous studies that have investigated the creep-rupture life and monotonic strength of C/SiC at elevated temperatures. However, the effect that cyclic loading frequency has on the oxidation of the carbon fibers within C/SiC at elevated temperatures has not been studied to a great extent.

Twenty-five tests on C/SiC at a temperature of 550°C were performed in this study. Cyclic loading of C/SiC was investigated at frequencies of 375 Hz, 10 Hz, 1 Hz, and 0.1 Hz. Creep-Rupture tests and tests that were combinations of creep-rupture and fatigue were also accomplished at 550°C and compared to the cyclic data. A monotonic tensile test was performed at 550°C and compared to a room temperature monotonic tensile test conducted by Staehler et al. (14). Strain histories and modulus data were analyzed to show how C/SiC degraded and ultimately failed during the different tests. Microscopic evidence also identified to what extent carbon fibers were oxidized within C/SiC during the various tests.

This study showed that an elevated temperature of 550°C has very little effect on the Ultimate Tensile Strength (UTS) of C/SiC. The UTS of C/SiC at 550°C was 487 MPa, while the room temperature UTS is 493 MPa (14).

The three creep-rupture tests in this study performed at 350 MPa, 175 MPa and 105 MPa had lives of less than 11 hours despite the fact that the UTS of C/SiC is 487 MPa at

550°C. The short life of the specimens is due to the oxidation of the carbon fibers within the C/SiC composite. The data from these tests were similar to that of Verilli's (8) tests at 550°C.

S-N curves were developed from the data of fatigue tests performed in this experiment. The S-N curves indicate that there is an increase in cycles to failure as the frequency is increased at 550°C. This is opposite of the room temperature results in Staehler's et al. (14) study. Their research found that there was a reduction in cycles to failure as frequency is increased at room temperature. Another very important discovery in this study was the fact that oxidation of the carbon fibers within C/SiC is reduced when frequency of fatigue is increased. At high frequency fatigue (10Hz to 375 Hz), C/SiC composites have longer cycle lives and time lives than at low cycle fatigue. This occurs because the internal friction between the fibers and the matrix at high frequencies cause an increase in the internal temperature of the composite. The micro-cracks within the matrix began to close as the temperature of the sample approaches the approximate processing temperature of 1100°C (2:8). At this processing temperature, the thermal expansion of the carbon fibers and the SiC matrix are matched. At high internal temperatures, growth of a silica scale (SiO_2) also occurs as the SiC matrix oxidizes. The silica scale helps to fill in matrix cracks, which seal off the fibers from the outside air. The matrix micro-crack closure that occurs due to these two occurrences reduces the flow of oxygen within C/SiC, which then reduces oxidation of the carbon fibers

The Microscopic and SEM analysis verified that oxidation of carbon within C/SiC is slowed as frequency of fatigue is increased. The SEM photographs showed that high frequency fatigued C/SiC specimens had less sample edge oxidation as well. Micro-

cracks within the SiC matrix are also closed in SEM photographs of high frequency fatigued samples.

Further studies should focus on different temperature levels and fatigue frequencies between 10 Hz and 375 Hz. The studies should also investigate the mechanistic reasons that cause high frequency fatigue to reduce oxidation at elevated temperatures. This further research would bring closure to the effect that frequency of fatigue plays in the failure of C/SiC composites at elevated temperatures.

Appendix A: Additional SEM Photographs

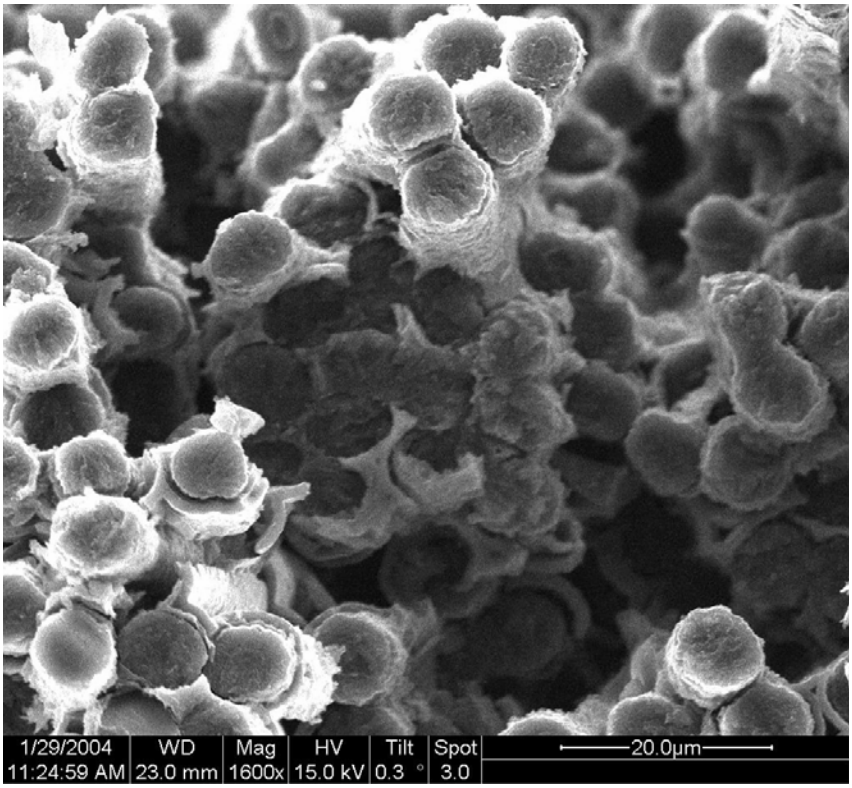

Figure A-1. Sample 02-325 (350 MPa, 0.1 Hz, 0.59 hours)

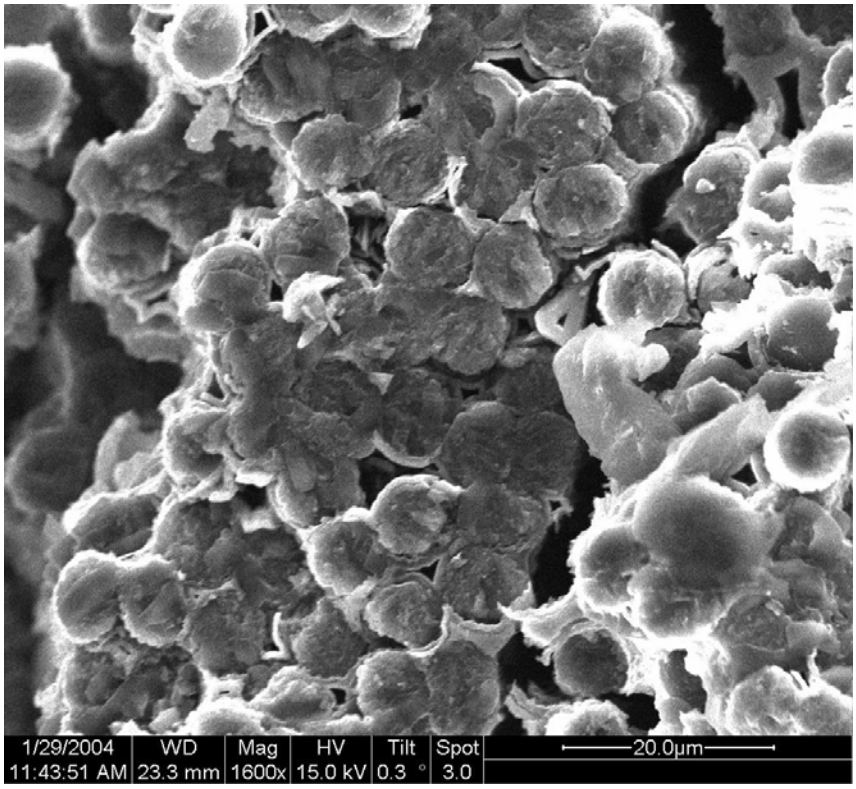

Figure A-2. Sample 02-326 (350 MPa, Creep, 0.43 hours)

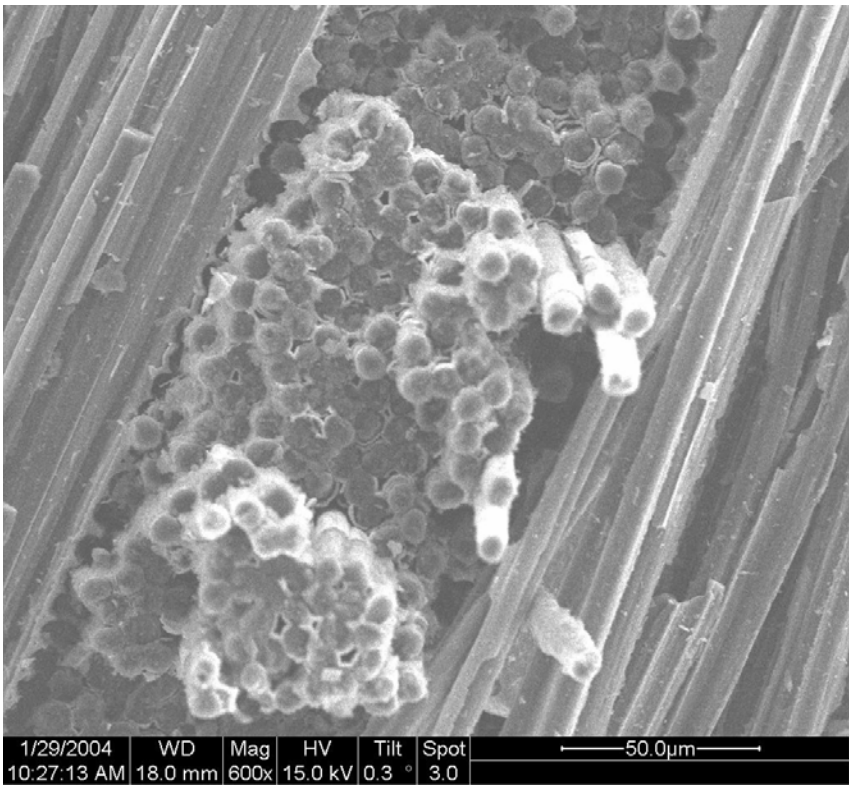

Figure A-3. Sample 02-271 (425 MPa, 375 Hz, 0.23 hours)

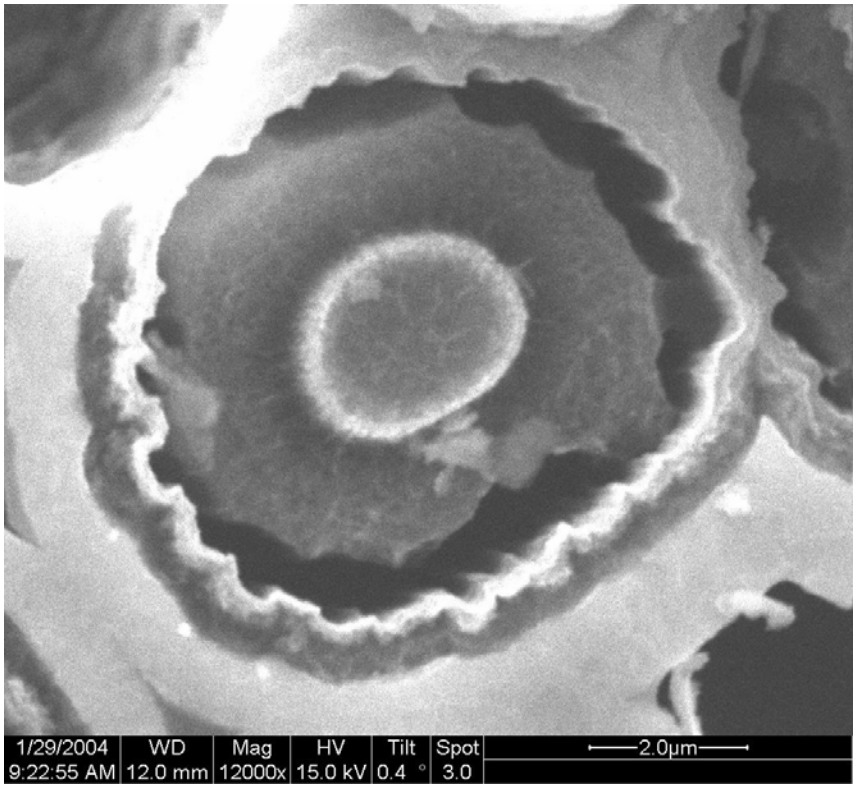

Figure A-4. Sample 02-304 (175 MPa, 375 Hz, 55.75 hours)

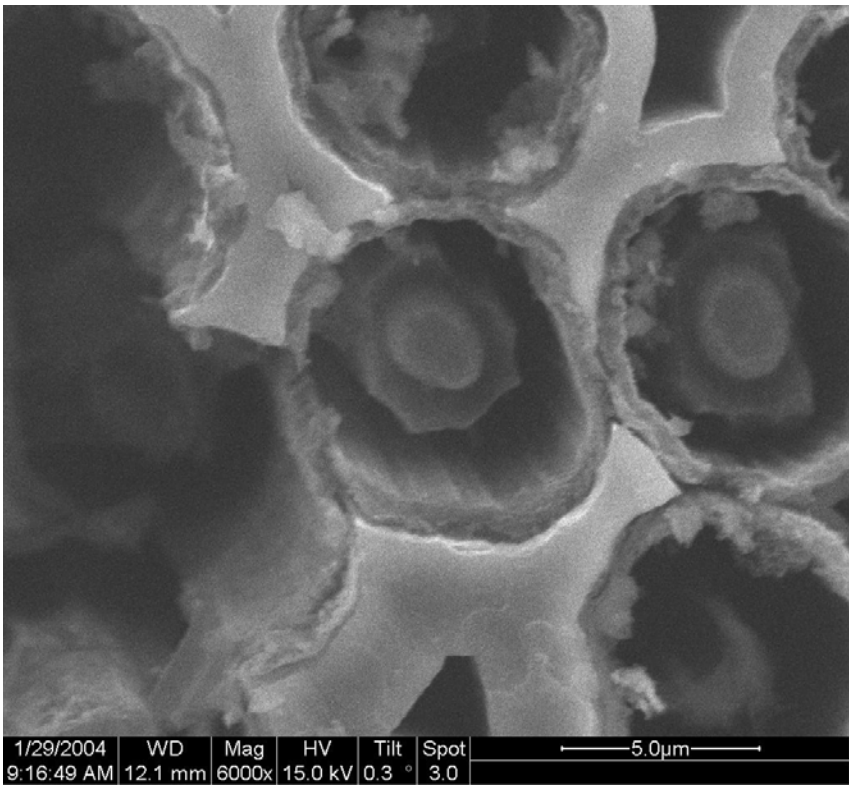

Figure A-5. Sample 02-304 (175 MPa, 375 Hz, 55.75 hours)

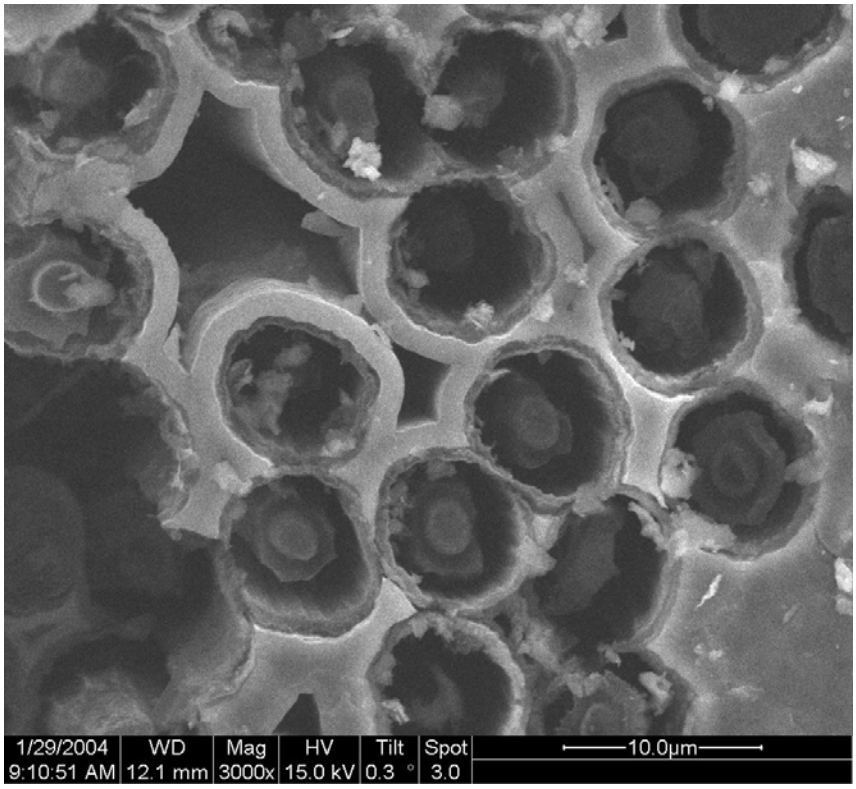

Figure A-6. Sample 02-304 (175 MPa, 375 Hz, 55.75 hours)

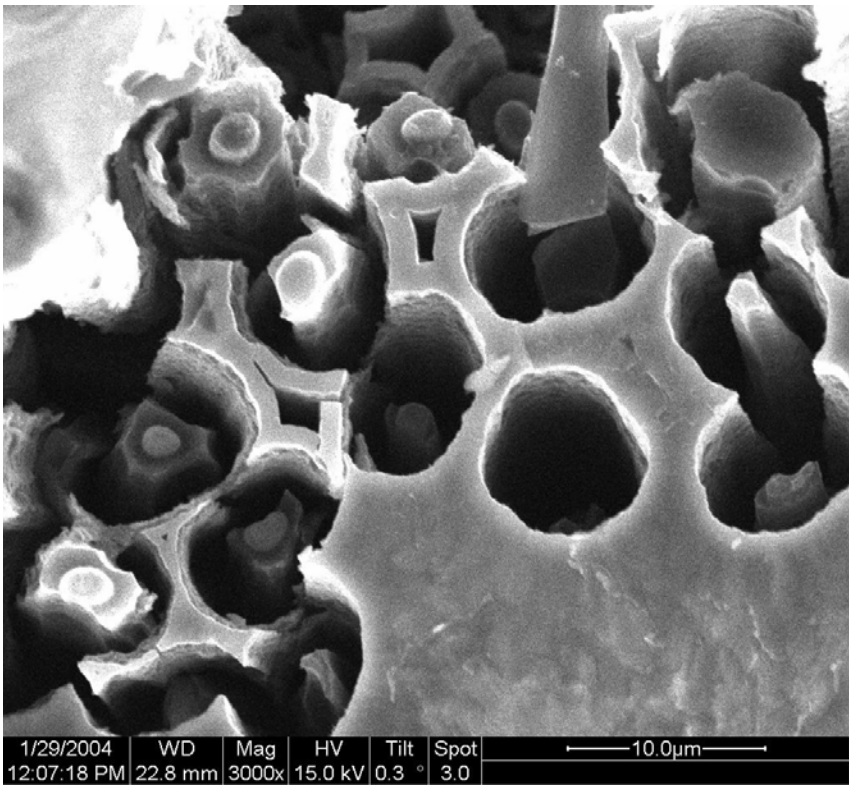

Figure A-7. Sample 02-314 (105 MPa, Creep, 10.59 hours)

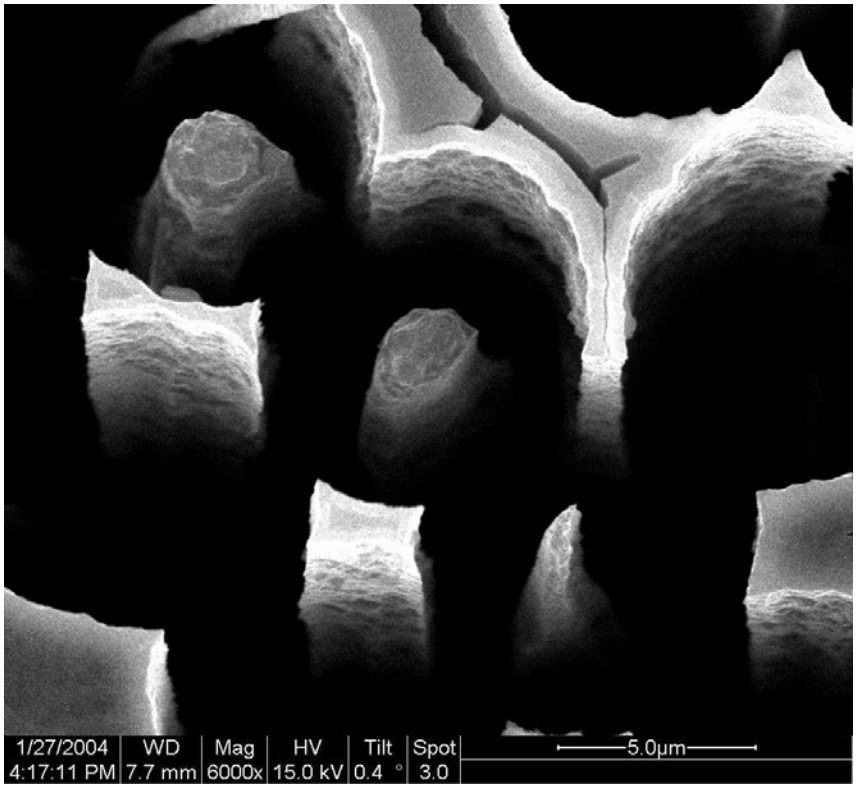

Figure A-8. Sample 02-314 (105 MPa, Creep, 10.59 hours)

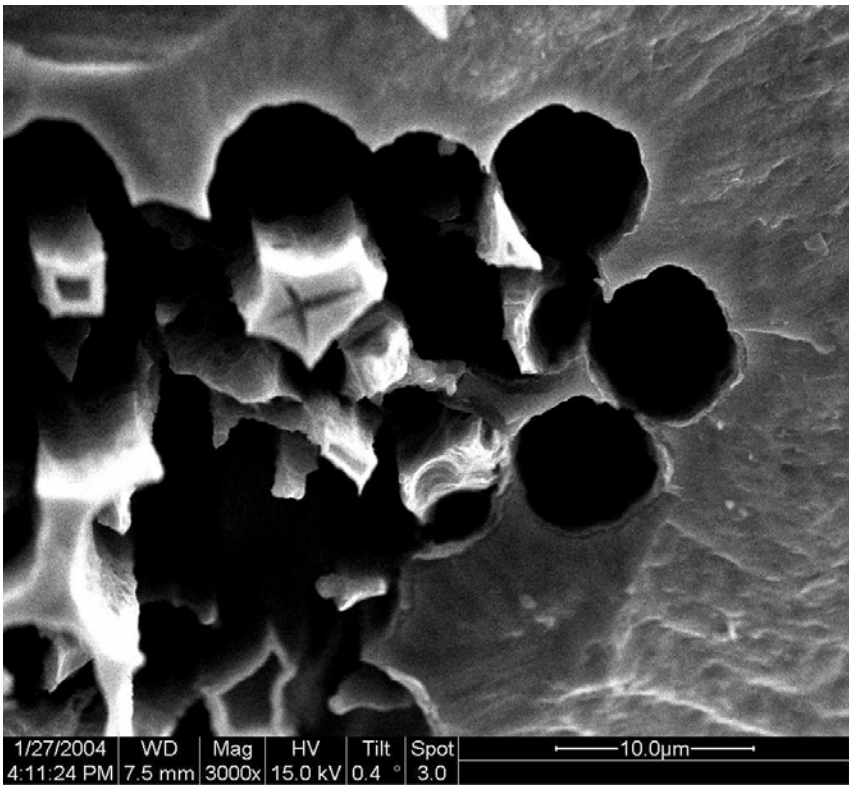

Figure A-9. Sample 02-314 (105 MPa, Creep, 10.59 hours)

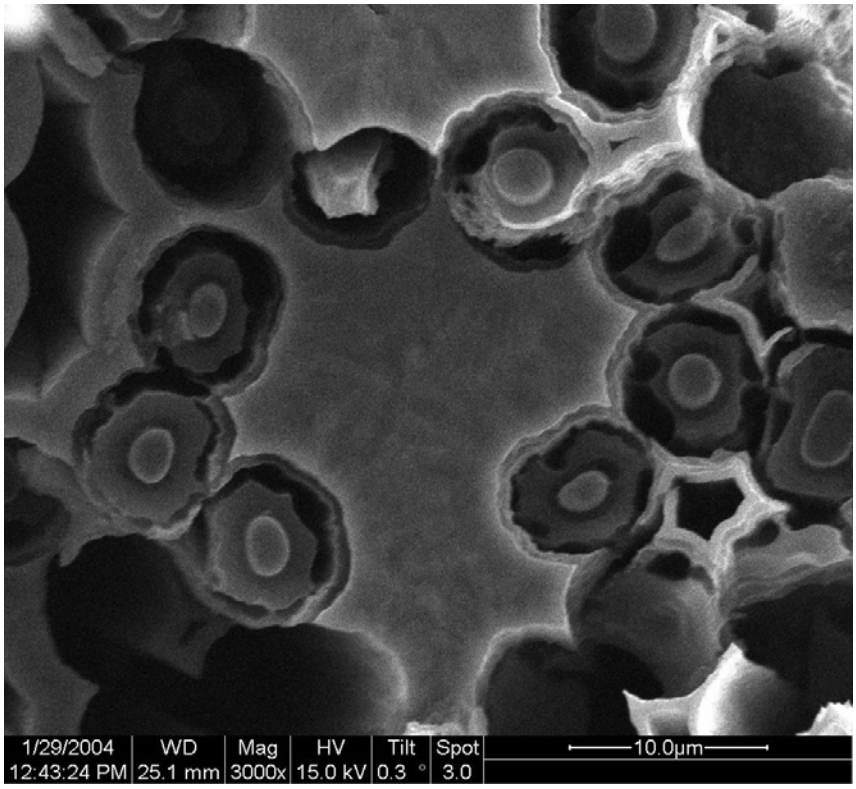

Figure A-10. Sample 02-315 (105 MPa, 0.1 Hz, 13.09 hours)

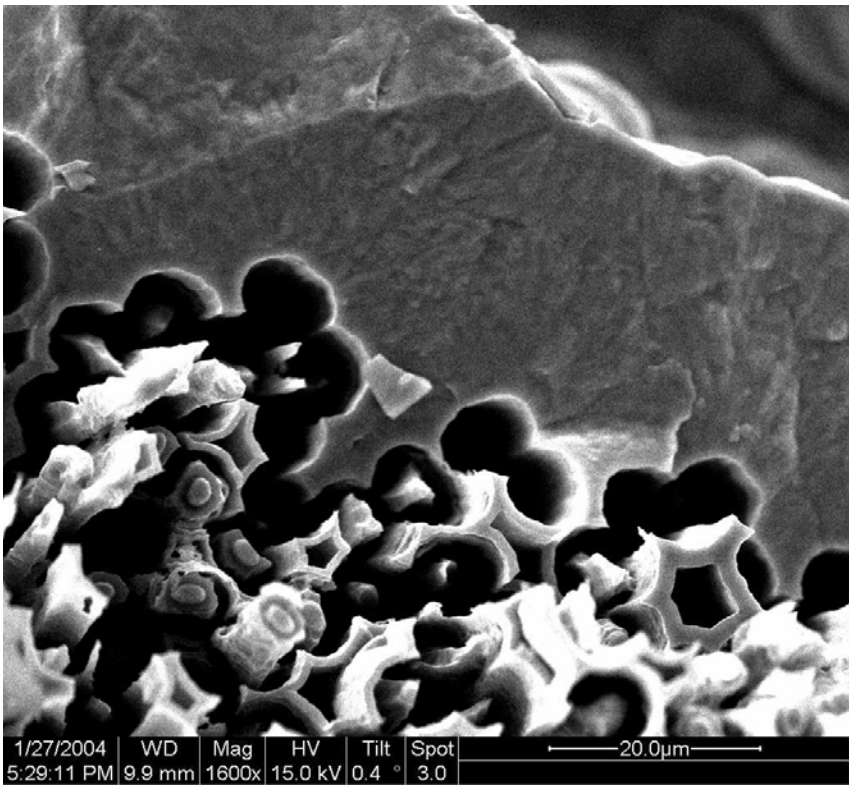

Figure A-11. Sample 02-315 (105 MPa, 0.1 Hz, 13.09 hours)

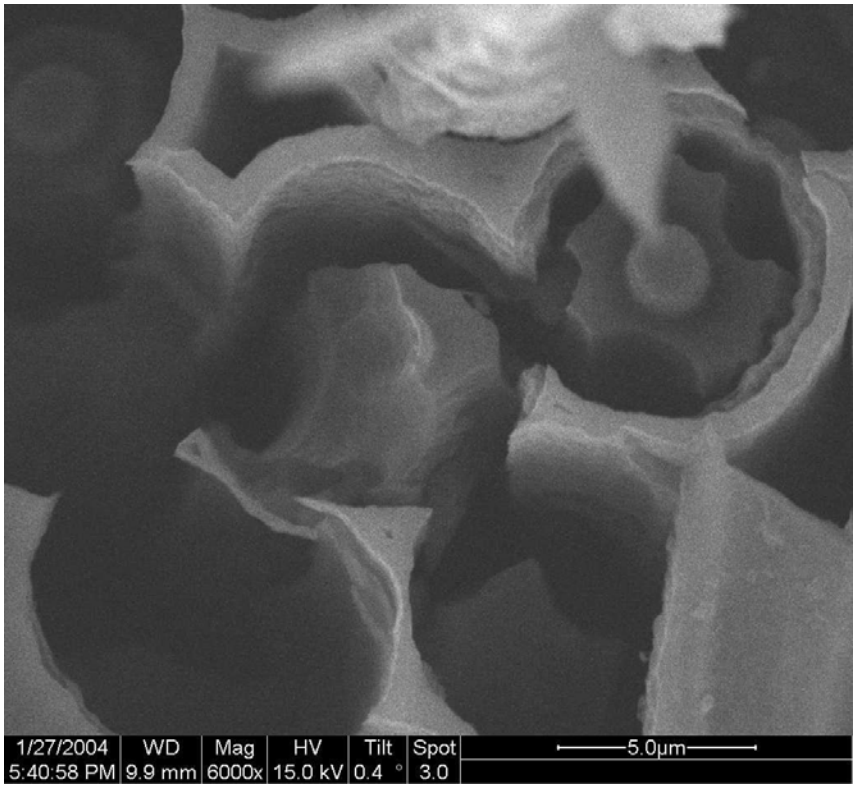

Figure A-12. Sample 02-315 (105 MPa, 0.1 Hz, 13.09 hours)

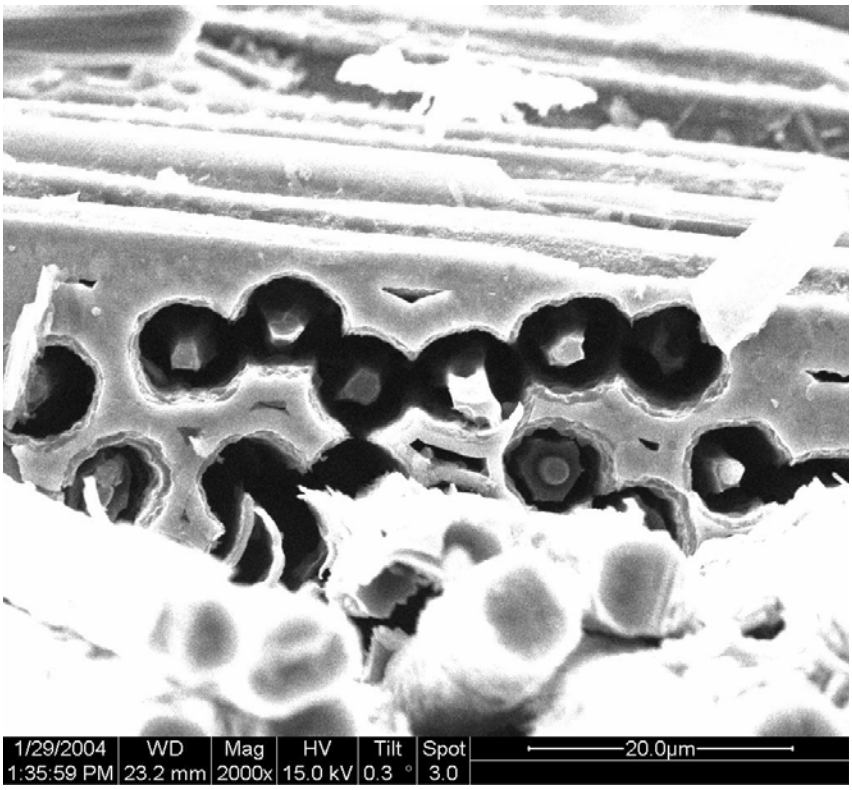

Figure A-13. Sample 02-320 (105 MPa, 10 Hz, 19.84 hours)

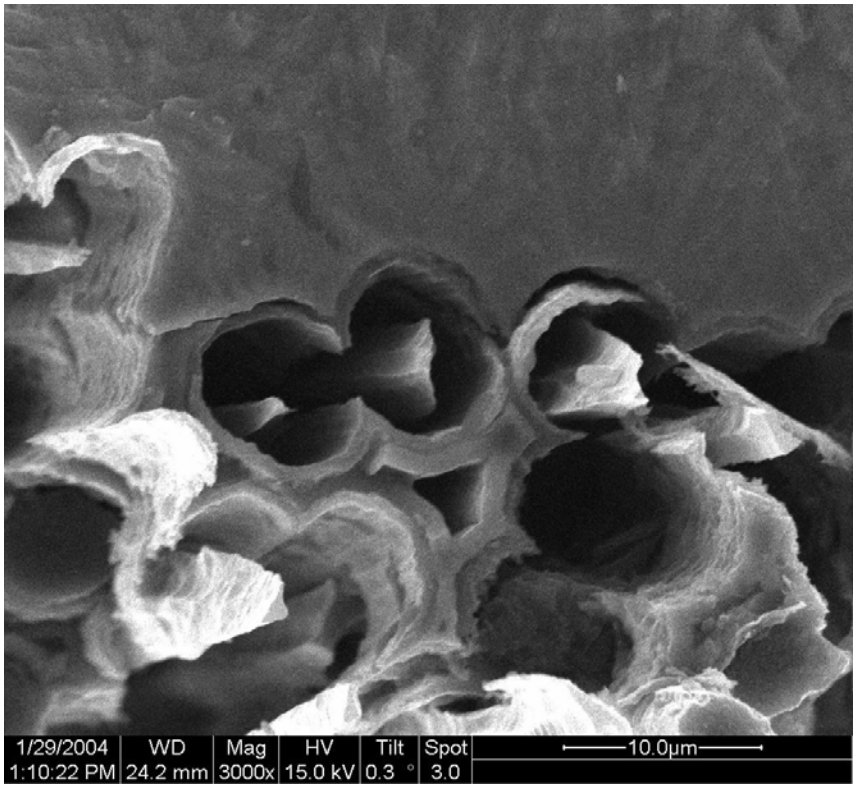

Figure A-14. Sample 02-320 (105 MPa, 10 Hz, 19.84 hours)

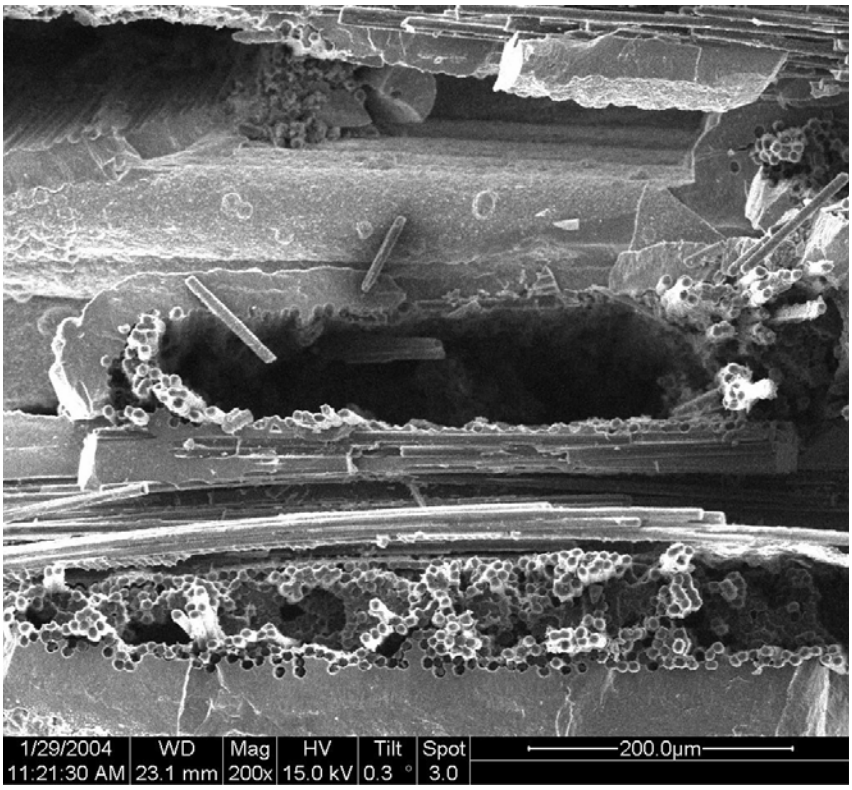

Figure A-15. Sample 02-325 (350 MPa, 0.1 Hz, 0.59 hours)

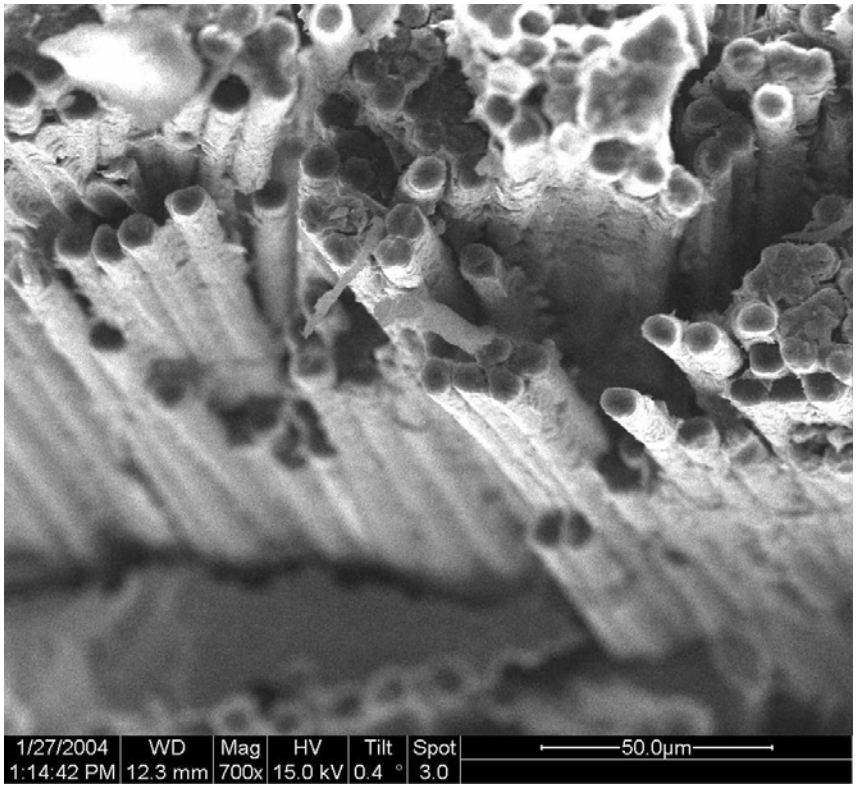

Figure A-16. Sample 02-321 (350 MPa, 10 Hz, 0.22 hours)

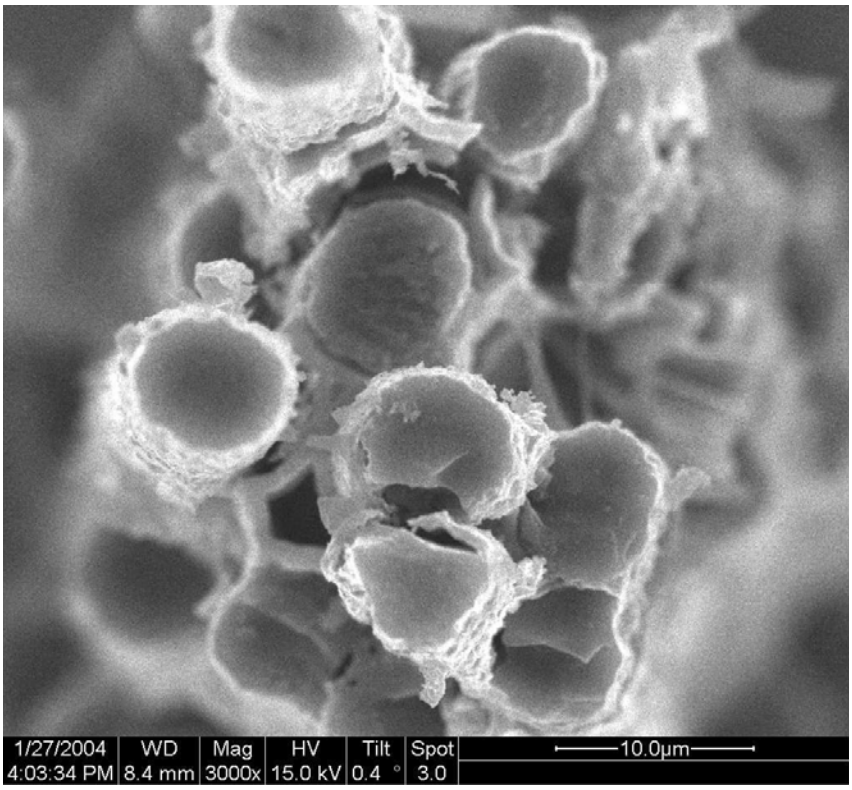

Figure A-17. Sample 02-314 (105 MPa, Creep, 10.59 hours)

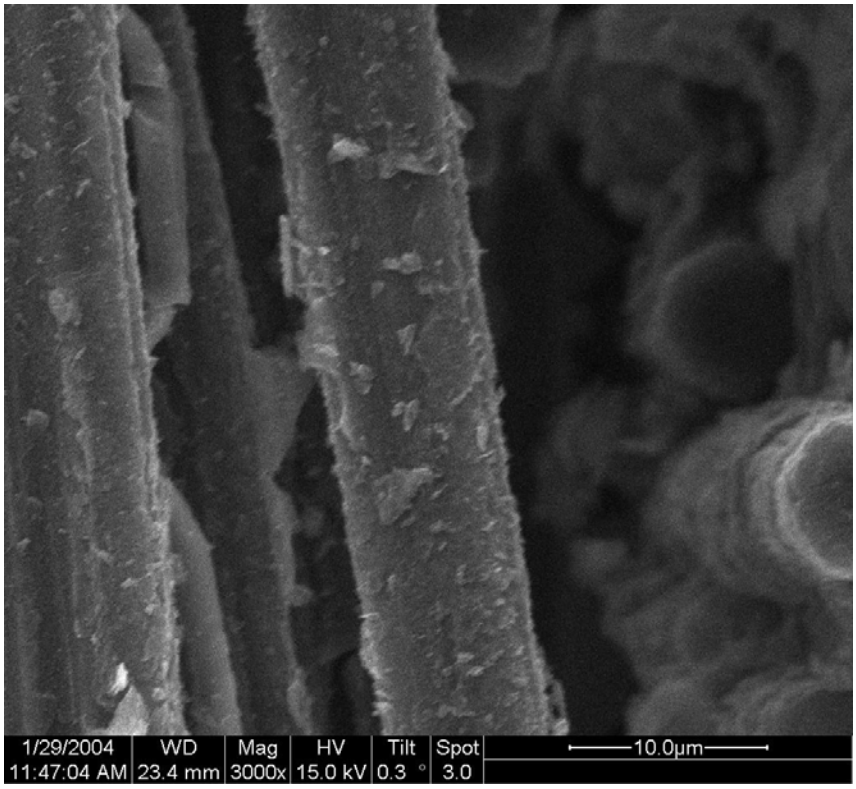

Figure A-18. Sample 02-326 (350 MPa, Creep, 0.43 hours)

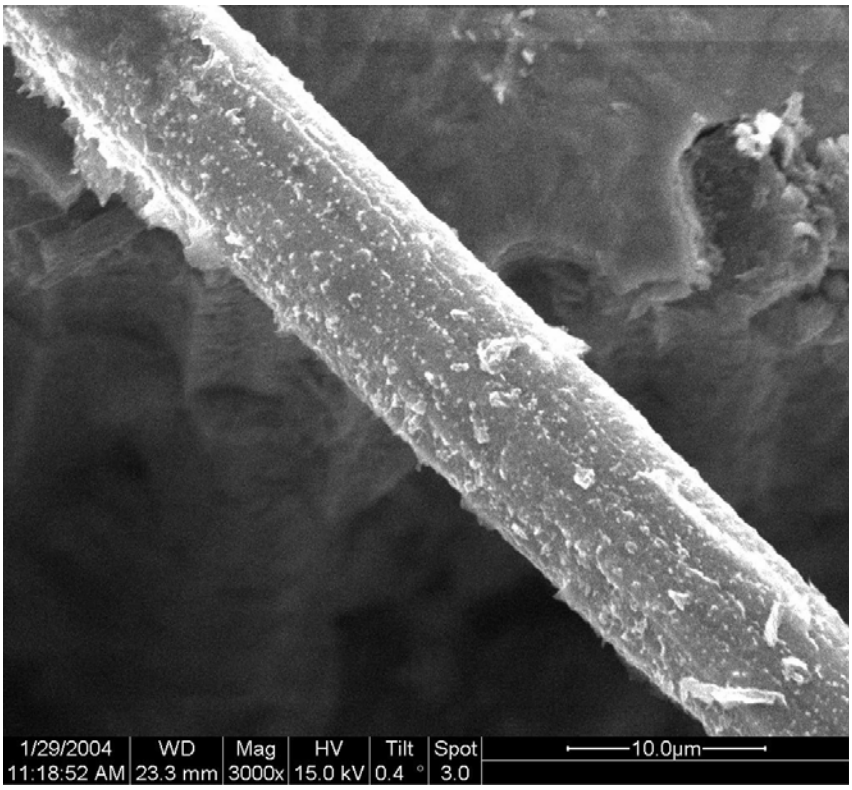

Figure A-19. Sample 02-325 (350 MPa, 0.1 Hz, 0.59 hours)

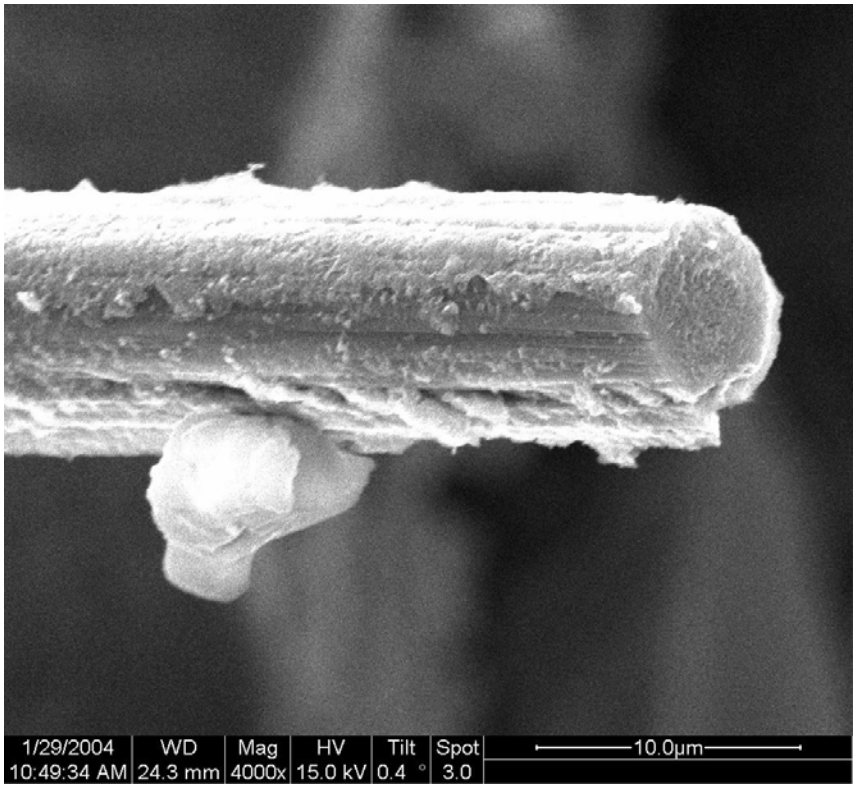

Figure A-20. Sample 02-310 (175 MPa, 1 Hz, 3.13 hours)

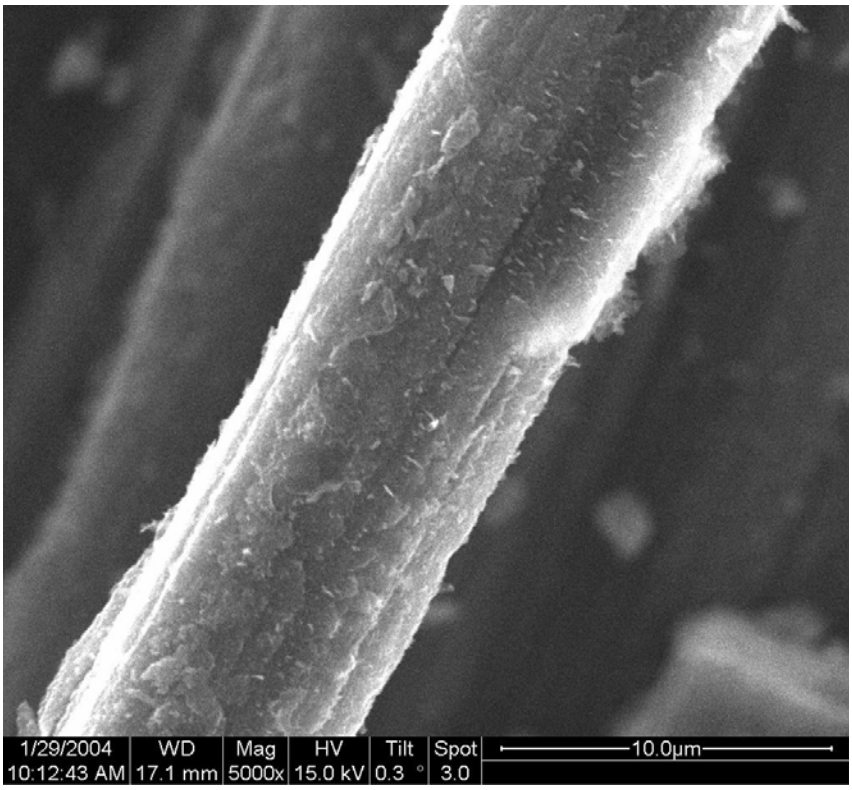

Figure A-21. Sample 02-304 (175 MPa, 375 Hz, 55.75 hours)

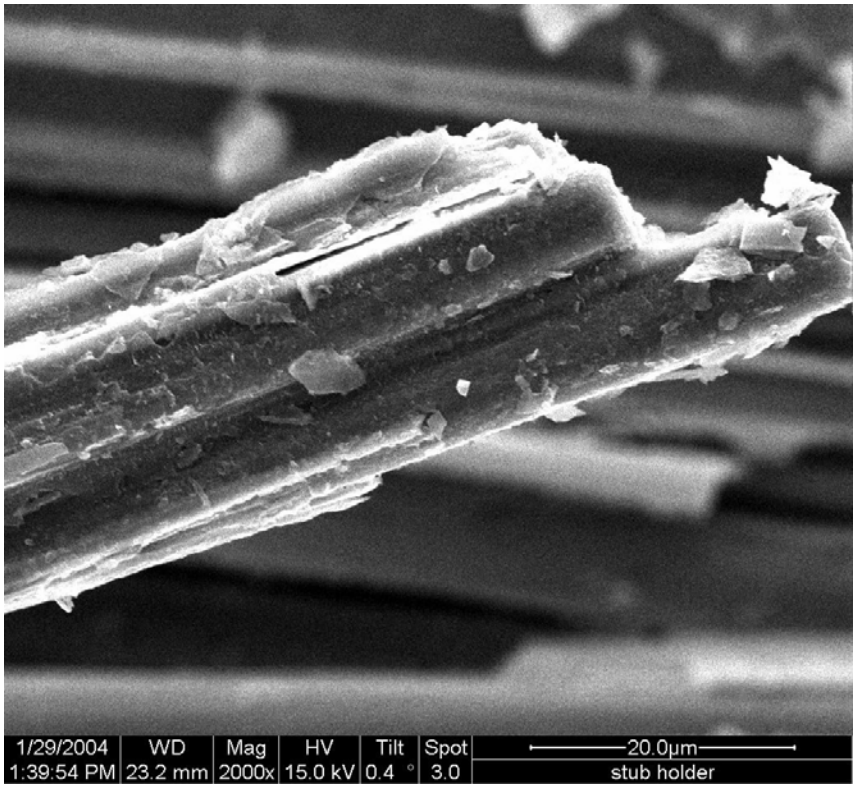

Figure A-22. Sample 02-320 (105 MPa, 10 Hz, 19.84 hours)

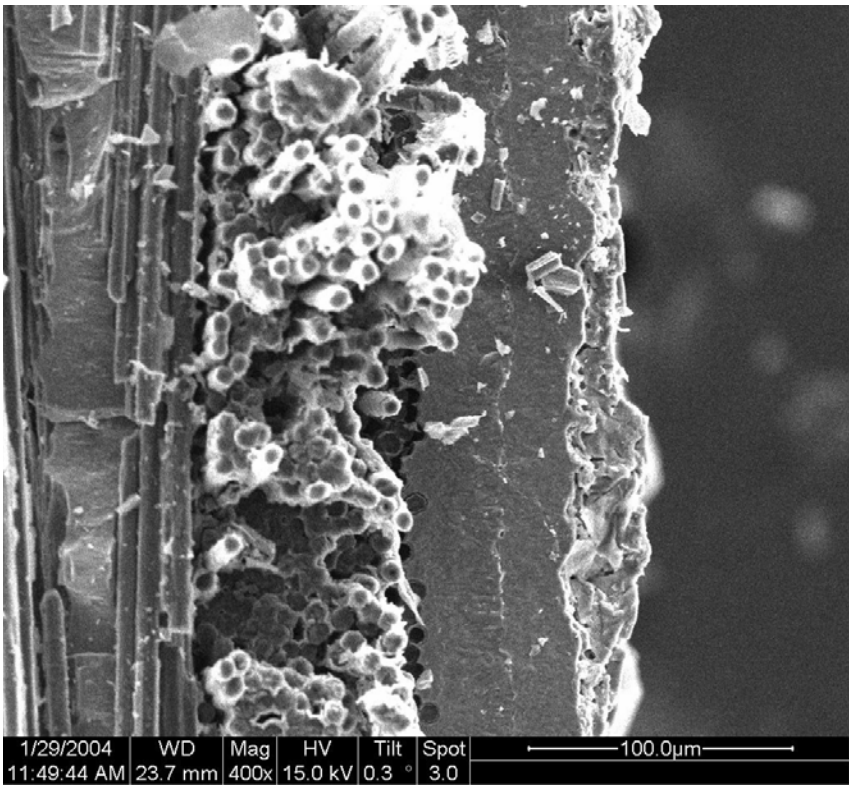

Figure A-23. Sample 02-326 (350 MPa, Creep, 0.43 hours)

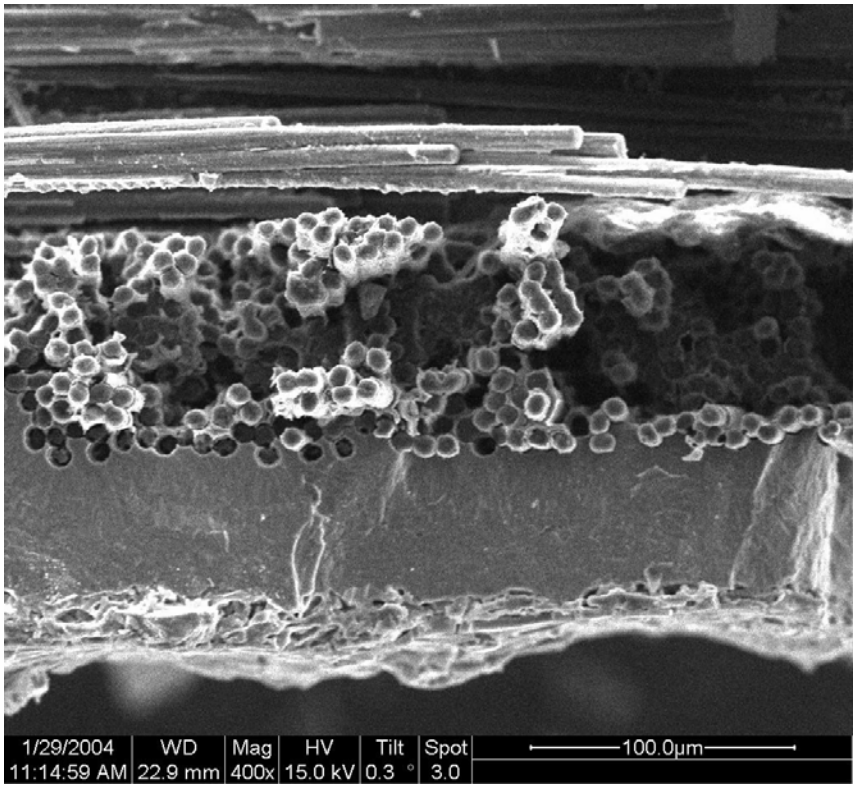

Figure A-24. Sample 02-325 (350 MPa, 0.1 Hz, 0.59 hours)

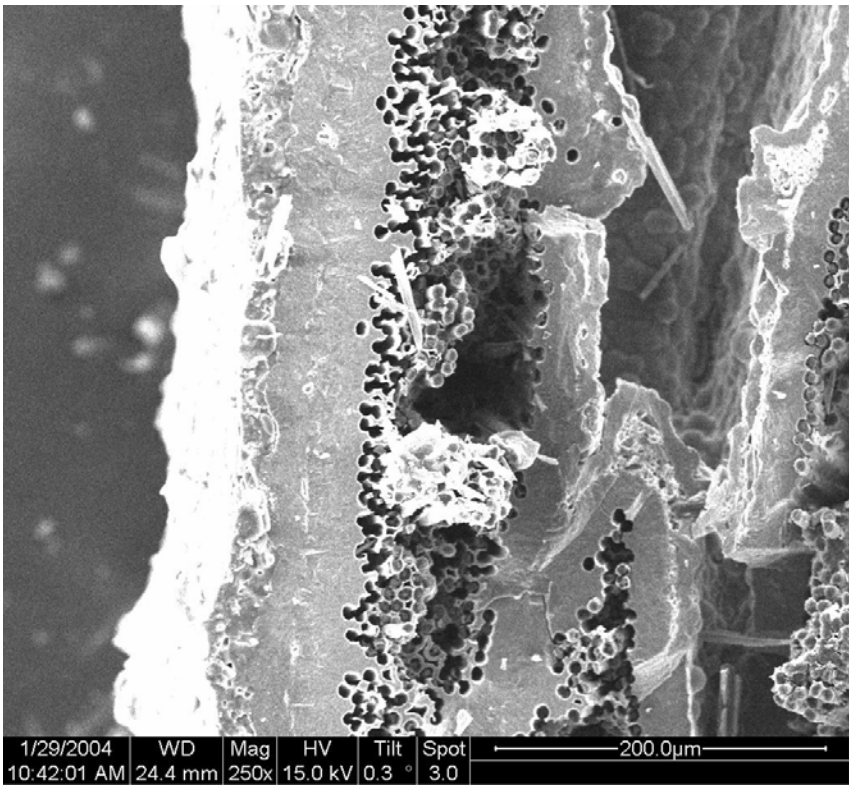

Figure A-25. Sample 02-310 (175 MPa, 1 Hz, 3.13 hours)

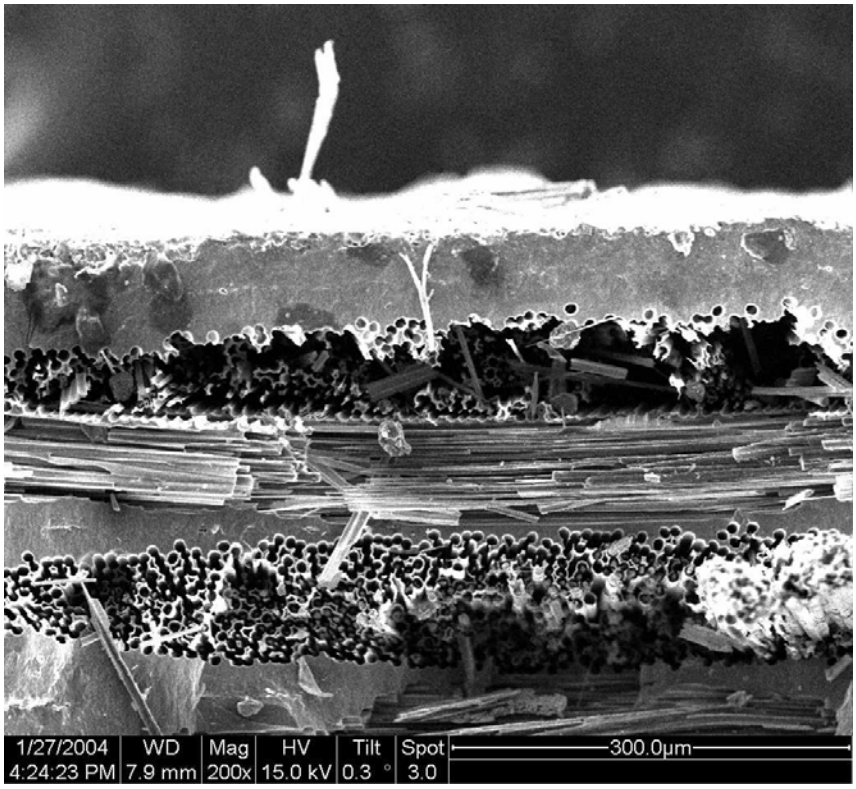

Figure A-26. Sample 02-314 (105 MPa, Creep, 10.59 hours)

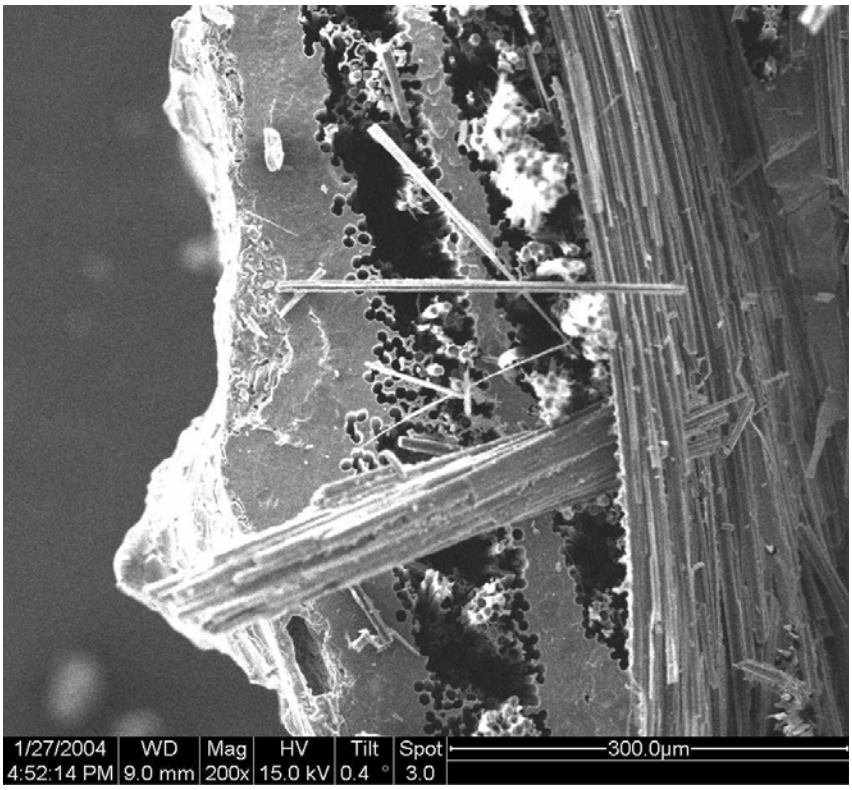

Figure A-27. Sample 02-320 (105 MPa, 10 Hz, 19.84 hours)

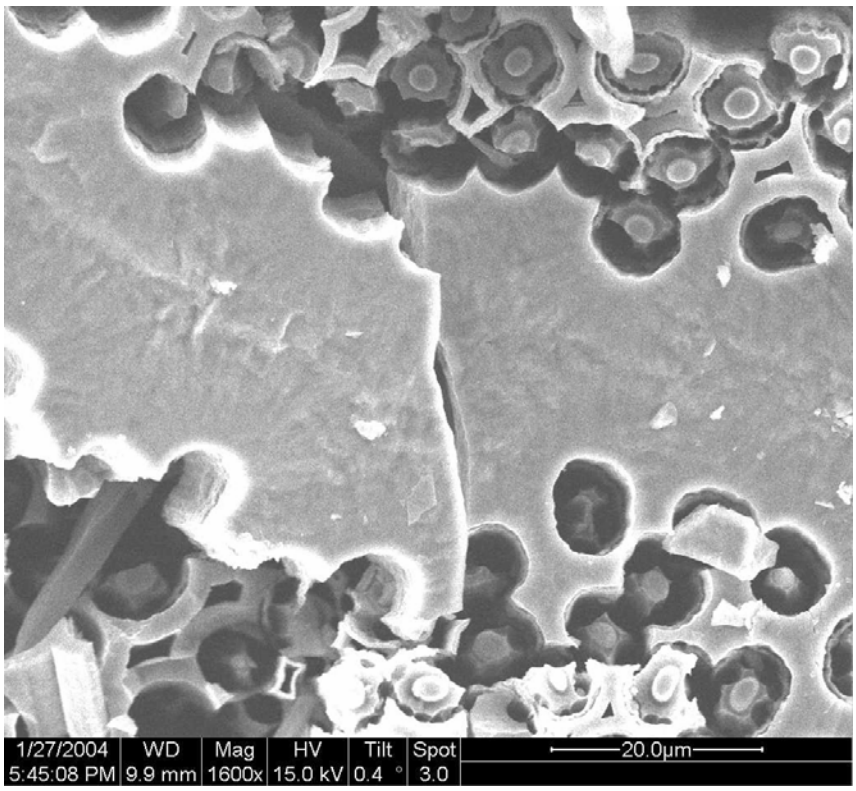

Figure A-28. Sample 02-315 (105 MPa, 0.1 Hz, 13.09 hours)

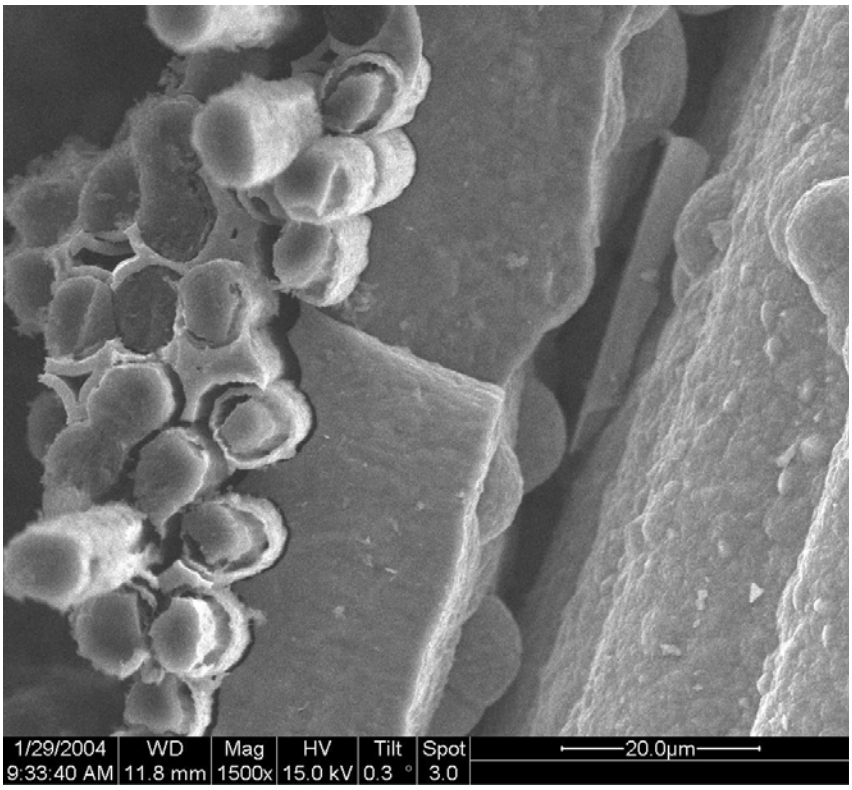

Figure A-29. Sample 02-304 (175 MPa, 375 Hz, 55.75 hours)

Bibliography

1. Daniel, Isaac M. and Ori Ishai. *Engineering Mechanics of Composite Materials*. New York: Oxford University Press, Inc., 1994.

2. Verilli, Michael J., Kantzos, Peter and Jack Telesman. "Characterization of Damage Accumulation in a Carbon Fiber-Reinforced Silicon Carbide Ceramic Matrix Composite (C/SiC) Subjected to Mechanical Loadings at Intermediate Temperature," *Mechanical, Thermal and Environmental Testing and Performance of Ceramic Composites and Components*, ASTM STP 1392, M.G. Jenkins, E. Lara-Curzio, and S. T. Gonczy, Eds., American Society for Testing and Materials, West Conshohocken, PA, 2000.

3. Verilli, Michael J., Calomino, Anthony M. and David J. Thomas. "Stress Life Behavior of a C/SiC Composite in a Low Partial Pressure of Oxygen Environment - Part I: Static Strength and Stress Rupture Database," *Proceedings of the 26th Annual Conference on Composites, Advanced Ceramics, Materials, and Structures*. 435-442. Cocoa Beach, Florida: The American Ceramic Society, 2002.

4. Halbig, Michael C. and Andrew J. Eckel. *Oxidation of Continuous Carbon Fibers Within a Silicon Carbide Matrix Under Stressed and Unstressed Conditions*. NASA/TM-2000-210224. Washington: NASA. ARL-TR-2194. Maryland: U.S. Army Research Lab, July 2000.

5. Thomas, David J., Calomino, Anthony M. and Michael J. Verilli. "Stress Life Behavior of a C/SiC Composites in a Low Partial Pressure of Oxygen Environment - Part III: Life Prediction Using Probabilistic Residual Strength Model," *Proceedings of the 26th Annual Conference on Composites, Advanced Ceramics, Materials, and Structures*. 453-461. Cocoa Beach, Florida: The American Ceramic Society, 2002.

6. Calomino, Anthony M., Verilli, Michael J. and David J. Thomas. "Stress Life Behavior of a C/SiC Composites in a Low Partial Pressure of Oxygen Environment - Part II: Stress Rupture Life and Residual Strength Relationship," *Proceedings of the 26th Annual Conference on Composites, Advanced Ceramics, Materials, and Structures*. 443-451. Cocoa Beach, Florida: The American Ceramic Society, 2002.

7. Steel, Steven G. *Monotonic and Fatigue Loading Behavior of an Oxide/Oxide Ceramic Matrix Composite*. MS Thesis, AFIT/GMS/ENY/00M-02. School of Engineering and Management, Air Force Institute of Technology (AU), Wright-Patterson AFB OH, March 2000.

8. Azom.com. "Silicon Carbide." Excerpt from unpublished article. n. pag. http://www.azom.com/details.asp?ArticleID=42. August 2003.

9. Papenburg, Ulrich, Deerler, Michael, Pfrang, Wilhelm and G. Siegfried Kutter. "Carbon Fiber-Reinforced Silicon Carbide (C/SiC) Technology." Excerpt from unpublished article. BDM/IABG and Dornier Satellite Systems (DSS). n. pag. http://www.ngst.nasa.gov/public/unconfigured/doc_0170/rev_01/CsiCTechnology1.pdf. August 2003.

10. Clarke, D. R. "Interpenetrating Phase Composites," *Journal of the American Ceramic Society,* 75 [4]: 739-758 (1992).

11. Xu, Yongdong, Cheng, Laifei and Litong Zhang. "Carbon/Silicon Carbide Composites Prepared by Chemical Vapor Infiltration Combined With Silicon Melt Infiltration," *Carbon,* 37: 1179-1187 (1999).

12. Ultramet. "Composites." Excerpt from unpublished article. n. pag. http://www.ultramet.com/old/composit.htm. Pacoima, CA. August 2003.

13. Deng, Jingyi, Wei, Yongliang and Wenchuan Liu. "Carbon-Fiber-Reinforced Composites with Graded Carbon-Silicon Carbide Matrix Composition." *American Ceramic Society,* 82 [6]: 1629-1661 (June 1999).

14. Staehler, James M., Mall, Shankar and Larry P. Zawada. "Frequency Dependence of High-Cycle Fatigue Behavior of CVI C/SiC at Room Temperature," In Press, (September 2003).

15. Verilli, Michael J., Kiser, Douglas, Calomino, Anthony M. and Elizabeth Opila. "Effect of Environment on Stress-Rupture Behavior of a Carbon Fiber-Reinforced Silicon Carbide (C/SiC) Ceramic Matrix Composite," *Proceedings of 2001 National Missile Materials Symposium*. Monterey, CA. June 2001.

16. Calomino, Anthony M. and Michael J. Verilli. "Specimen-Scale-Effect in the Durability Behavior of Continuous Carbon Fiber Reinforced Silicon Carbide Composites," *Proceedings of 2003 National Space and Missile Materials Symposium*. Colorado Springs, CO. June 2003.

17. NASA. *Affordable Fiber Reinforced Ceramic Matrix Composite Technology*. Space Act Award Application. NASA Case Number, LEW-15, 449-1, LEW-16, 221-1. NASA, 9 January 2001.

18. Gadow, Rainer. "Carbon Fiber Reinforced SiC Ceramic For Brake Disks." Excerpt from unpublished article. n. pag. http://www.uni-stuttgart.de/IFKB/en/research/17-e.pdf. University of Stuttgart. August 2003.

19. SGL Carbon AG. "High Performance Automotive Brakes." Excerpt from unpublished article. n. pag. http://sglcarbon.com/sgl_t/brakedisc/products/auto.html. SGL Technologies Section. August 2003.

20. Halbig, Michael C. "The Influence of Temperature, Stress, and Environment on the Oxidation and Life of C/SiC Composites," *Proceedings of the 26th Annual Conference on Composites, Advanced Ceramics, Materials, and Structures*. 419-426. Cocoa Beach, Florida: The American Ceramic Society, 2002.

21. Htcomposites.com. "Hyper-Therm High-Temperature Composites, Inc." Excerpt from unpublished article. n. pag. http://www.htcomposites.com/. Capabilities Section. August 2003.

22. Lamouroux, F. and G. Camus. "Kinetics and Mechanics of Oxidation of 2D Woven C/SiC Composites: I, Experimental Approach," *Journal of the American Ceramic Society,* 77 [8]: 2049-2057 (1994).

23. Effinger, M. R., Tucker, D. S. and T. R. Barnett. "Tensile and Interlaminar Shear Evaluation of Dupont Lanxide CMCs," *Proceedings of the 20th Annual Conference on Composites, Advanced Ceramics, Materials, and Structures*. Ceramic Engineering and Science Proceedings, 18 [4]: 316-323. (1996).

24. Verilli, Michael J. and Anthony M. Calomino. "Temperature Dependence on the Strength and Stress Rupture Behavior of a Carbon-Fiber Reinforced Silicon Carbide Matrix (C/SiC) Composite," In Press, *Ceramic Engineering and Science Proceedings*, September 2003.

25. Berbon, Min Z., Rugg, Kevin L., Dadkhah, Mahyar S. and David B. Marshall. "Effect of Weave Architecture on Tensile Properties and Local Strain Heterogeneity in Thin-Sheet C-SiC Composites," *Journal of the American Ceramic Society,* 85 [8]: 2039-2048 (2002).

26. Shuler, S.F., Holmes, J.W., Wu, X, and D. Roach. "Influence of Loading Frequency on the Room-Temperature Fatigue of a Carbon-Fiber/SiC-Matrix Composite," *Journal of the American Ceramic Society,* 76 [9]: 2327-2336 (1993).

Vita

Captain John Mark Engesser graduated from Grand Rapids High School in Grand Rapids, Minnesota. He attended the United States Coast Guard Academy for one year. He then enrolled at the University of Minnesota in Duluth, Minnesota where he graduated with a Bachelor of Science degree in Chemical Engineering in 1998. He was commissioned through the Detachment 420 AFROTC program at the University of Minnesota where he was recognized as a Distinguished Graduate.

His first assignment was at Detachment 420 where he was a special assistant to the Commander in July 1998. In October 1998, he was assigned to Vandenberg AFB, California where he was a student in Undergraduate Space and Missile Training (USMT). After USMT graduation, he was stationed at F. E. Warren AFB, Wyoming as a missile operations officer. He entered the Graduate School of Engineering and Management, Air Force Institute of Technology in August 2002. Upon graduation, he will be assigned to the Air Force Research Lab Materials Directorate at Wright-Patterson AFB, Ohio.

REPORT DOCUMENTATION PAGE		Form Approved OMB No. 074-0188

1. REPORT DATE *(DD-MM-YYYY)*	**2. REPORT TYPE**	**3. DATES COVERED** *(From – To)*
23-03-2004	Master's Thesis	August 02 – March 04

4. TITLE AND SUBTITLE

MONOTONIC, CREEP-RUPTURE, AND FATIGUE BEHAVIOR OF CARBON FIBER REINFORCED SILICON CARBIDE (C/SIC) AT AN ELEVATED TEMPERATURE

5a. CONTRACT NUMBER

5b. GRANT NUMBER

5c. PROGRAM ELEMENT NUMBER

6. AUTHOR(S)

Engesser, John, M., Captain, USAF

5d. PROJECT NUMBER

5e. TASK NUMBER

5f. WORK UNIT NUMBER

7. PERFORMING ORGANIZATION NAMES(S) AND ADDRESS(S)
Air Force Institute of Technology
Graduate School of Engineering and Management (AFIT/EN)
2950 Hobson Way
WPAFB OH 45433-7765

8. PERFORMING ORGANIZATION REPORT NUMBER

AFIT/GMS/ENY/04-M01

9. SPONSORING/MONITORING AGENCY NAME(S) AND ADDRESS(ES)
AFRL/MLLN
Attn: Mr. Allan Katz
2230 10th Street \r\nB655 R181
WPAFB OH 45433-7817 DSN: 785-7817

10. SPONSOR/MONITOR'S ACRONYM(S)

11. SPONSOR/MONITOR'S REPORT NUMBER(S)

12. DISTRIBUTION/AVAILABILITY STATEMENT
APPROVED FOR PUBLIC RELEASE; DISTRIBUTION UNLIMITED.

13. SUPPLEMENTARY NOTES

14. ABSTRACT

The main objective of this research effort was to examine the impact that cyclic loading frequency has on the life of a C/SiC composite at an elevated temperature of 550°C. Cyclic loading of C/SiC was investigated at frequencies of 375 Hz, 10 Hz, 1 Hz, and 0.1 Hz. Creep-Rupture tests and tests that were combinations of creep-rupture and fatigue were also accomplished. A monotonic tensile test was performed at 550°C and compared to a room temperature monotonic test. This study showed that an elevated temperature of 550°C has very little effect on the Ultimate Tensile Strength (UTS) of C/SiC. The UTS of C/SiC at 550°C was 487 MPa, while the room temperature UTS is 493 MPa. The three creep-rupture tests in this study performed at 350 MPa, 175 MPa and 105 MPa had lives of less than 11 hours despite the fact that the UTS of C/SiC is 487 MPa at 550°C. The short life of the specimens is due to the oxidation of the carbon fibers within the C/SiC composite. S-N curves developed from the fatigue tests indicate that there is an increase in cycles to failure as the frequency is increased. Another important discovery in this study was the fact that oxidation of the carbon fibers within C/SiC is reduced when frequency of fatigue is increased. At high frequency fatigue (10Hz to 375 Hz), C/SiC composites have longer cycle lives and time lives than at low cycle fatigue. Microscopic and SEM analysis verified that oxidation of carbon within C/SiC is slowed as frequency of fatigue is increased.

15. SUBJECT TERMS
Ceramic Matrix Composites (CMCs), C/SiC, Carbon, Silicon Carbide, Temperature, Fatigue, Creep-Rupture

16. SECURITY CLASSIFICATION OF:			**17. LIMITATION OF ABSTRACT**	**18. NUMBER OF PAGES**	**19a. NAME OF RESPONSIBLE PERSON**
REPORT	**ABSTRACT**	**c. THIS PAGE**			Dr. Shankar Mall
U	**U**	**U**	**UU**	127	**19b. TELEPHONE NUMBER** *(Include area code)* (937) 255-3636, ext 4587; e-mail: Shankar.Mall@afit.edu